Institut für Phytopathologie

der Justus-Liebig-Universität Gießen

---

dsRNA as a novel tool to fight *Verticillium* diseases - from basics to future applications

INAUGURAL-DISSERTATION

zur Erlangung des Doktorgrades (Dr. rer. nat.)
im Fachbereich Agrarwissenschaften, Ökotrophologie und Umweltmanagement der Justus-Liebig-Universität Gießen

vorgelegt von
Mohamed Abdeldayem
aus Kairo, Ägypten

Gießen, 2025

Mit Genehmigung des Fachbereichs Agrarwissenschaften, Ökotrophologie und Umweltmanagement der
Justus-Liebig-Universität Gießen

Prüfungskommission:

1. Gutachter(in):	Prof. Dr. Karl-Heinz Kogel
2. Gutachter(in):	Prof. Dr. Marc F. Schetelig
Prüfer(in):	Prof. Dr. Patrick Schäfer
Prüfer(in):	Prof. Dr. Volker Wiessemann
Vorsitzende(r):	Prof. Dr. Keding Gudrun
Tag der Disputation:	09.01.2026

Table of Contents

Author Declaration

Gemäß der Promotionsordnung des Fachbereichs 09, Agrarwissenschaften, Ökotrophologie und Umweltmanagement der Justus-Liebig-Universität Gießen (Ausgabe vom 29.05.2019) § 17 (2):

„Ich erkläre: Ich habe die vorgelegte Dissertation selbständig und ohne unerlaubte fremde Hilfe und nur mit den Hilfen angefertigt, die ich in der Dissertation angegeben habe.

Alle Textstellen, die wörtlich oder sinngemäß aus veröffentlichten Schriften entnommen sind, und alle Angaben, die auf mündlichen Auskünften beruhen, sind als solche kenntlich gemacht.

Bei den von mir durchgeführten und in der Dissertation erwähnten Untersuchungen habe ich die Grundsätze guter wissenschaftlicher Praxis, wie sie in der „Satzung der Justus-Liebig-Universität Gießen zur Sicherung guter wissenschaftlicher Praxis“ niedergelegt sind, eingehalten.“

_____

Mohamed Abdeldayem

List of figures:

Chapter I: Introduction

Chapter III: Results

Chapter IV: Discussion

Supplementary information

List of tables:

Chapter II

Chapter III

Abbreviations

AGO	Argonaute protein	**MCS**	Multiple cloning site
Amp	Ampicillin	**miRNA**	micro-ribonucleic acid
APS	Ammonium Persulfate	**MNase**	Micrococcal nuclease
AUDPC	Area under disease progression curve	**mRNA**	messenger ribonucleic acid
BCA	Biological control agent	**NP**	Nanoparticle
bp	base pair	**nt**	nucleotide
BSA	Bovine serum albumin	**NTO**	Non-target organism
cDNA	Complementary deoxyribonucleic acid	**OECD**	Organisation for Economic Co-operation and Development
CIA	Chloroform: Isoamyl alcohol	**PAMP**	Pathogen associated molecular pattern
CLSM	Confocal laser scanning microscopy	**PC**	Polymerase complex
DCL	Dicer like enzyme	**PCR**	Polymerase chain reaction
dd-H2O	double distilled water	**PDA**	Potato dextrose agar
DEPC	Diethyl pyrocarbonate	**PDB**	Potato dextrose broth
DNA	deoxyribo-nucleic acid	**PTGS**	Post transcriptional gene silencing
dNTP	deoxyribonucleotide triphosphate	**PTI**	Pattern triggered immunity
dsRNA	double stranded ribonucleic acid	**RdDM**	RNA directed DNA methylation
ECL	Enhanced chemiluminescence	**RdRP**	RNA dependent RNA polymerase
EFSA	European food safety authority	**RISC**	RNA induced silencing complex
EPPO	European public prosecutor's office	**RNAi**	Ribonucleic acid interference
EtOH	Ethanol	**RPM**	Revolutions per minute
FACS	Fluorescence activated cell sorting	**RT-qPCR**	Real-time quantitative reverse transcription Polymerase chain reaction
FAO	Food and Agriculture Organization	**shRNA**	small hairpin ribonucleic acid
GC	Guanine-Cytosine	**SIGS**	Spray induced gene silencing
gDNA	genomic deoxyribo-nucleic acid	**siRNA**	small interfering ribonucleic acid
GFP	Green fluorescence protein	**ssRNA**	single stranded ribonucleic acid
GMO	Genetically modified organism	**SXM**	Simulated xylem medium
HIGS	Host induced gene silencing	**TBE**	Tris-Borate-EDTA
hpt	hours post treatment	**TBS-T**	Tris buffered saline buffer + Tween 20
HRP	Horseradish Peroxidase	**TEMED**	Tetramethyl ethylenediamine
IgG	Immunoglobulin G	**TGS**	Transcriptional gene silencing
IPEC	Interpolyelectrolyte complexes	**TMV**	Tobacco mosaic virus
IPPC	International Plant Protection Convention	**ToBRFV**	Tomato brown rugose fruit virus
IPTG	Isopropyl-β-D-thiogalactopyranosid	**UTP**	Uracil triphosphate
Kan	Kanamycin	**UV**	Ultra-violet
kb	Kilo base pair	**VIGS**	Virus induced gene silencing
mAB	monoclonal antibody	**wpi**	weeks post infection

Chapter I: Introduction

1.1 Impact of plant pathogenic fungi

Plant pathogenic fungi are among the biggest causes of crop losses (Steinberg and Gurr 2020), leading the biotic stress group in limiting yields and devastating a wide range of plant hosts, with an estimated 10-23% pre-harvest losses and 10-20% post-harvest loses. According to a ranking of various plants pests and pathogens, plant pathogenic fungi occupy the first six places and are considered the biggest threats to food security worldwide (Savary et al. 2019). Modern cropping strategies for mass production (ex. monocultures) have contributed to the emergence of many fungicide resistant pathogens, leading to an immense increase in the amounts of fungicides needed to limit or eliminate infectious abilities of these pathogens (Heick et al. 2017). Another crucial factor in this arms race is the environmental factors influencing the so called "*disease triangle*", namely the continuous rise in global temperatures, more frequent extreme weather events and precipitation fluctuations (Goessling et al. 2025). These rapid environmental changes will be affecting the whole agricultural ecosystem, for instance it might alter virulence of existing pathogens, as well as a growing risk of the emergence of novel pathogen species that are better suited for the new climate conditions. Additionally, the re-introduction of pathogens previously restricted to the Southern hemisphere towards the colder Northern hemisphere and threatening crops previously not susceptible to such diseases and vice versa (Singh et al. 2023). All these factors ring an alarm to enhance the toolkit of plant protection and put more pressure on developing alternative strategies, to ensure food security and meet the nutritional needs for an ever-growing population.

1.2 *Verticillium* wilt – genus classification and disease lifecycle

The management strategies for fungal plant pathogens vary depending on the severity of infections, the ability to diagnose these infections, and the historic experiences from previous cropping seasons. Many practices and guidelines exist for known plant pathogens to limit loses as much as possible, which are usually available on local, regional (ex. EFSA, EPPO) and international levels (ex. FAO, IPPC). Common practices include careful rotation of crops with varying susceptibilities to pathogens, using resistant varieties for known pathogens from previous seasons and most commonly, the use of chemical fungicides or biological control agents (BCA) to protect crops in commercial applications. However, these plant protection approaches offer varying protection levels, in some cases these strategies offer only a very limited protection or no curative options, as in the case of Verticillium wilt caused by various *Verticillium* species (Pegg and Brady 2002, Subbarao et al. 2007).

Verticillium is a small genus of ascomycete fungi that currently contains 10 species (Inderbitzin et al. 2011), of which *V. dahliae* and *V. albo-atrum* are the most common plant pathogens and well characterized species, due to their broad host range and economical relevance. They are known to infect tomato, cotton, lettuce, potato, strawberries and many other commodity crops. The "nearly diploid" species *V. longisporum* was first characterized in Germany in 1961 (Stark 1961) having conidia isolated from infected Horseradish twice as long as *V. dahlia*e conidia, later classified as a separate species based on phylogenetic and morphological differences (Karapapa et al. in 1997). *V. longisporum* is believed to have originated from multiple hybridization events of *V. dahliae* and an unidentified *V. alfalfae* related species, it has a narrower host range, as it is known to infect primarily plants belonging to family *Brassicaceae*. *V. longisporum* causes considerable losses to *Brassica napus* when fields are infested with their resilient resting microsclerotia (Depotter et al. 2016, Inderbitzin and Subbarao 2014).

V. longisporum is a soil-borne hemi-biotrophic pathogen, the infection is monocyclic and consists of an initial endophytic phase, followed by a semi-necrotrophic phase (Figure 01). Resting microsclerotia is stimulated to germinate once roots exudates can be detected, which leads to germination and penetration typically through lateral roots. The growing hyphae spreads through the plant vasculature and when a systemic infection is established, water transport through xylem vessels is impeded, leading to the common disease symptoms like chlorosis, stunting and eventually wilting. A semi-necrotrophic phase takes place at the later stages of the disease, where microsclerotia - melanized, thick-walled clusters of fungal cells - are formed due to the increased senescence of the host plant. The microsclerotia are then released back to the soil and can survive in a dormant state for over 10 years in the soil (Wilhelm 1955), mostly found 10-30 cm below ground surface, but also can reach up to 40 cm below ground surface (Palanga et al. 2021).

The complex disease cycle and infection site contribute to the difficulty of managing such pathogen, soil fumigation has been an effective strategy to eliminate the danger of infection by *Verticillium* species using Methyl bromide (MeBr) and chloropicrin (Subbarao et al. 2007). However, due to increasing environmental concerns of their negative effects on stratospheric ozone and tight regulatory limits for chloropicrin acceptable levels (Enebak 2011), the use of MeBr has been limited to specific quarantine applications and equally effective alternatives are still being investigated (Rosskopf et al. 2024). Soil solarization can be an effective alternative that showed a decline in the viable microsclerotia levels; however it is possible only in certain warmer climate areas like Mediterranean, tropical environments and deserts (Stapleton 2000).

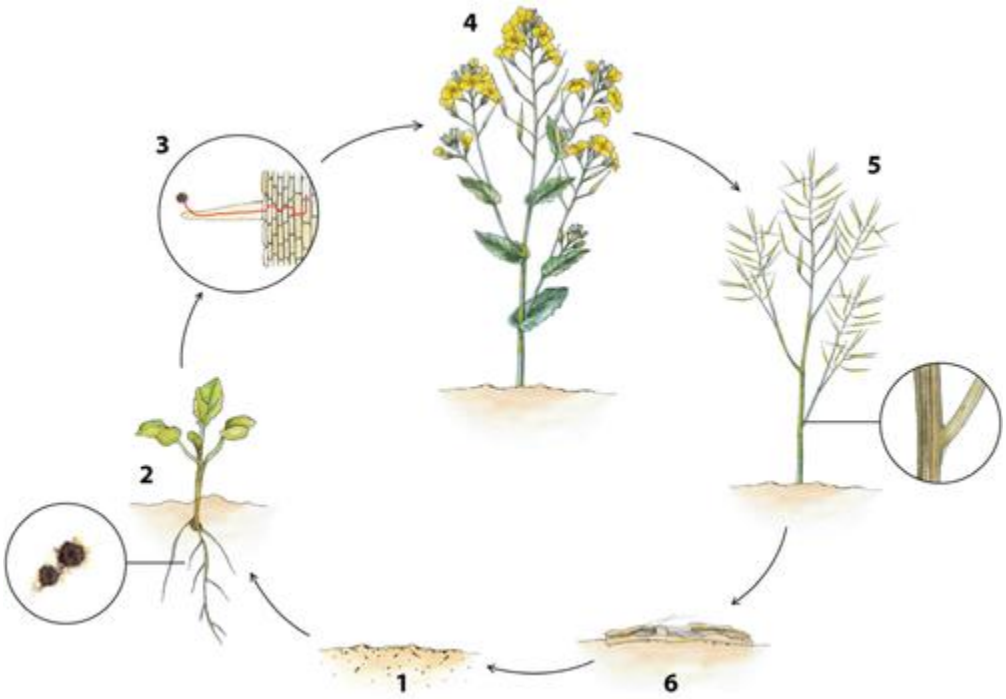

Figure 01. Adopted from Depotter et al. 2016 (Verticillium longisporum, the invisible threat to oilseed rape and other brassicaceous plant hosts - Depotter - 2016 - Molecular Plant Pathology - Wiley Online Library) Disease cycle of *Verticillium longisporum* on oilseed rape. **1.** Microsclerotia are persistent resting structures that reside in the soil and bridge the gap between hosts. **2.** Triggered by root exudates, microsclerotia start to germinate and hyphae grow towards the root of the plant. **3.** The fungus enters the root through wounds, or by direct penetration of epidermal cells of lateral roots or root hairs. In the root, hyphae grow intercellularly and intracellularly towards the central cylinder and enter the xylem. **4.** No disease symptoms are observed during a major part of the growing season. **5.** Dark unilateral striping develops on the stem of oilseed rape during the ripening of the crop. Ultimately, black microsclerotia are formed in the stem cortex. **6.** Microsclerotia are released into the soil on decomposition of plant debris.

1.3 Current *Verticillium* wilt management strategies

Verticillium infections are currently managed mostly through using known resistant cultivars if available. For instance, *Ve1* is a known race-specific resistance gene found originally in 2001 in tomato (Kawchuk et al. 2001), and homologues were later identified in cotton (Zhang et al. 2011), lettuce (Hayes et al. 2011) and *Nicotiana glutinosa* (Zhang et al. 2013). The presence of this resistance gene demonstrated protection against race 1 isolates of *Verticillium* species, that includes *V. dahliae* and *V. albo-atrum,* but not yet established as a known resistance gene against *V. longisporum* infections (Depotter et al. 2016).

Being the only diploid member of *Verticillium* species, *V. longisporum* isolates are classified according to their different lineages to A1 x D1/2/3, where different hybridization events took place to produce the current three lineages of *V. longisporum* (A1D1, A1D2, A1D3) (Depotter et al. 2021). In a recent phylogenetic analysis, lineage A1/D1 of *V. longisporum* was identified as the most virulent lineage after studying 271 isolates from 61 geographical locations in Europe and Canada (Vega-Marin et al. 2025). However, due to a high variation in the pathogenicity levels observed between different isolates from the same location or phylogenetic clade, it was not possible to identify specific virulence genes. The group concluded that various virulence factors must be involved - even in closely related isolates - and subsequently decrease the chances of identifying cultivars exhibiting broad resistance capabilities to different *V. longisporum* isolates.

Other possible strategies for limiting infections of *Verticillium* species include crop rotation or biological control agents (BCA) to decrease the microsclerotia load in soil. Crop rotation using broccoli showed a decreased in microsclerotia load in soil and *V. dahliae* infection severity on cotton (Zhao et al. 2023), eggplant (Ikeda et al. 2015), cabbage (Banno et al. 2011), and strawberries (Subbarao et al. 2007). However, no similar big scale studies were done to demonstrate these effects of crop rotation programs against *V. longisporum* infections, which is capable of infecting broccoli that belongs to the susceptible *Brassicaceae* family.

BCA research has shown many promising applications for non-pathogenic fungal strains like *Fusarium oxysporum* isolates (Zhang et al. 2015) and *Verticillium isaacii* (Deketelaere et al. 2020) were reported to reduce infections by *Verticillium* wilt causing species. In a small-scale application, non-aggressive *V. longisporum* strains from A1D2 lineage showed decreased disease severity when co-inoculated with the virulent strain Vl43 from A1D1 lineage, indicating a possible competition on active sites or a priming effect that leads to less severe infections (Vega-Marin and Von Tiedemann 2022).

Several bacterial BCA were also reported to decrease severity of *Verticillium* infections, beneficial effects against *V. longisporum* infections were reported with using *Serratia plymuthica* HRO-C48 (Müller and Berg 2008) and *Bacillus amyloliquefaciens* (Niazi et al. 2014). However, none of the aforementioned strategies were established in large scale field application for protection against *V. longisporum* infections.

1.4 RNAi as an alternative strategy for *Verticillium* wilt management

Since the first recorded observation of RNA interference (RNAi) phenomenon in 1990 on Petunia (Napoli et al. 1990), the interest to understand the mechanism behind it yielded the first reported application of dsRNA on *Caenorhabditis elegans* in 1998 (Fire et al. 1998). The phenomenon was later characterized as a conserved immune response against dsRNA, which is naturally present in viruses as part of their genome, or a product of ssRNA viral replication process (Chen and Hur 2022). Upon dsRNA recognition in an eukaryotic cell, the RNAi machinery is recruited to ensure that complementary mRNAs are not further translated, by cleaving long dsRNA molecules to small interfering RNA (siRNA), thereby preventing viral replication or the hijacking of cellular resources by the invading virus. siRNAs can also be generated through the cleavage of endogenously produced small hairpin RNA (shRNA) - also referred to as micro-RNA (miRNA) - involved in gene regulation pathways (Carthew and Sontheimer 2009). The plant RNAi machinery is therefore involved in viral immune response, transcription regulation and epigenetic modifications, which was found to be carried out by different variants of DICER and ARGONAUTE (AGO) proteins (Deleris et al 2006). The two separate pathways are usually referred to as post transcriptional gene silencing (PTGS) (Hammond et al. 2001), while RNA directed DNA methylation (RdDM) and chromatin remodelling lead to transcriptional gene silencing (TGS) (Erdmann and Picard 2020).

The RNAi machinery comprises many proteins with various functions and variants, depending on the activated pathway. DICER is the central enzyme involved in cleavage of long dsRNA or pre-microRNA (pre-miRNA) to shorter fragments of siRNA (Vergani-Junior et al. 2021). It contains the dsRNA binding domain and RNase III domains, generating siRNAs/miRNAs, which will then be loaded to AGO proteins and form the RNA-induced silencing complex (RISC). In mammals, DROSHA is another enzyme belonging to RNase III endonuclease family, it is involved in cleaving primary-micro-RNA (pri-miRNA) found in the nucleus, to produce pre-miRNA that will later be transported to the cytoplasm for DICER cleavage steps (Carthew and Sontheimer 2009).

DROSHA has not been characterized in plants, where the initial processing of miRNAs is carried out by DICER like enzyme I (DCL1) (Li and Patel 2016). The size of the generated siRNAs varies between different species and usually some variation is also observed within the same system. For instance, in *A. thaliana*, a pool of siRNAs between 21-24 nucleotides (nt) is expected, depending on which DICER enzyme is involved and the source of the diced siRNA (Henderson et al. 2006). RNA dependent RNA polymerase (RdRP) can amplify the gene silencing effects when secondary siRNAs are produced. In plants, when siRNA binds the complementary target mRNA, RdRP recruitment would lead to the transcription of complementary RNA using siRNA as a primer, and thereby producing a new long dsRNA that would re-enter the gene silencing process and generate new siRNAs, referred to as “secondary” or “transitive” siRNAs (Sanan-Mishra et al. 2021).

The history of RNAi discovery and characterization in plants was comprehensively reviewed (Rosa et al. 2018), it started by studying the cross protection observed against related viral pathogens (Lindbo et al. 1993) and later the range of RNAi functions were better understood. It was found that RNAi is also involved in the immune response against other bacterial pathogens like *Pseudomonas syringae, Agrobacterium tumefaciens* and *Verticillium dahliae* through miRNAs (Li at al. 2010, Zhang et al. 2011, Zhang et al. 2016 respectively).

This growing knowledge led to a surge in research approaches to employ RNAi in plant protection, through genetic transformation of host plants to express certain dsRNAs, known as host-induced gene silencing (HIGS) (Koch and Wassenegger 2021), spray-induced gene silencing (SIGS) (He et al. 2024) and for fungal pathogens specifically (Mosquera et al. 2025), and virus-induced gene silencing (VIGS) (Dommes et al. 2019). All these strategies aim to gene target reduction using the "knock-down" effect, which could be a host gene leading to decreased susceptibility, a desired phenotype, or targeting a pathogen gene leading to decreased virulence or disease severity, with the difference being the method used to deliver the siRNAs to target cells. In HIGS, the host is genetically modified to continuously express hairpin siRNA, that will then be processed by RNAi machinery. In SIGS, dsRNA with variable length (≈155-1500 nt) is sprayed to host plants and then uptaken by insects or fungi to achieve the intended effects, or directly act on virus associated transcripts.
Another key difference between these strategies is their compliance to current regulations regarding genetically modified organisms (GMO) use, which is allowed in many countries worldwide for commercial crop production but not in the European union, where HIGS & VIGS would be considered GMO applications ((EC) No 1829/2003).

To date, one commercial SIGS product is officially licensed for field application in plant protection, developed by GreenLight Biosciences, "Calantha" offers protection to potato leaves from Colorado potato beetle (US EPA 2023). The commercial application was possible due to their patented low-cost dsRNA production system in a cell free system, reaching as low as 0.5$ per 1 g dsRNA (US10858385B2, Cunningham et al. 2018). Bacterial dsRNA production systems also offer lower cost for dsRNA production compared to the more expensive (≈200$/g) *in-vitro* transcription kits. Certain limitations exist for each production system depending on the producing bacterial strains, involvement of IPTG for transcription induction which could reach cytotoxic levels if not purified properly (da Rosa et al. 2024), size limitation of the produced dsRNA constructs and the costs involved with purification of dsRNA from unwanted nucleic acids (reviewed by Hashiro and Yasueda 2022).

Beside cost of production, many challenges still face SIGS approach for large scale field application. Environmental degradation is another challenge for efficient RNAi effects, where UV, light, rain, nucleases from target and non-target organisms and heat in some locations rapidly degrades dsRNA. To address this rapid degradation, various formulation strategies showed promising degrees of protection following spray application for a prolonged protection window compared to naked dsRNA spray application like carbon dots (Wang et al. 2023), clay nanosheets (Mitter et al. 2017), star polycation (Tao et al. 2025) and chitosan based nanoparticles (Moorlach et al. 2025). However, the prolongation of environmental dsRNA survival should still be handled carefully, as it also increases the probability of non-target organisms (NTO) exposure to dsRNA, and thus a higher potential off-target effects.

In risk assessment studies conducted by the Organisation for Economic Co-operation and Development (OECD), no risks to human health were found, due to the poor bioavailability and rapid degradation of dsRNA/siRNA when ingested orally. On the other hand, the environmental risk is much more challenging to estimate, given the significant variations observed in the RNAi machinery between different species, and the absence of information in some cases about the expected effects from dsRNA or siRNA on different organisms (OECD 2020 and OECD 2023). These risks include saturation of RNAi machinery, activation of immune responses, and heritable histone modifications/DNA methylation that take place in the TGS pathway (Dalakouras et al. 2024, Joga et al. 2016). Despite these uncertainties, RNAi is proving to be a powerful tool with a huge potential in studying gene functions, limiting certain pest populations as shown in susceptible insects (Pallis et al. 2023), and offering an alternative customisable strategy for combating plant pathogens such as fungi and viruses.

The success of RNAi using exogenously applied dsRNA would depend on the i) characterization of lethal/virulence limiting gene targets, ii) efficient delivery of the necessary dsRNA concentration before systemic infection is established, and iii) avoiding any unwanted negative effects for host plants/NTO.

Many studies were conducted to uncover the molecular mechanisms behind the virulence and viability of *V. dahliae*, due to their broad host spectrum and more abundant genomic data. Genetic manipulation through studying knock-out variants in infection assays (Bui et al. 2019, Chen et al. 2023, Fradin et al. 2009, Lv et al. 2023, Wang et al. 2022 and Zhang et al. 2022), as well as using genetically modified plant hosts (HIGS) expressing siRNA (Jin et al. 2019, Song and Thomma 2018, Su et al. 2020 and Zhang et al. 2022) represents the best reservoir for initial gene targets screening in the less studied *V. longisporum*. Homologues of *VdClp-1* (Zhang Tao et al. 2016), *VdCYP1* (Zhang Dan-Dan et al. 2016) and *VdIC* (Protein ID VDAG_00647) (Su et al. 2020) in *V. longisporum* were selected for evaluating the available information from *V. dahliae* on gene functions, and to assess if a similar protection can be achieved through exogenous application of dsRNA.

The first selected gene target is a *Calpain-9* like protein (*VlClp-1*), which encodes a Calcium dependent cysteine protease. Zhang Tao et al. (2016) investigated the role of small RNAs in regulating *V. dahliae* pathogenesis on infected cotton plants through deep sequencing of total small RNAs isolated from *V. dahliae* (strain V592) grown on infected cotton plants (Xinluzao No.16). They identified *VdClp-1* as a target for cotton miRNA 166 and reported a reduced virulence mediated through *V. dahliae* mRNA cleavage. The second gene target investigated for limiting *V. longisporum* infection belongs to the Cytochrome P450 protein superfamily, known for being involved in diverse metabolic pathways and are actively involved in pathogenesis, making it a target for the commercially available fungicide family "Azoles". It was illustrated that *VdCYP1* is a pathogenesis related gene in cotton infections (Zhang Dan-Dan et al. 2016), where *VdCYP1* knock-out through T-DNA insertion mutant generation led to almost complete loss of virulence. Both genes are closest to the optimal required sizes for *in-vivo* dsRNA production in *P. syringae* and were therefore selected for molecular cloning of dsRNA production vectors. *VdIC* is the third gene target investigated through *in-planta* infection assay and *in-vitro* growth assay, it showed the lowest disease severity index among various gene targets targeted through HIGS (Su et al. 2020).

While HIGS approach provide a direct and consistent cellular supply of siRNAs through the host transcription machinery, SIGS approach faces a challenge to consistently deliver dsRNA, and might require more frequent application in order to reach the same protection efficacy and a sustained gene silencing effect. Thus, understanding the stability timeframe of exogenously applied dsRNA and the flexibility of application methods are crucial for developing SIGS based plant protectants.

The previous studies employing SIGS on *V. dahliae* (Qiao et al. 2021, Tao et al. 2025) relied on root dipping of seedlings in conidia solutions mixed with dsRNA targeting the gene of interest then transferring back to soil, which allows only a single application of dsRNA alongside inoculation before an infection is established. Therefore, more flexible approaches will be investigated to enable repeated dsRNA application for root pathogens, and simplify dsRNA detection procedures for dsRNA stability monitoring.

1.5 Aims of the study

This study aims to explore the potential use of dsRNA as an alternative approach to limit infections caused by *V. longisporum* using RNAi pathway, through assessing the effect of targeting different genes on the disease severity, in a patho-system with the model dicot plant *Arabidopsis thaliana*. This study provides data on dsRNA uptake in liquid fungal cultures and targeted down-regulation of endogenous genes in *V. longisporum*, as a function of different dsRNA molecules and delivery methods. The ability to limit fungal virulence was studied in a hydroponic system, which allows access to root tissues as a treatment site, as well as fungal biomass quantification after treatment with different forms of dsRNA (i.e. non-formulated vs. formulated). The study also provides novel approaches for high-throughput growth monitoring, aimed to accelerate the gene target selection process, and to evaluate the direct effects of different dsRNA sequences on *in-vitro* growth of *V. longisporum*. To this end, assessment of dsRNA stability and PTI effects after foliar spray application were investigated *in-planta*, using qRT-PCR and an immunoblotting approach optimized for a highly specific detection of intact dsRNA. These assays are meant to i) offer the basic tools needed to develop a non-toxic, degradable formulation that efficiently protects dsRNA from environmental degradation, ii) identify gene targets that directly limits the pathogen growth, and iii) identify the best application strategy to achieve maximal protection against *V. longisporum* infections.

Chapter II: Materials and Methods

2.1 Fungal isolates

Two strains of *Verticillium longisporum* were used. *Verticillium longisporum* wild type strain (Vl41) was provided by Prof. Andreas von Tiedemann (Georg-August-Universität Göttingen, Germany); it was isolated from the region of Mecklenburg-Vorpommern, Germany. *Verticillium longisporum* (Vl43) *GFP*, which exhibits a stable expression of *GFP* by *A. tumefaciens* mediated transformation, was transformed and provided by Prof. Andreas von Tiedemann as well (Eynck et al. 2007).

2.2 Growth Media for *V. longisporum*

The fungus was grown on potato dextrose agar (PDA, Formedium TM) plates. The liquid cultures were prepared in sterile Erlenmeyer flasks with one third fill on an orbitary shaker, at about 150-160 RPM for four to five days incubation at room temperature.

Xylem simulated medium (SXM) was later adopted for growth assay and *in-vitro* silencing experiments, prepared as previously described (Neumann 2003) including sodium polypectate 2 g/L, vitamin free casamino acids 4 g/L, KCl 0.52 g/L, $MgSO_4$ heptahydrate 0.52 g/L, KH_2PO_4 1.52 g/L, 0.1 µM biotin and 1x trace elements* (Bennett and Lasure, 1991).

*Trace elements were prepared as 1000x stock solution and added freshly to each batch of liquid medium (1 mL for each 1 L medium prepared)

Table 01. Trace elements components for SXM preparation

Trace elements 1000x	Weight (g)/100 mL
$ZnSO_4.7H_2O$	2.2 g
H_3BO_3	1.1 g
$MnCl_2.4H_2O$	0.5 g
$FeSO_4.7H_2O$	0.5 g
$CuCl_2.5\ H_2O$	0.16 g
$CuSO_4.5H_2O$	0.16 g
$(NH_4)_2Mo_7O_{24}.\ 4H_2O$	0.11 g
Na_2EDTA	5 g

Conidia isolation and counting: Liquid culture was filtered over sterile Miracloth placed in a sterilized funnel, the Miracloth was then pressed using a sterile glass rod and washed with 0.002% Tween H_2O. The flow through from PDB/SXM culture and 0.002% Tween 20 H_2O was centrifuged in 50 mL Falcon tubes for 10 min at 4000 RPM. The supernatant was then discarded, and conidia pellets were resuspended in a suitable volume of Tween H_2O. Hemocytometer was used for counting conidia and estimating the conidia/mL for each liquid culture. Cryo-cultures can be prepared using a 1:1 ratio of conidia solution and sterile 25% glycerol to be stored for longer durations in -80 °C.

2.3 dsRNA synthesis

In-vitro dsRNA synthesis was used for all the experiments using T7 Megascript RNAi kit (Thermofischer) following the manufacturer protocol, with the exception of fluorescently labelled dsRNA experiment where 35 % of UTP was replaced by Aminoallyl-PEG-Atto488 UTP (Jena biosciences) for confocal microscopy analysis. Shortly, DNA template for the gene of interest was amplified with primers containing flanking T7 promoter sequences (Supplementary information), followed by dsRNA synthesis using T7 polymerase and the relevant buffers/nucleotides mix (Table 02). The synthesised dsRNA was then visualised on 1% agarose gel to confirm correct product size, annealing and absence of unspecific amplification products. Purified dsRNA was aliquoted and stored in -80 °C to prevent any thaw/freezing degradation.

Table 02. Megascript RNAi reaction mix

Component	Amount
Nuclease-free Water	to 20 µL
Linear template DNA	1 µg
10X T7 Reaction Buffer	2 µL
ATP Solution	2 µL
CTP Solution	2 µL
GTP Solution	2 µL
UTP Solution	2 µL
T7 Enzyme Mix	2 µL

2.4 Fluorescently labelled dsRNA uptake evaluation

The uptake of fluorescently labelled dsRNA was evaluated through observation of the growing hyphae under confocal microscope (Leica, TCS SP8), green fluorescence of dsRNA labelled with A488 UTP was detect by filter AF488 (λexc494, λem515 nm). *V. longisporum* wild type strain Vl41 was used for this experiment, 500 conidia were aseptically added to 500 µL Potato dextrose broth (PDB) and 1 µg of labelled dsRNA was added after 24 h. To investigate whether the fluorescence signal observed was due to intracellular uptake of dsRNA, 100U of Micrococcal nuclease (MNase) were used to degrade all extracellular nucleic acids prior to microscopy, growing mycelia were centrifuged and the pellet was resuspended in MNase digestion buffer (50 mM Tris-HCl with pH 8.0 and 5 mM $CaCl_2$). Samples were checked at 6 and 24 h after dsRNA addition.

2.5 Gene expression analysis

For the gene expression analysis experiments, 6-well-plates were used to grow mycelia. Under sterile conditions 500 conidia in 2 mL SXM were added to each well. Hereafter, the plates were shaken at room temperature at 50 RPM to stimulate the *V. longisporum* conidia to grow mycelia for 3 days before adding dsRNA. The 6-well-plates were wrapped in aluminium foil to keep them in darkness. At harvesting timepoints the liquid medium and growing colonies from each well were transferred under aseptic conditions to 2 mL Eppendorf tubes, followed by centrifugation at 16,000 RPM for 10 min, the supernatant was discarded, and the remaining pellet was directly frozen in liquid nitrogen and stored at -80°C for further analysis.

2.6 Total RNA extraction

Frozen pellets were homogenized using mortar and pestle, followed by Trizol extraction using miniprep Total RNA extraction kit (Zymo research) following the kit protocol. 700 µL Trizol was added per sample, and the eluted total RNA was quantified using Nanodrop, and then aliquoted to prevent freeze/thaw cycles.

To ensure integrity of total RNA, an equivalent to 1 µg was loaded in 1% agarose gel and ribosomal RNA bands were visualised after gel electrophoresis at 100V for 45 min.

2.7 First strand cDNA synthesis

After the concentration of the RNA was measured using Nanodrop, the amount of mRNA to be reverse-transcribed could be determined. An equivalent of 2 µg of total RNA was placed in a PCR tube and then filled up with water to 11.5 µL. Afterwards, 1 µL oligo(dT) primer (0.5 µg; 100 pmol) was added. The sample was incubated at 65°C for 5 min to allow for primer binding, then samples were placed on ice. The following components were added to the sample in a next step: 5x Reaction Buffer 4 µL, Thermo ScientificTM RiboLock RNase Inhibitor (#EO0381) 0.5 µL (20 U), dNTP Mix 10 mM 2 µL, Revert Aid RT (Reverse Transcriptase) 1 µL (200 U). The samples were then incubated at 42°C for 60 min. Afterwards the reaction was terminated by heating at 70 °C for 10 min. The cDNA was brought to a concentration of 10 ng/µL by diluting it with nuclease free water and was then stored at -20°C.

2.8 RT-qPCR

cDNA was diluted to 10 ng/µL by adding 180 µL RNase free water, Master mix contains 17.5 µL SYBR green (Merck) ,3.15 µL gene specific primers, 5.6 µL H_2O and 8.75 µL cDNA, bringing it to a total of 35 µL, which was then distributed to three technical replicates of 10 µL each. RT-qPCR program had three steps; 1) Initial denaturation 95°C 5 min – 2) 40 cycles of: 95 °C for 30 sec, 60°C for 30 sec, 72°C for 20 sec – 3) Melt curve stage. Relative gene expression was calculated using ΔΔCt method, using *Actin* expression as a housekeeping gene (Livak and Schmittgen, 2001).

2.9 dsRNA detection using immunoblotting

Dot blot assay was established for the detection of dsRNA, using J2 monoclonal antibody (Jena bioscience) that specifically binds to dsRNA molecules longer than 40 bp, regardless of the dsRNA sequence or modification. Total RNA was diluted to 1 µg/8 µL and directly applied to a positively charged nylon membrane (Hybond™-N+ Amersham) and left to dry, after around 30 min no more drop marks were visible, and the membrane was crosslinked in a UV crosslinker (Biorad Gene linker) for 30 sec on 40 mj/sec^2. The membrane was then blocked in 5% low fat milk (Roth) in Tris buffered saline buffer (TBS-T) (20 mM Tris, 0.15 M NaCl and adjust pH to 7.6 using HCl, 0.1% Tween 20) for 1 h while rocking at low speed in a suitable sterile container.

The blocking solution was then discarded and replaced with the primary antibody solution, containing J2 mAB 1:2000 in 1% low fat milk in TBS-T for 1 h, while rocking at low speed. The membrane was thoroughly washed 3 times while rocking at low speed in 40 mL TBS-T, 5 min each followed by the addition of the secondary antibody solution, containing the secondary antibody Goat Anti-mouse IgG (Thermofischer scientific) 1:2000 in 1% low fat milk in TBS-T for 1 h while rocking at low speed. The membrane was thoroughly washed 3 times while rocking at low speed in 40 mL TBS-T, 5 min each before visualising signals using enhanced chemiluminescence kit (ECL Amersham), signal generation and imaging were done using Chemidoc MP (Biorad) with multiple images taken on exposure between 60-120 sec. For dsRNA size detection, the protocol for the detection of viral dsRNA (Poynter and DeWitte-Orr 2017) was adopted with some modifications. Total RNA was separated by gel electrophoresis on 12% native polyacrylamide gel (600 µL 10x TBE, 100 µL 10% APS, 5 µL TEMED, 4 mL ddH2O, 2 mL Acrylamide/Bis-solution 30 (29:1)) for 120 min and 120V in 1xTBE buffer. Following the gel electrophoresis, RNA was transferred to the positively charged nylon membrane (Hybond™-N+ Amersham) using electric transfer with 400 mA (limit voltage 25V) for 45 min, the membrane was carefully placed between 2 sets of 4 layers Whatman filter paper, followed by UV crosslinking for 30 sec on 40 mj/sec^2.

The membrane was then transferred to a suitable container for blocking in 5% skimmed milk in TBS-T buffer for 1 h and gentle rocking, followed by rinsing with TBS-T for three times. J2 mAB was diluted 1:2000 in TBS-T with 2% BSA and incubated overnight at 4°C on a rocking platform set to a low speed. Primary antibody solution was removed and could be collected for reuse, followed by rinsing 3 times with TBS-T. Secondary antibody, goat-anti mouse IgG HRP, 1:2000 in 5% skim milk TBS-T was added for 1 h on a rocking platform set to a low speed at room temperature. Signal was visualised using enhanced chemiluminescence kit (ECL Amersham), signal imaging was done using Chemidoc MP (Biorad) with multiple images taken on exposure between 60-120 sec.

2.10 Growth assay in 96-well-plate

The growth assay was developed to assess direct effects of dsRNA on conidial germination and viability using *GFP* fluorescence signal intensity over time. For this purpose, *V. longisporum GFP* (Vl43) was used to evaluate growth curves over the time period showing high correlation coefficient (R^2) between number of starting conidia and the observed signal. Black 96-well-plates with clear bottom (Thermofischer scientific) were used to offer best *GFP* fluorescence intensity measurement. Each treatment group consisted of six replicates with the same components and each well was measured in four spots to estimate bottom cover in a consistent manner. Xylem simulated medium (SXM) was selected as it offered the least background fluorescence and did not interfere with *GFP* fluorescence intensity measurement. 100 *V. longisporum GFP* conidia in 200 µL/well final volume was used for evaluation of the selected dsRNA gene targets, for each group the blank measurement was done on adjacent wells containing only the growth medium and the relevant dsRNA, where the final fluorescence intensity values used were after subtraction of these blank values. The plates were sealed with parafilm and covered with aluminium foil, to prevent evaporation and keep optimal dark conditions for growth respectively. *GFP* fluorescence intensity was measured daily at the same time using Tecan plate reader infinite 200 pro, with the following parameters: Multiple Reads per Well 2*2 (Border) 500 µm, Excitation

Wavelength: 485 nm, Emission Wavelength: 535 nm, Excitation Bandwidth: 9 nm, Emission Bandwidth: 20 nm, Gain: 189 Optimal (100%), Number of Flashes: 25, Integration Time: 100 µs, Lag Time: 0 µs, Settle Time: 0 ms.

2.11 Hydroponic infection assay

A. thaliana Col-0 sterile seeds were sowed in rockwool blocks, and were vernalized for 48 h at 4°C, using half strength hydroponic solution for the first week, and full strength for all remaining weeks. Root growth took around four to five weeks to allow for treatment and infection through root dipping, dsRNA was diluted in 50mL DEPC water for root treatment or directly sprayed on leaves. The infection was initiated by root dipping in $100*10^6$ *V. longisporum* conidia solution overnight, followed by adding fresh hydroponic solution on weekly basis. Roots and leaves could be harvested at many timepoints (weekly) without drastically affecting plant growth, however to keep the conditions equivalent in all groups, whole root and rosettes were harvested at the last screening timepoint for genomic DNA quantification.

Seed sterilization:

A. thaliana Col-0 seeds were surface-sterilized using sequential incubations in 70% (v/v) ethanol, 5% (v/v) hypochlorite solution and then washed at least 5 times with sterile water.

Growing conditions in growth chamber:

- Temperature day/night: 22°C/18°C
- light intensity: 50%
- day/night rhythm: 8h/16h

Hydroponic solution preparation:

Hydroponic solution was prepared according to Gibeaut et al. (1997) by mixing three different groups of solutions.

For preparing 1 litre of each group, the following components were required:

Table 03. Hydroponic solutions components

Group	Ingredient	Concentration (g/L)
Group I	H_3BO_3	0.48 g
	$MnCl_2$	0.3 g
	$ZnSO_4$	0.087 g
	$CuCl_2$	0.039 g
	$(NH_4)_6Mo_7O_{24}$	0.015 g
	Fe-EDTA-Na	3.966 g
	$MgSO_4$	13.55 g
Group II	KCl	0.57 g
	KNO_3	18.96 g
	KH_2PO_4	10.20 g
Group III	$Ca(NO_3)_2$	53.16 g

In each of the three solutions, Sterile Milli-Q water was added up to 1 L and then stored at 4°C. To obtain 1 L of full-strength hydroponic solution, 6.6 mL of each group were mixed. Instead, for the half-strength hydroponic solution 3.3 mL of each group were added together.

2.12 Genomic DNA extraction

Doyle & Doyle method was used to extract genomic DNA from roots/rosettes (Doyle 1991). Extraction buffer contains 100 mM Tris-HCl (pH 8.0), 20 mM EDTA (pH 8. 0), 1.4 M NaCl, 2% Cetyltrimethylammonium Bromide (CTAB), 1% $Na_2S_2O_5$ and 0.2% β-Mercaptoethanol was added freshly before each extraction. The frozen plant material was first homogenized using mortar and pestle in the presence of liquid nitrogen, the homogenized powder was then aliquoted to 0.4 mg aliquots in 2mL Eppendorf tubes. The extraction buffer was heated to 65°C beforehand, and 700 µL were added to each sample and mixed carefully by swirling or tilting gently before incubation for 30 min in a water bath at 65°C.

Afterwards, 700 µL Chloroform/Isoamyl alcohol 24:1 (CIA) was added and carefully swirled or tilted for 5 min, then centrifuged at 10,000 RPM and 4°C for 15 min. The aqueous (upper) phase was transferred to a new 2mL Eppendorf tube and 600 µL CIA was added.

The tubes were gently swivelled overhead for 5 min and centrifuged at 10,000 RPM at 4°C for 15 min. The aqueous phase was transferred to a new 2mL Eppendorf tube, and 50 µL of 10M NH_4OAc and 60 µL of 3M NaOAc (pH 5.5) were added and mixed by tilting. 500 µL isopropanol (2-propanol) was added and mixed carefully by tilting or swirling and the DNA was allowed to precipitate on ice for 1.5–2 h. The samples were then centrifuged at max. speed (13,000-14,000 RPM) for 10 min in a benchtop centrifuge and all liquid was carefully discarded.

The remaining pellet was washed by adding 500 µL of 70% EtOH/10 mM NH_4OAc and incubated for 10 min to remove salts, centrifuged for 10 min on max. Speed (13,000-14,000 RPM) in benchtop centrifuge and all liquid supernatant was carefully discarded. To dry the pellet, the samples were left with open lid under the flow hood until the pellet was clear, when the residual alcohol has completely evaporated, the pellet was resuspended in 100 µL nuclease free water.

2.13 Disease severity index

Using the images taken weekly, ImageJ analysis was done to estimate the percentage of leaves showing chlorosis symptoms by estimating the ratio between yellow area pixels (colour threshold to 50) to the overall green area (colour threshold to 120), the levels of disease severity estimation were adopted from Zhao et al. 2012 and was recorded as follows: Disease severity was divided into five classes using a disease score ranging from 0 to 5 as follows: 0 = no symptoms, 1 = less than 10% of leaves showing chlorosis and wilt, 2 = 10-25% of leaves displaying chlorosis and wilt, 3 = 25-50% of leaves displaying chlorosis and wilt, 4 = 50-75% of leaves displaying chlorosis and wilt, 5=>75% of leaves displaying chlorosis and wilt.

The area under the disease progress curve (AUDPC) was calculated based on the trapezoidal rule for area under the curve estimation method of Zhao et al. 2012:

$$\mathrm{AUDPC} = \sum_{i=1}^{n-1} \left[\left(\mathrm{DS}_i + \mathrm{DS}_{i+1} \right) /2 \right] \left(t_{i+1} - t_i \right)$$

where t is the number of days post inoculation, DS is the disease severity level caused by *V. longisporum*, and n is the total number of assessments.

2.14 Foliar spray of dsRNA for stability and PTI response evaluation

Four-week-old *A. thaliana* Col-0 plants were used to assess gene expression changes and dsRNA stability after foliar spray of dsRNA and chitosan-based formulations. 20 µg of 500 bp dsRNA was diluted in nuclease free water to a total volume of 1.5 mL and sprayed using 5 mL spray bottles. Two leaves were harvested from each plant at selected timepoints, one leaf was directly frozen in liquid nitrogen until further analysis, while the other was washed thoroughly under running water for 30 sec before freezing in liquid nitrogen. Leaves were homogenized using tissuelyser (Retsch) after adding 2 sterile glass beads for 60 sec at 30 Hz, then returned in liquid nitrogen before total RNA extraction as previously described.

2.15 Molecular cloning of dsRNA production vectors

A. **PCR amplification of target fragment:**

Gene target sequences were retrieved directly from NCBI database (National Center for Biotechnology Information (nih.gov)) if annotated in *V. longisporum* Vl43, otherwise *V. dahliae* annotated sequences was used as a query in BlastN suite (Nucleotide BLAST: Search nucleotide databases using a nucleotide query (nih.gov) to identify the corresponding sequence in *V. longisporum*. After confirming that the selected restriction sites were not present in the gene target insert fragment, Phusion polymerase (New England Biolabs) 50 µL reactions were used to amplify the target fragment, using primers containing the desired restriction sites.

Upon successful amplification and after confirming a single band of correct size on 1% agarose gel, the PCR product was purified using Wizard DNA clean up kit (Promega) following the kit protocol.

B. **Restriction reaction:**

Vectors used for dsRNA production where pMS2 and pLD18 carrying ampicillin resistance gene, the intended gene target fragment was inserted in the MCS located between a T7 polymerase promoter sequence and a T7 transcription termination site. 2 µg of empty vector or 1 µg of PCR fragment was used as a template in the following reaction and incubated for 2 h at 37 °C, followed by 10 min incubation at 65 °C for enzyme deactivation. The whole reaction product was loaded on 0.7% agarose gel and correct bands of restricted products were cut into gel slices, followed by purification of the restricted product using Wizard clean up kit (Promega) and concentration measurement using Nanodrop.

Table 04. Plasmid restriction reaction components

Nuclease free H_2O	to 50 µL
Template	≈1 µg
10x Fast digest buffer	5 µL
Restriction enzyme I (fast digest)	2 µL
Restriction enzyme II (fast digest)	2 µL
Total	50 µL

C. **Ligation:**

A ratio of 1:3 Vector: insert was found to be optimal for ligation, and exact amounts to be added can be calculated based on vector and insert size in bp. After adding all components from the table below, the reaction mix was incubated overnight at 16°C.

Example: for 4 kb insert (*VlClp-1* 4kb) in pMS2 (3.6 kb)

Table 05. Plasmid ligation reaction components

Ligation reaction components	Volume (µL)
Insert (after restriction and clean up)	330 ng
Vector (after restriction and clean up)	100 ng
10x ligation buffer	2 µL
T4 Ligase	1 µL
Nuclease free H_2O	to 20 µL
Total	20 µL

D. **Heat shock transformation:**

DH5α competent cells were used for heat shock transformation. 100 µL of DH5α cells were incubated with 5 µL Ligation product on ice for 10 min, the mixture was then transferred to a pre-heated heat block at 42°C for 45 sec and then returned to ice for 2 min. 1 mL of LB medium was added (no antibiotics included) and was incubated at 37°C for 1 h. 100 µL from each transformation reaction was then transferred to LB ampicillin plates in sterile conditions and incubated at 37°C for 16 h.

Ligation controls: restricted vector (Restriction confirmation) – unrestricted vector (Transformation confirmation) – Restricted/ligated empty vector (Ligation confirmation).

E. **Colony selection and confirmation:**

Growing single colonies were picked using sterile pipette tips for streaking LB ampicillin plates and the rest were suspended in 50 µL nuclease free H_2O. Streaking plate can be used for later propagation of correctly transformed/ligated plasmids. Colony PCR was used for selecting colonies carrying the correct plasmid, using Taq. Polymerase PCR reaction with M13 or insert specific primers, initial denaturation step was carried out at 95°C for 10 min, followed by 32 cycles (10 sec 95°C, 30 sec 55°C and 30 sec at 72°C) and 5 min at 72°C.

Table 06. Colony PCR reaction components

Colony PCR reaction	Volume (µL)
Nuclease free H_2O	7.5
Template (colony suspension)	5
10x buffer	2
25 mM $MgCl_2$	1.6
Forward primer	1
Reverse primer	1
Taq polymerase	0.3
dNTPs	1.6
Total	20

2.16 dsRNA off-target analysis in *A. thaliana* Col-0 and *B. napus*

dsRNA sequences used for targeting *V. longisporum* genes of interest were checked for potential off-targets using "*pssRNAit: Designing Effective and Specific Plant RNAi siRNAs with Genome-wide Off-target Gene Assessment"* (Ahmed et al. 2020), the open access online tool (https://www.zhaolab.org/pssRNAit/Home.gy) offers analysis of template sequences – between 30 and 15,360 nt in length – to predict the number of possible siRNAs and off-target analysis in various plant and fungi species. Default parameters were used to have a wider estimate of all possible matches, with a maximum of 20 off targets for each predicted siRNA.

Materials

Table 07. Chemicals and reagents

Material	Chemical Ref. No	Manufacturer
1kb Plus DNA Ladder	10787018	Thermo Fisher Scientific Inc., Lithuania
2-Mercaptoethanol	4227.3	Carl Roth GmbH, Germany
2-propanol	6752.3	Carl Roth GmbH, Germany
6x Purple Loading Dye	#B7024S	New England Biolabs, Inc., USA
Agarose	50004	BMA Products, Rockland, USA
Amersham Hybond™-N+	GERPN203B	Cytiva, USA
Aminoallyl-UTP-ATTO-488	NU-821-488	Jena Bioscience GmbH, Germany
Ammonium acetate	7869.2	Carl Roth GmbH, Germany
Ammonium heptamolybdate tetrahydrate	7311.1	Carl Roth GmbH, Germany
Ammonium Peroxodisulfate (APS)	9592.3	Carl Roth GmbH, Germany
Ampicillin sodium salt	HP62.1	Carl Roth GmbH, Germany
Anti-dsRNA monoclonal antibody J2	RNT-SCI-10010200	Jena Bioscience GmbH, Germany
Biotin	B4501	Sigma Aldrich - Merck KGaA., Germany
Boric acid	6943.3	Carl Roth GmbH, Germany
Bovine serum albumin (BSA)	3737.1	Carl Roth GmbH, Germany
$Ca(NO_3)_2$	P740.2	Carl Roth GmbH, Germany
$CaCl_2$	C5670	Sigma Aldrich - Merck KGaA., Germany
Casamino acids vitamin free	AE41.1	Carl Roth GmbH, Germany
Cetyltrimethylammonium Bromide	9161.1	Carl Roth GmbH, Germany
Chloroform	6340.2	Carl Roth GmbH, Germany
$CuSO_4$	CP86.1	Carl Roth GmbH, Germany
DEPC	K028.1	Carl Roth GmbH, Germany
dsRNA ladder	N0363S	New England Biolabs, Inc., USA
EDTA Disodium Salt	8043.2	Carl Roth GmbH, Germany
Ethanol	9065.4	Carl Roth GmbH, Germany
Ethidium Bromide Solution	2218.1	Carl Roth GmbH, Germany
Fe-EDTA-Na	6498.2	Carl Roth GmbH, Germany
Glass Beads	HH56.1	Carl Roth GmbH, Germany
Goat anti-Mouse IgG	31430	Thermo Fisher Scientific Inc., Lithuania

H_3BO_3	6943.3	Carl Roth GmbH, Germany
HCl	6792.2	Carl Roth GmbH, Germany
Isoamyl alcohol	T870.1	Carl Roth GmbH, Germany
Isopropanol	AE73.2	Carl Roth GmbH, Germany
KCl	6781.1	Carl Roth GmbH, Germany
KH_2PO_4	3904.1	Carl Roth GmbH, Germany
KNO_3	P021.2	Carl Roth GmbH, Germany
LB medium	X968.1	Carl Roth GmbH, Germany
LB Medium+ Agar-Agar	6494.4	Carl Roth GmbH, Germany
$MgSO_4$	0261.1	Carl Roth GmbH, Germany
$MgSO_4.7\ H_2O$	P027.2	Carl Roth GmbH, Germany
Micrococcal Nuclease Solution	88216	Thermo Fisher Scientific Inc., Lithuania
$MnCl_2$	T881.1	Carl Roth GmbH, Germany
NaCl	9265.2	Carl Roth GmbH, Germany
PDA medium	PDA0102	FORMEDIUM LTD, England
PDB medium	PDB0102	FORMEDIUM LTD, England
ROTIPHORESE®NF	A124.2	Carl Roth GmbH, Germany
Skimmed milk powder	T145.2	Carl Roth GmbH, Germany
Sodium acetate	3856.5	Carl Roth GmbH, Germany
Sodium Hydroxide	6771.1	Carl Roth GmbH, Germany
Sodium hypochlorite - NaOCl	9062.1	Carl Roth GmbH, Germany
Sodium metabisulphite $Na_2S_2O_5$	8554.1	Carl Roth GmbH, Germany
Sodium polypectate	P3850	Sigma Aldrich - Merck KGaA., Germany
Tetramethylethylenediamine	2367.3	Carl Roth GmbH, Germany
Tris	5429.3	Carl Roth GmbH, Germany
Tris-HCl	9090.4	Carl Roth GmbH, Germany
Trizol	15596018	Thermo Fisher Scientific Inc., Lithuania
TWEEN 20	9127.1	Carl Roth GmbH, Germany
$ZnSO_4$	2293.1	Carl Roth GmbH, Germany

Table 08. Buffers and Growth media

Buffers & Solutions Components	**Ingredient**	**Final concentration**	**Catalog No.**	**Manufacturer**
TBE 10x buffer	Tris	1 M	5429.3	Carl Roth GmbH, Germany
	Boric acid	1 M	6943.3	Carl Roth GmbH, Germany
	EDTA Disodium Salt	20 mM	8043.2	Carl Roth GmbH, Germany
DNA extraction buffer pH 8.0	Tris-HCl	100 mM	5429.3	Carl Roth GmbH, Germany
	NaCl	1.4 M	9265.2	Carl Roth GmbH, Germany
	EDTA Disodium Salt	20 mM	8043.2	Carl Roth GmbH, Germany
	$Na_2S_2O_5$	1%	8554.1	Carl Roth GmbH, Germany
	β-Mercaptoethanol	0.20%	4227.3	Carl Roth GmbH, Germany
	Cetyltrimethylammonium Bromide	2.00%	CN30.3	Carl Roth GmbH, Germany
TWEEN water	TWEEN 20	0.002%	9127.1	Carl Roth GmbH, Germany
PDA medium	Potato Dextrose Agar	4.1 % (w/v)	PDA0102	FORMEDIUM LTD, England
PDB medium	Potato Dextrose Broth	2.4 % (w/v)	PDB0102	FORMEDIUM LTD, England
LB medium	LB Broth	2.5% (w/v)	X968.1	Carl Roth GmbH, Germany
LB-Agar Amp.	LB Medium+ Agar-Agar	1.5 % (w/v)	6494.4	Carl Roth GmbH, Germany
	Ampicillin sodium salt	50 µg/ml	HP62.1	Carl Roth GmbH, Germany

Table 09. Kits

Kit	Ref. No / Cat. No	Manufacturer
DCSPol DNA Polymerase	DPT-500	DNA Cloning Service eK, Germany
Direct-zol RNA Miniprep Plus	R2070, R2071, R2072, R2073	Zymo Research Europe, Germany
FastDigest NheI	FD0974	Thermo Fisher Scientific Inc., Lithuania
FastDigest PstI	FD0614	Thermo Fisher Scientific Inc., Lithuania
FastDigest SacI	FD1133	Thermo Fisher Scientific Inc., Lithuania
MEGAscript™ RNAi-Kit	AM1626	Invitrogen/ Thermo Fisher Scientific Inc., Lithuania
Monarch® Plasmid Miniprep Kit	NEB #T1010S/L	New England Biolabs, Inc., USA
Phusion High-Fidelity DNA Polymerase	#M0530L	New England Biolabs, Inc., USA
RevertAid Reverse Transcriptase (200 U/µL)	#EP0441	Thermo Fisher Scientific Inc., Lithuania
SYBR® Green JumpStart™ Taq ReadyMix™	S4438	Merck KGaA., Germany
T4 DNA Ligase (5 U/µL)	EL0011	Thermo Fisher Scientific Inc., Lithuania
TURBO DNA-free™ Kit	AM1907	Invitrogen/ Thermo Fisher Scientific Inc., Lithuania
Wizard PCR product clean-up kit	A9282	Promega, Germany

Table 10. Consumables and equipment

Article	Ref. No / Cat. No	Manufacturer
384-well microtiter plate	HSP3805	Bio-Rad Laboratories GmbH, Germany
96-Well Plate - Black - transparent bottom	165305	Thermo Fisher Scientific Inc., Lithuania
Blue Cap Bottle	C78.7	Carl Roth GmbH, Germany
Confocal microscope	TCS SP8	Leica Mikrosysteme Vertrieb GmbH, Germany
Electrophoresis gel chamber	Sub-Cell Model 192 Cell	Bio-Rad Laboratories GmbH, Germany
Electrophoresis power supply	PowerPac™ Basic Power Supply #164-5050	Bio-Rad Laboratories GmbH, Germany
Eppendorf Centrifuge Tabletop Centrifuge	5417R	Eppendorf AG, Hinz GmbH, Germany
Eppendorf tubes▪ SafeSeal micro tube, 2ml	PP 72.695.500	Sarstedt AG & Co. KG, Germany
Erlenmeyer flasks	PC49.1	Carl Roth GmbH, Germany
Falcon Centrifuge	5810 R	Eppendorf AG, Hinz GmbH, Germany
Falcon tubes	50 ml:227 261 / 15 ml: 188271-N	Greiner BIO-ONE GMBH, Germany
Fuchs Rosenthal Chamber	T731.1	Carl Roth GmbH, Germany
Glass slides	H 876	Carl Roth GmbH, Germany

Glass slips	AA00000102E01 MNZ10	Gerhard Menzel GmbH, Germany
Heat Block MHR	11 8 107	HLC BioTech, Germany
Heidolph UNIMAX 2010	542-10020-00	MAGV, Germany
INFORS HT Ectron shaker	14595	Infors AG, Switzerland
Lab microscope	H 600 PH	Plan Helmut Hund GmbH, Germany
Macroplate, 6-well	657102	Greiner BIO-ONE GMBH, Germany
Miracloth	475855-1R	Merck KGaA., Germany
Parafilm	H666.1	Carl Roth GmbH, Germany
PCR cycler	T100 Thermal Cycler #1861096	Bio-Rad Laboratories GmbH, Germany
PCR SingleCap 8er-SoftStrips 0.2 ml	710980	Biozym Scientific GmBH, Germany
Petri dishes	633180	Greiner BIO-ONE GMBH, Germany
Photo-spectrometer	6135CO501556	Eppendorf AG, Hinz GmbH, Germany
Pipette tips (10/100/1000 µl)	775350/ 771350/777350	Greiner BIO-ONE GMBH, Frickenhausen, Germany
Plate reader	infinite 200 pro	Tecan Austria GmbH
qPCR Machine QuantStudio 5 Real-Time PCR Instrument (384-Well Block)	A28135	Thermo Fisher Scientific Inc., Lithuania (Applied Biosystems)
Rotor	F45-30-11	Eppendorf AG, Hinz GmbH, Germany
Rotor	A-4-62	Eppendorf AG, Hinz GmbH, Germany
Tissuelyser II	9003240	Retsch/Qiagen, Germany
Trans-Blot Turbo	1704150	Bio-Rad Laboratories GmbH, Germany
UV Cross linker	Gene linker	Bio-Rad Laboratories GmbH, Germany
UV Transilluminator	Chemidoc MP	Bio-Rad Laboratories GmbH, Germany
Vortexer MS1	3.004092	IKA-Works, INC. US

Chapter III. Results

3.1 Uptake of labelled dsRNA in liquid cultures

To assess the ability of *V. longisporum* to uptake exogenously added dsRNA molecules, *V. longisporum* Vl41 was grown in liquid medium (PDB) for 24 h at room temperature, and low speed orbitary shaking. Labelled dsRNA was synthesized by *in-vitro* transcription of T7 promoter sequence containing templates with the addition of fluorescently labelled Uracil triphosphate (Figure 01.B Aminoallyl-UTP-Atto488). Labelled dsRNA was added to the liquid cultures and growing colonies were observed at 6 and 24 h after dsRNA addition (Figure 01.A). Micrococcal nuclease (MNase) was used to evaluate the nature of the observed signal, whether it is only extracellular attachment to the cell wall or intracellular uptake is taking place as well. In theory, MNase should degrade all kinds of extracellular nucleic acids after 30 min incubation at 37 °C. Accumulation of fluorescence signal was observed in treated samples after 6 h of treatment and was still visible after 24 h with lower intensity, implying the processing or degradation of labelled dsRNA over time. The fluorescence signal was still present after treatment with MNase (100U) suggesting that the observed fluorescence is not entirely extracellular. Aminoallyl-UTP-Atto488 did not show any accumulation of fluorescence when applied to growing colonies, even at 10 times the concentration used for dsRNA labelling, which confirms that the observed fluorescence is from intact labelled dsRNA molecules and not an unspecific fluorescence from the fluorescently labelled nucleotides on their own. These results confirm the ability of *V. longisporum* to uptake exogenously applied dsRNA and go in line with previous reports from the closely related strain *V. dahliae* (Qiao et al. 2021).

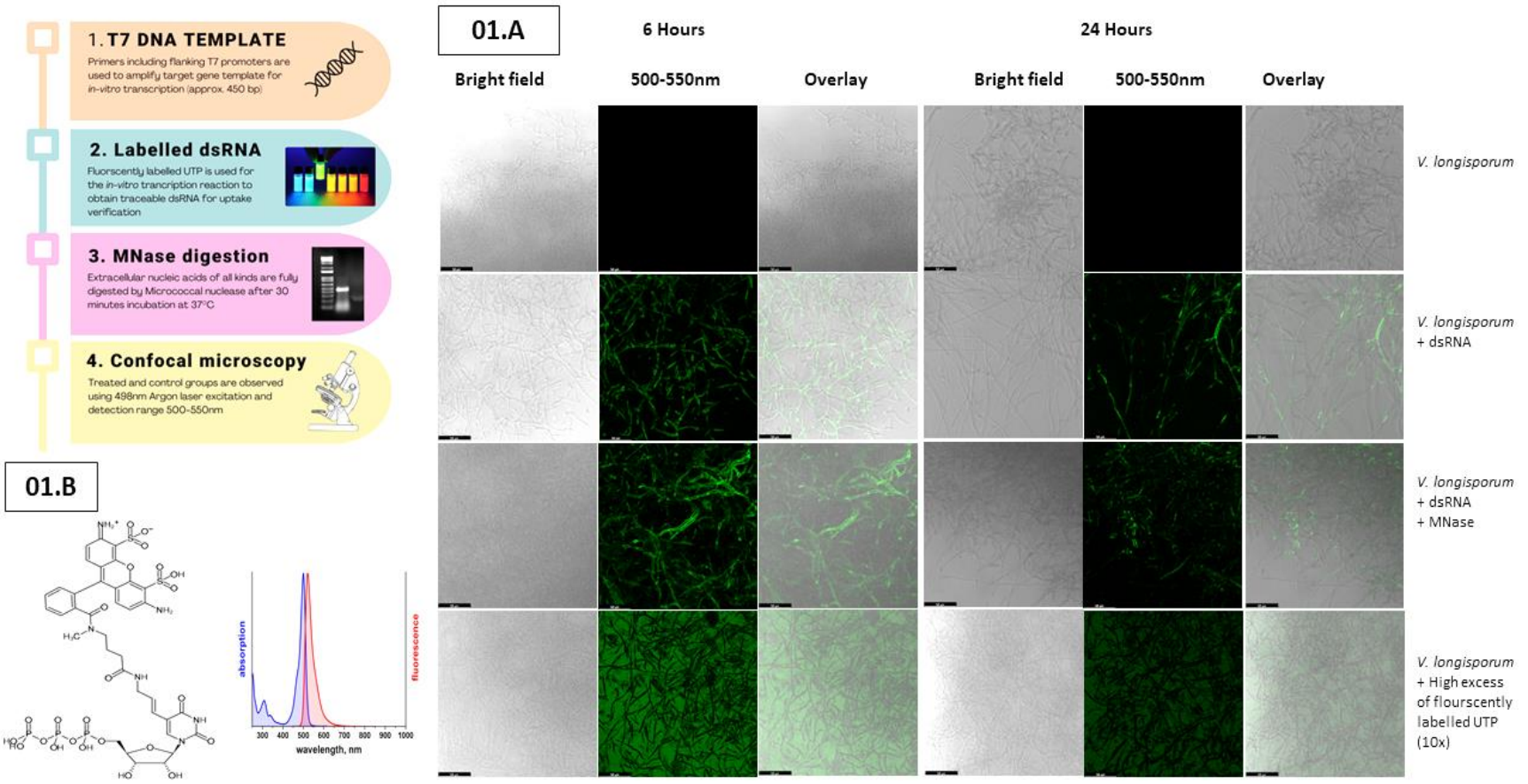

Figure **01.A** CLSM images from different channels of *V. longisporum* wild type (Vl41) mycelia captured at 6 and 24 h after addition of fluorescently labelled dsRNA (476 bp), scale bar is 50 µm. **01.B** Chemical structure and excitation/emission spectra of fluorescently labelled nucleotides (Aminoallyl-UTP-ATTO-488).

3.2 *In-vitro* gene silencing

3.2.1 *In-vitro* silencing of green fluorescence protein (*GFP*) expression in genetically modified *V. longisporum*

V. longisporum expressing *GFP* (Eynck et al. 2007) was used to assess gene silencing effects using 476 bp long dsRNA targeting the *GFP* sequence. *GFP* transcripts are expressed constitutively due to the 35S promoter used in the transformation of Vl43 wild type strain, thus offering a stable baseline expression needed to assess the effect of the applied dsRNA on the *GFP* transcript levels via post transcriptional gene silencing (PTGS). The level of *GFP* gene expression was estimated using RT-qPCR primers amplifying a 120 bp fragment of *GFP*, outside of the region targeted by dsRNA to avoid any unspecific amplification products. In a time-course *in-vitro* feeding experiment, the relative expression of *GFP* gene normalized to *V. longisporum Actin, GFP* showed a downregulation trend with a statistically significant reduction of *VlGFP* transcript levels at 72 hpt (Figure 02.A).

3.2.2. *In-vitro* silencing of endogenous gene targets in *V. longisporum*

3.2.2.1 *VlClp-1*

Following the confirmation of exogenously applied dsRNA uptake and targeted *GFP* silencing in *V. longisporum* expressing *GFP,* endogenous gene targets were selected for further evaluation of RNAi as a protectant against *V. longisporum*. Gene targets were adopted from the more widely studied and closely related species *V. dahliae* in HIGS reported experiments. Two gene targets were selected for further investigation of target gene silencing and infection assay.

The possible homologue of *VdClp-1 in V. longisporum* Vl43 was identified using BLASTP function on NCBI, showing a high similarity (98.5% identity) and annotated as Calpain-9 like protein with a sequence ID KAG7110543.1. The retrieved nucleotide sequence was used to identify regions predicted to contain the most siRNA candidates and a similar size of dsRNA

(≈476 bp) was selected for gene silencing assessment. Relative gene expression analysis of *VlClp-1* in liquid cultures revealed a similar down-regulation trend to *GFP* silencing (Figure 02.B), where a significant reduction of *VlClp-1* transcripts was reached after dsRNA treatment by 72 h, suggesting that this time frame represents the time needed for dsRNA uptake, processing and RNAi activation following their application to the liquid culture medium.

3.2.2.2 *VlCYP1*

The homologue of *VdCYP1* was identified in *V. longisporum* Vl43 and showed a high degree of sequence similarity (98%) with nucleotide sequence ID KAG7125432.1. The nucleotide sequence was used to design dsRNA construct with 471 bp length, in the region of coding sequence predicted to produce the highest number of siRNAs, predicted by sequence analysing open-source tools. Relative gene expression analysis of *VlCYP1* showed a similar down-regulation trend with statistically significant reduction achieved after 72 h (Figure 02.C).

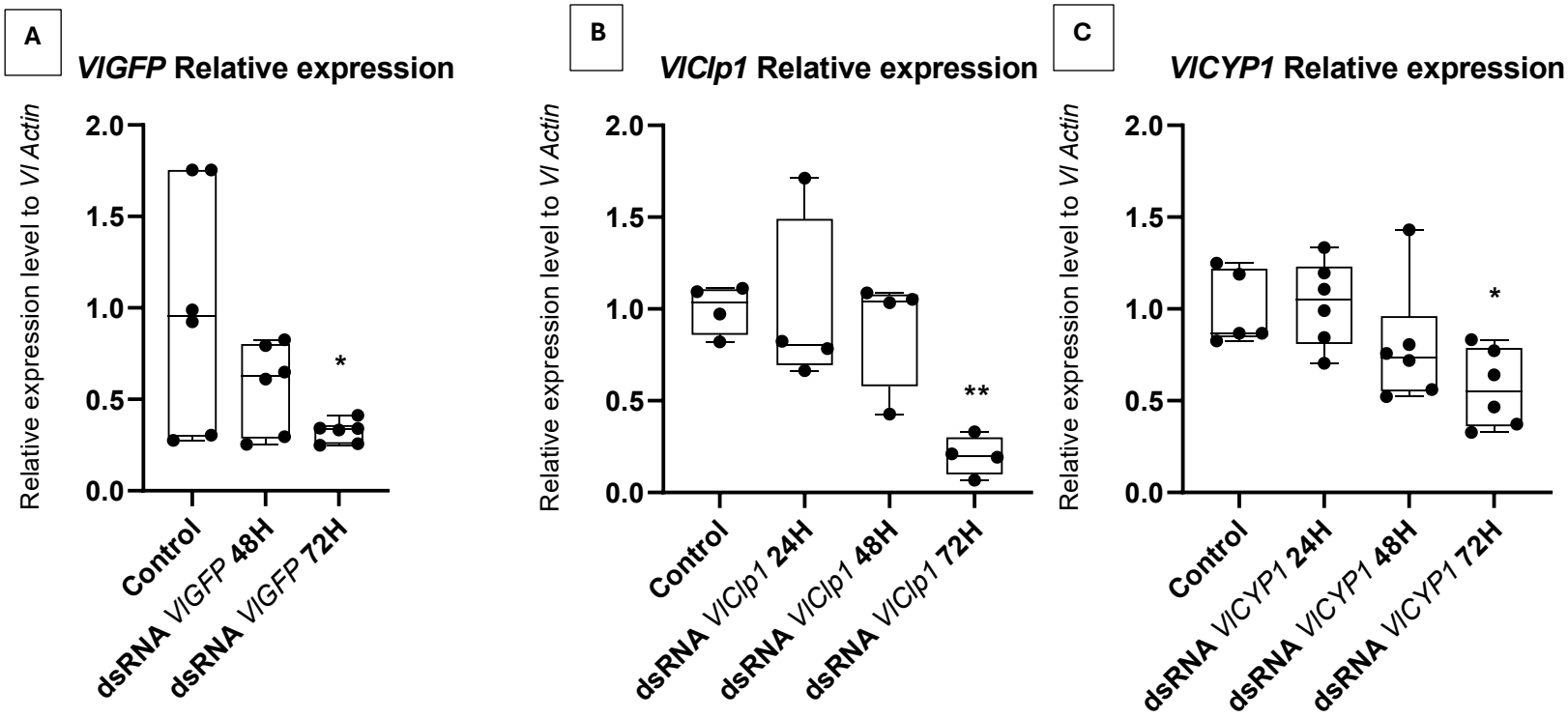

Figure 02. Relative gene expression of target genes after dsRNA targeting (**A.** *VlGFP* **B.** *VlClp-1* **C.** *VlCYP1*) were added to *V. longisporum* liquid cultures, 1 µg dsRNA was added to each replicate with a final concentration of 0.5 ng/µl, and growing colonies were harvested in the selected timepoints (24, 48, 72 h). *VlActin* was used as a housekeeping gene for normalization of Ct values obtained from qRT-PCR analysis, and relative gene expression was calculated according to ΔΔCt method. Statistical significance was analysed with one-way ANOVA for 6 biological replicates (*VlGFP/VlCYP1*) or 4 biological replicates (*VlClp1)*, error bars represent standard deviation (SD) and stars demonstrate statistical significance from the control (* p≤0.05, ** p≤0.001) according to Dunnett test.

3.3 Infection assay (soil/hydroponic)

3.3.1 Assessment of *V. longisporum* infections in soil grown *A. thaliana* plants

To evaluate the severity of *V. longisporum* infections on *A. thaliana*, Col-0 plants grown in soil were uprooted after two weeks from germination. Infection was done through root dipping in a Tween20 water 0.002% w/v solution containing *V. longisporum* Vl43 conidia, adjusted to $1*10^6$ conidia/ml or $3*10^6$ conidia/ml for 30 min, then returned back to soil. Infection symptoms like chlorosis could be observed 2 weeks post infection and increased after the third week post inoculation. *V. longisporum* gDNA could be detected in the infected leaves by using PCR primers amplifying 300 bp fragment of *VlCYP1* gene after 2 weeks, however the same detection of *V. longisporum* gDNA could not be achieved in gDNA extracted from infected roots (Figure 03), thus limiting the possibility of quantitative analysis of root infection severity through gDNA quantification, most likely due to the known inhibitory effect of soil particles on PCR amplification reactions (Schrader et al. 2012). Beside the limitation of detection to leaves only without further purification of gDNA extracted from root tissue, this approach was found to be time consuming and introduces abiotic stresses associated with uprooting and root dipping for a long duration. The results confirm the ability of *V. longisporum* to infect *A. thaliana* plants in the used concentrations and growing conditions, as well as the possibility to monitor infections in the leaves starting from second week post infection.

Table 01. Samples loaded to 1% agarose gel in **figure 03,** *A. thaliana Actin* primers were used to check the integrity of gDNA extracted from roots and leaves, *V. longisporum CYP* primers were used to track infection progression.

Gel lane #	Sample (*A. thaliana Actin* primers)	Sample (*V. longisporum CYP* primers)
1-4	Leaf samples from 1st infection group (Uninfected)	
5	Root sample from 1st infection group (Uninfected)	
6-9	Leaf samples from 2nd infection group (Infected using $1*10^6$ conidia)	
10	Root sample from 2nd infection group (Infected using $1*10^6$ conidia)	
11-14	Leaf samples from 3rd infection group (Infected using $3*10^6$ conidia)	
15	Root sample from 3rd infection group (Infected using $3*10^6$ conidia)	
16	Positive control (gDNA *A. thaliana*)	Positive control (gDNA *V. longisporum*)
17	Negative control (gDNA *V. longisporum*)	Negative control (gDNA *A. thaliana*)
18	No template control (NTC)	
L	1 kb-plus ladder	

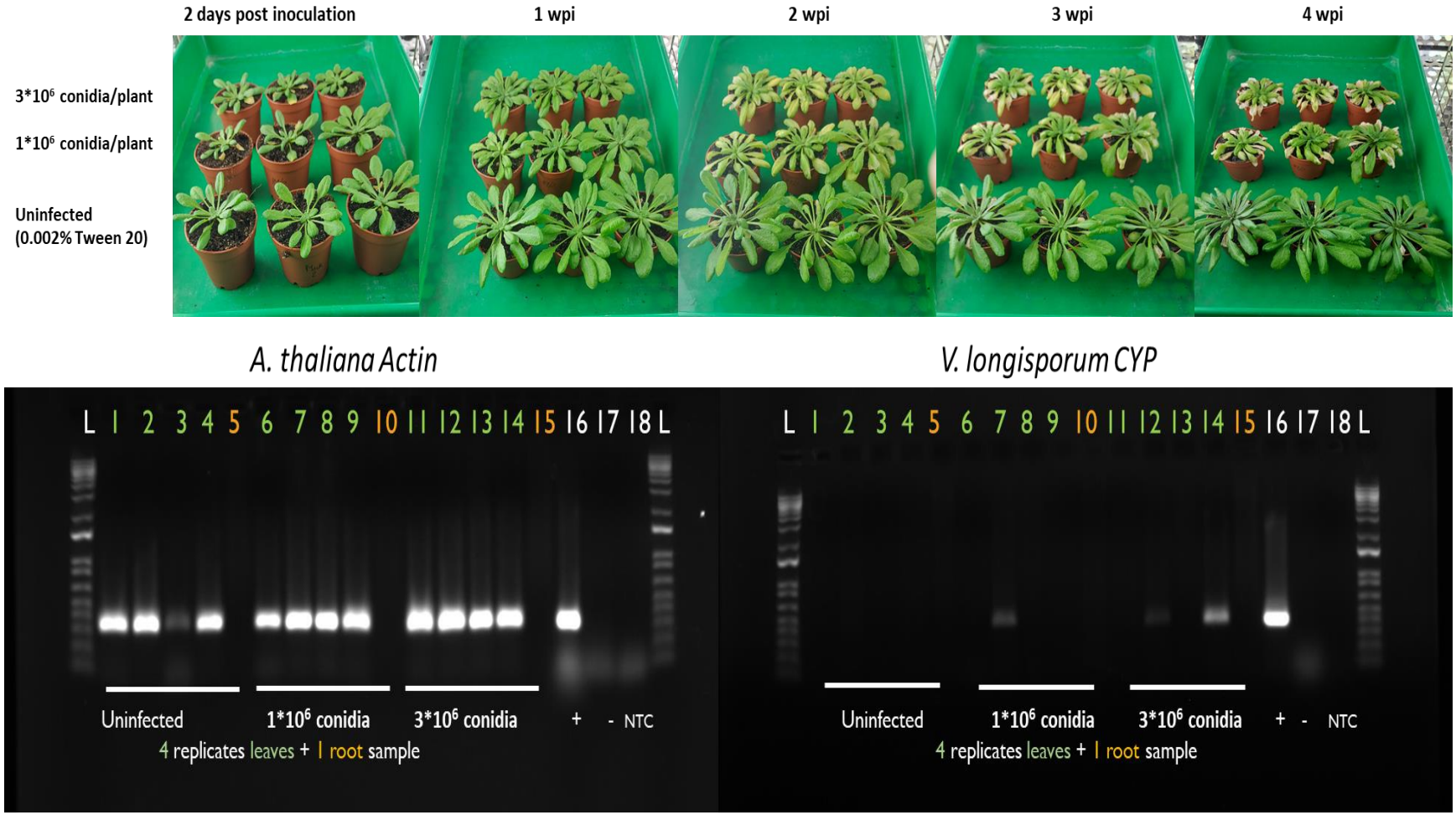

Figure 03. Infection of soil grown *A. thaliana* plants using root dipping method in two different concentrations of *V. longisporum* conidia solutions ($1*10^6$ or $3*10^6$ conidia/plant), and PCR analysis of gDNA extracted from root and leaf tissues after 4 weeks post inoculation (wpi). *A. thaliana Actin* was used to assess the integrity of the extracted gDNA and *V. longisporum CYP* to track infection success and detectability. Samples description provided in Table 01.

3.3.2 Assessment of *V. longisporum* infections in hydroponically grown *A. thaliana* plants

A hydroponic system was tested to avoid the disadvantages observed in the previous soil grown system, which allows the direct introduction of *V. longisporum* conidia without further preparation steps and eliminate abiotic stress as a factor in the infection assessment. *A. thaliana* seeds were sowed on rockwool and were allowed to germinate after 48 h vernalisation at 4 °C. Half-strength hydroponic solution containing all essential elements for plant growth was used for the first week followed by a weekly change of full-strength hydroponic solution (Gibeaut et al. 1997). Infections were achieved by using a total of $50*10^6$ conidia and $100*10^6$ conidia, with the later concentration showing more prominent disease symptoms after overnight incubation with *V. longisporum* conidia (Figure 04.A). The extracted gDNA from roots and leaves could be used for *A. thaliana* and *V. longisporum* specific gene fragments PCR amplification (Figure 04.B), thus enabling quantitative analysis of root infections and offering a more flexible treatment approach, for instance allowing root treatment without the associated hurdles of uprooting from soil, as well as the possibility of repeated treatments and easier scalability.

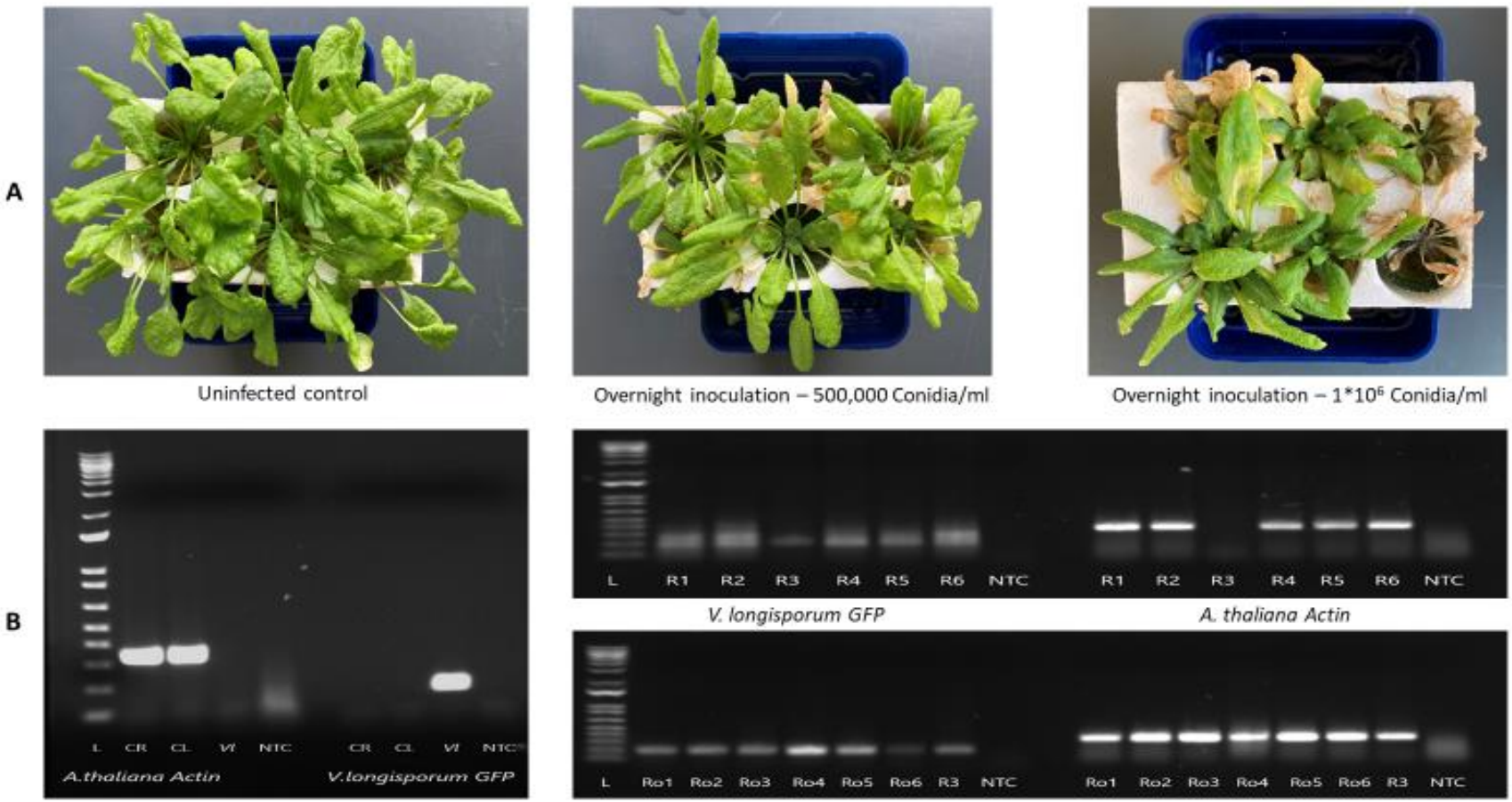

Figure 04. **A.** Infected *A. thaliana* Col-0 plants grown in hydroponic solution after either lower conidia concentration (centre) or higher conidia concentration (upper right) overnight infection with *V. longisporum GFP* (Vl43) compared to uninfected plants (upper left), captured at 4 weeks post inoculation. **B.** Agarose gel electrophoresis following PCR amplification of target gene fragments from *A. thaliana Actin* gene and *V. longisporum GFP* gene, left panel shows the specificity of primers used for gDNA biomass quantification, where the templates used were **CR**: Control uninfected root, **CL**: Control uninfected leaves, **Vl**: *V. longisporum GFP* genomic DNA, **NTC**: no template control. In the right panel the infected plant tissues showed successful detection of *V. longisporum* gDNA in all root (**R**1-6) and rosette (**Ro**1-6) samples harvested four weeks post inoculation, as well as confirmation of genomic DNA integrity through amplification of *A. thaliana Actin* gene.

3.4 Vector cloning for dsRNA *in-vivo* production in bacterial system

Niehl et al. developed a bacterial dsRNA production system employing a phi6 bacteriophage in a non-pathogenic strain of *Pseudomonas syringae,* where target dsRNA sequences replace the coding regions in two (M-segment & S-segment) of the three phi6 genome segments, with an upstream T7 promoter and T7 terminator to stop the transcription reaction at the required length of ssRNA (Figure 05), while L- segment remains unchanged and carries components necessary for the polymerase complex formation. After the transformation of the three vectors, T7 polymerase enzyme from *P. syringae* initiates ssRNA production from the three vectors, alongside other components of the phi6 replication complex. The T7 polymerase enzyme produced ssRNA are then packed to polymerase complexes where they will be replicated to dsRNA molecules. This system was used to produce dsRNA sequences targeting Tobacco mosaic virus (TMV) and showed a significant plant protection action through inhibition of TMV propagation (Niehl et al. 2018), with a higher yield and lower cost than *in-vitro* transcription method, which enables larger scale dsRNA production and testing.

3.4.1 M-Segment vector cloning for dsRNA production

A 2904 bp fragment from *VlClp-1* coding sequence amplified from cDNA (Figure 06.C) and was selected to be cloned to pMS2 vector for dsRNA production (Figure 06.A), the sequence is intended to replace the M-segment in the phi6 genome. The plasmid pMS2 is 3602 bp and contains a multiple cloning site (MCS) and T7 promoter for dsRNA production, as well as ampicillin resistance gene for colony selection. The insert size was confirmed by restriction digest using the restriction enzymes *NheI* and *PstI* (Figure 06.B), the plasmid integrity was confirmed using an *in-vitro* transcription kit and a fragment of ssRNA of the expected size was transcribed (Figure 08). Following an unsuccessful initial trial for *in-vivo* dsRNA production, a longer insert was cloned to the same vector in order to exclude insert size limitation as a reason for unstable constructs. The original M-segment from phi6 bacteriophage genome is 4023 kb, thus a longer 4000 bp insert (amplified from gDNA) from *VlClp-1* gene was cloned to pMS2 (Figure 06.D).

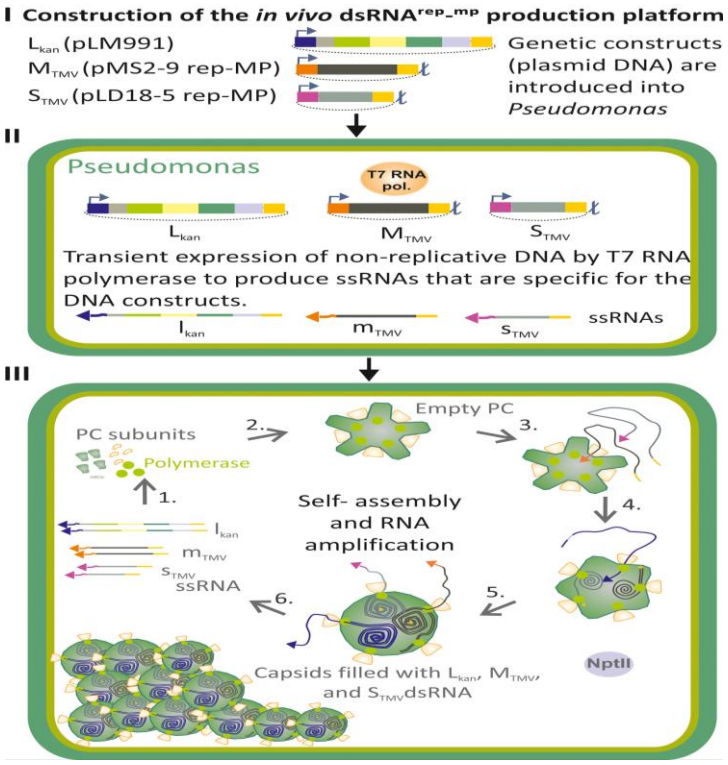

Figure 05. Schematic representation of the *in-vivo* dsRNA production system, adopted from Niehl et al. 2018 https://doi.org/10.1111/pbi.12904. **I**. Constructs for *P. syringae* transformation. L_{kan} encodes the components of the phi6 polymerase complex (PC), L-segment-specific RNA replication and packaging signals and the kanamycin resistance gene nptI. STMV and MTMV contain TMV-specific sequences (without open reading frames) flanked by phi6 S- or M-segment-specific signal sequences, respectively. Each construct carries a T7 RNA polymerase promoter upstream of the segment-specific phi6 packaging signal. **II**. Transformation of the plasmids into *P. syringae* cells, which express T7 RNA polymerase, leads to the transcription of L_{kan}-, MTMV- and STMV-specific ssRNA molecules (l_{kan}, mTMV and sTMV). T7 terminators ensure correct length of the MTMV-, and STMV-specific ssRNA transcripts. **III**. Translation of l_{kan} ssRNA (1.) leads to production of empty PCs (2.), which are sequentially packaged with sTMV, mTMV and l_{kan} ssRNAs (3.). During packaging, the PC synthesizes the complementary strand for each packaged ssRNA carrying the phi6-specific RNA replication signal (4.). Following the first round of dsRNA synthesis, the PCs continue to synthesize more sTMV, mTMV and l_{kan} ssRNAs (6.), which lead to the amplification of PCs containing L_{kan}, MTMV and STMV dsRNAs (dsRNArep-MP) until the host cell is filled with such particles. The plasmids used for the initial transformation (**I–II**) do not replicate in *P. syringae* and are not present in the cell lines in which dsRNA production is established (**III**).

3.4.2 S-Segment vector cloning for dsRNA production

A 1780 bp fragment from *VlCYP1* coding sequence amplified from cDNA (Figure 07.B) was cloned to pLD18 vector (Figure 07.A), intended to replace the S-segment in phi6 genome. The plasmid pLD18 is 3539 bp and contains a multiple cloning site (MCS) and T7 promoter for dsRNA production, as well as ampicillin resistance gene for colony selection. The insert size was confirmed by restriction digest using the restriction enzymes *NheI* and *SacI* (Figure 07.C), the plasmid integrity was confirmed using an *in-vitro* transcription kit and a fragment of ssRNA of the expected size was transcribed (Figure 08).

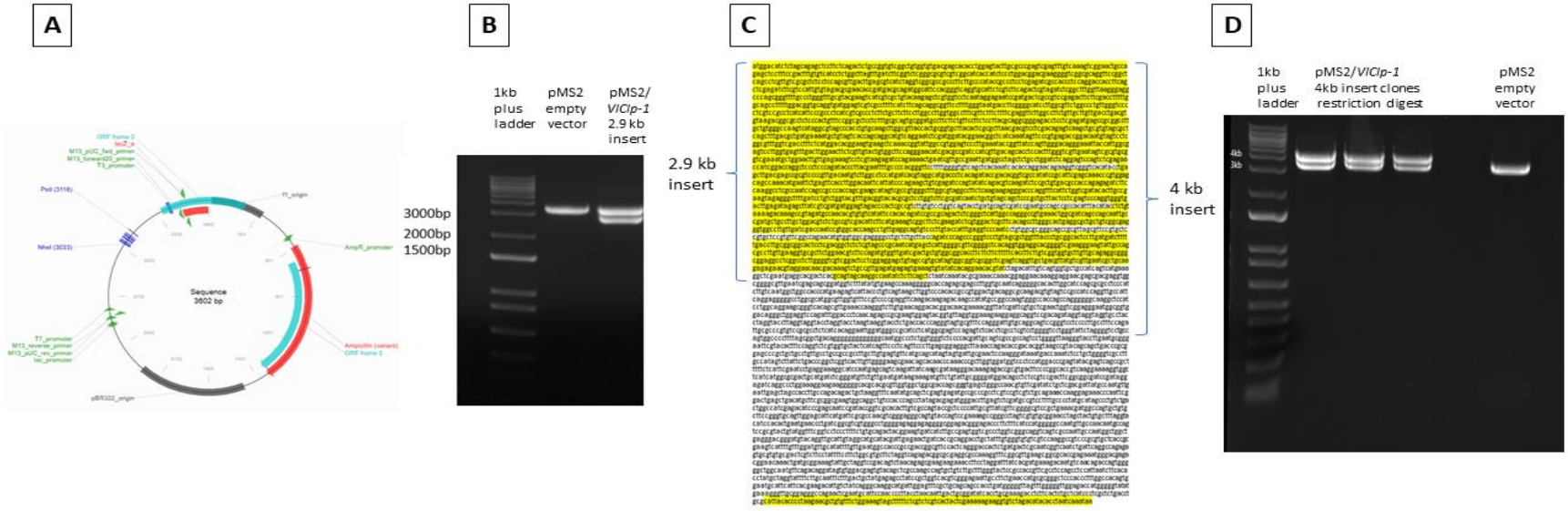

Figure 06. **A**. pMS2 vector for M-segment phi6 genome, NheI and PstI restriction sites used for *VIClp-1* insert cloning. **B**. Restriction digest using NheI and PstI fast digest, after cloning *VIClp-1* 2.9 kb insert. **C**. Full coding sequence of *VIClp-1* gene, exons highlighted in yellow (Available as text in supplementary information). **D**. Restriction digest using NheI and PstI fast digest for a longer 4 kb insert for *in-vivo* dsRNA production troubleshooting.

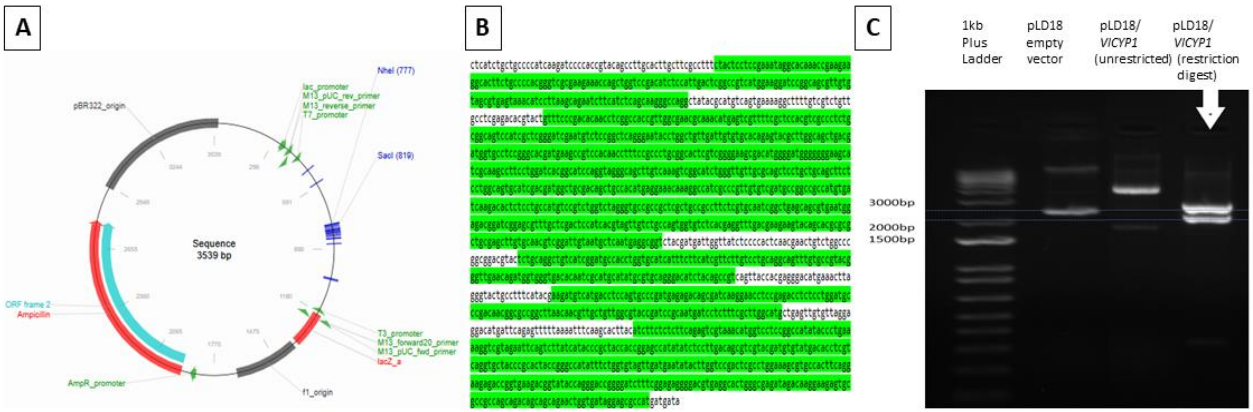

Figure 07. **A**. pLD18 vector for S-segment phi6 genome cloning, NheI and SacI restriction sites used for *VICYP1* insert cloning. **B**. Full coding sequence of *VICYP1* gene, exons highlighted in green (Available as text in supplementary information). **C**. Restriction digest using NheI and SacI fast digest, after cloning 1.8 kb insert.

3.4.3 *In-vivo* dsRNA production

Data provided by the partner lab in the Bioprotect project- University of Helsinki

Stable dsRNA production in the bacterial *in-vivo* system has not been achieved using the two constructs for *V. longisporum* (plasmids pLD18_*VlCYP1* and pMS2_*VlClp-1*). At least, three electroporation attempts were performed for each combination of the plasmids, and 194 clones were screened for *V. longisporum* specific dsRNA content. Most clones contained only L-segment dsRNA, and only four clones for *V. longisporum* contained three dsRNA segments of expected lengths. These clones were stored in glycerol at -80°C. However, already after several weeks the dsRNA pattern was different from what was initially detected. In alternative experiments, only two plasmids were used for electroporation, pLM991 which is required for the production of phi6 polymerase complexes and either pLD18_*VlCYP1* or pMS2_*VlClp-1*. For each pair of plasmids, 30 clones were screened to no avail.

In general, upon the electroporation of plasmids containing fungal sequences, the frequency of correct clones was scant compared to viral sequences, irrespective whether there were one or two fungal-specific plasmids present. The rare correct clones obtained were unstable. The production of dsRNA from the provided plasmids was assessed using *in-vitro* transcription (IVT) with T7 polymerase coupled with the replication by phi6 polymerase. Both T7 polymerase and purified recombinant RNA polymerase of bacteriophage phi6 accepted all fungal sequences and produced ssRNA and dsRNA *in-vitro* (Figure 08). Hence, the inability to produce dsRNA *in-vivo* from these sequences might be related to the properties of polymerase complexes or some host-specific factors.

According to the current understanding of ssRNA packaging and dsRNA synthesis within the bacteriophage phi6 polymerase complex, it is crucial that heterologous dsRNA molecules match the lengths of the natural phi6 genomic segments. Therefore, a longer version mimicking the M-segment of bacteriophage phi6, a plasmid pMS2_CLP_4kb, was cloned

with a longer 4000 bp insert (Figure 06.D). However, the electroporation performed with this plasmid did not help to get a correct dsRNA-producing bacterial clone.

It should be noted, that from the plasmid mimicking the S-segment, pLD18_CYP, a shorter dsRNA sequence is expected, 2374 bp instead of 2948 bp characteristic for the phi6 S-segment. To investigate if using a longer dsRNA sequence will increase the chances of obtaining correct clones and promote their stability, in the electroporation experiment pLD18-CYP was replaced with pMH4. This plasmid carries the cDNA copy of the natural phi6 S-segment, wherein a lytic gene was inactivated. Despite all three plasmid inserts mimicked the lengths of phi6 genomic segments, no clear clones with the expected dsRNA patterns were generated.

Similar *in-vivo* dsRNA production issues were also observed with other vectors cloned to produce dsRNA targeting a different set of genes in the pathogenic fungus *M. oryzae,* thus suggesting a specific incompatibility of these fungal genes with the bacterial *in-vivo* dsRNA production system, that leads to unstable packaging into polymerase complex. Further investigation is needed to determine the deciding factors for stable dsRNA production, the GC content and insert size doesn't seem to be the limiting criteria (Table 02), possible other factors could be an absence of specific regulatory sequence elements, differences in secondary ssRNA structures or a higher susceptibility to recombination in the fungal gene sequences compared to the successfully produced viral gene sequences.

Table 02. Analysis of the sequences used for dsRNA production *in-vivo*

Sequence	Length	GC content	*In-vivo* production
phi6 S segment	2948 bp	55%	+
phi6 M segment	4063 bp	57%	
TOTAL	**7011 bp**		
pLD18_ToBRFV	3208 bp	42%	+
pLD18 ToBRFV (second option)	2282 bp	43%	
pMS2 ToBRFV	4106 bp	43%	
TOTAL	**7314 bp or 6388 bp**		
pLD18 TuMV	3174 bp	47%	+
pMS2 TuMV	3930 bp	47%	
TOTAL	**7104 bp**		
pLD18_CYP	2374 bp	54%	-
pMS2_CLP	3544 bp	56%	
TOTAL	**5918 bp**		
pLD18_PMK1	2166 bp	53%	-
pMS2_MST7	2744 bp	53%	
TOTAL	**4910 bp**		
pLD18_CYP	2374 bp	54%	-
pMS2_CLP_4kb	4021 bp	57%	
TOTAL	**6395 bp**		
pMH4	2948 bp	55%	-
pMS2_CLP_4kb	4021 bp	57%	
TOTAL	**6969 bp**		

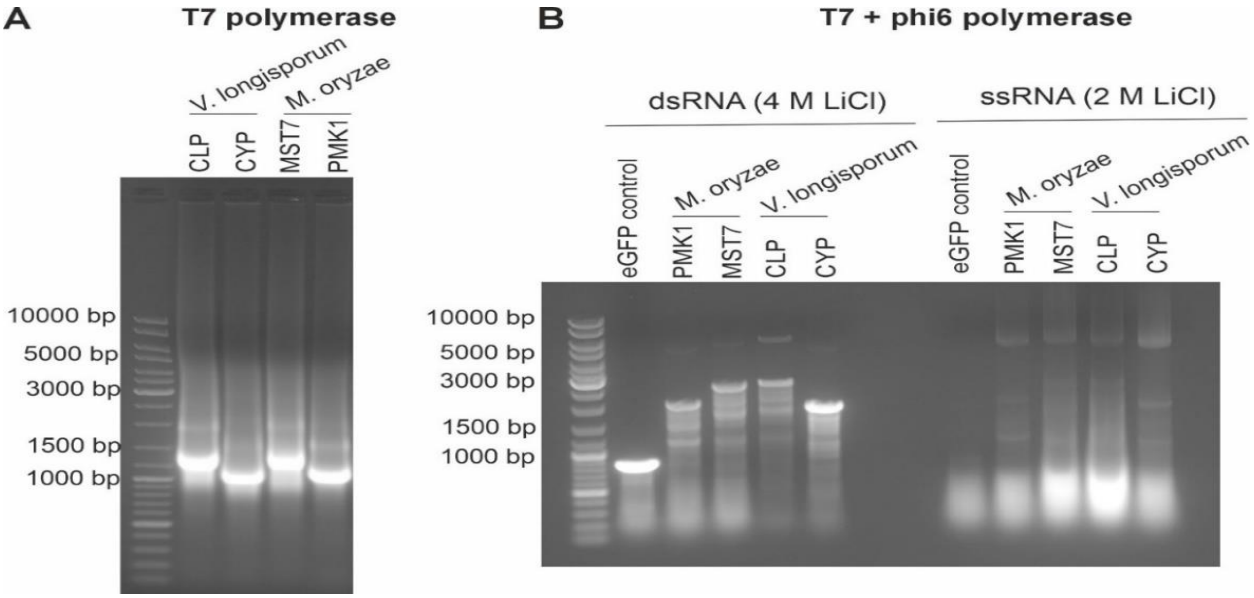

Figure 08. *In-vitro* synthesis evaluation of ssRNA/ dsRNA on the cloned fungal gene targets vectors, provided by the collaborating group in University of Helsinki **(A)** *In-vitro* transcription of ssRNA by T7 polymerase of the fungal gene target sequences from *V. longisporum* (*VlCYP1/VlClp-1*) and *M. oryzae* (*MoMST7/MoPMK1*). **(B)** A coupled transcription and replication reactions catalysed by T7 and phi6 polymerases, leading to replication of ssRNA to dsRNA using the same enzymatic process of the *in-vivo* dsRNA production in *P. syringae,* Lithium chloride molarity gradient used to differentiate between ssRNA that precipitates at 2 M concentration, and dsRNA that precipitates at 4 M concentration.

3.5. dsRNA formulation using chitosan/alginate nanoparticles

Developed in a collaboration within Bioprotect project - Fachhochschule Bielefeld

3.5.1 Protection against RNase III digestion

To protect dsRNA from rapid degradation by the abundant environmental nucleases and to mask the negative charge that is expected to influence foliar uptake, and to prolong its shelf-life, chitosan nanoparticles were developed by a partner group in Fachhochschule Bielefeld. Chitosan is a biodegradable polymer, comprised of β(1→4)-linked monomers of N-acetyl-D-glucosamine (acetylated or chitin monomer), and D-glucosamine (deacetylated or chitosan monomer), it exhibits a positive net charge in physiological pH due to protonation of the amine groups, which is employed to bind negatively charged dsRNA molecules intended for target gene silencing, with the help of alginate to form interpolyelectrolyte complexes (IPEC) (Moorlach et al. 2024). The formation of such complexes was hypothesized to protect dsRNA from nuclease digestion, which was observed using RNase III digestion assay (Figure 09), where unformulated dsRNA was rapidly degraded in the presence of 0.05U RNase III (lanes 2-6) while formulated dsRNA still shows bands of intact phi6-dsRNA produced *in-vivo* with the expected sizes of 7599 bp, 4063 bp and 2948 bp (lanes 7-12) after EDTA addition to release dsRNA from the formulated nanoparticles.

3.5.2 Nanoparticles size detection using Dynamic light scattering

The size of the obtained nanoparticles varied based on size of dsRNA, where longer dsRNA molecules obtained from phi-6 bacterial production system (L/M/S segments with sizes 7599 bp, 4063 bp and 2948 bp respectively) yielded smaller nanoparticles with a mean hydrodynamic diameter 97.77 ± 6.07 nm when measured by dynamic light scattering, compared to shorter ≈500 bp dsRNA molecules transcribed *in-vitro,* which yielded larger nanoparticles with a mean hydrodynamic diameter 125.54 ± 11.55 nm. The phosphate to nitrogen (P: N) ratio and the net charge was maintained by adjusting chitosan and alginate concentrations based on the size of dsRNA to be formulated, with a final ratio of 1.25 (+/−) for positively charged formulated nanoparticles, and 0.9 (+/−) for negatively charged ones.

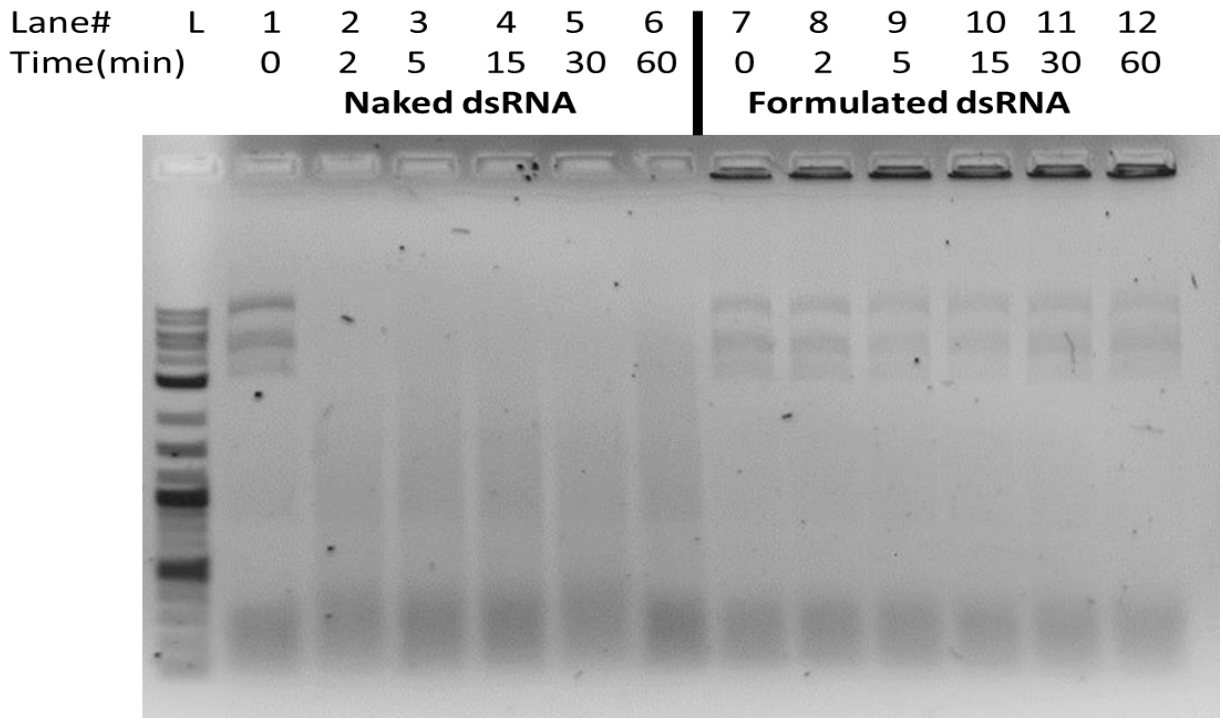

Figure 09. Free and formulated dsRNAphi6 (1196 ng, 26 ng/µL) treated with 0.05 U RNase III at 37 °C for 0 to 60 min. The reaction was stopped with 11 µmol EDTA (final conc. 152.8 mM EDTA). The mixture was incubated at 37 °C for 60 min, and the formulation was dissolved by thoroughly mixing every 30 min for 30 sec. The gel electrophoresis was performed in a 1 % high resolution agarose gel with ROTI gelstain for 40 min at 110 V.

3.5.3 Chitosan concentration optimization

3.5.3.1 Antimicrobial effect

Chitosan is obtained through deacetylation of chitin, which is readily present in fungal cell walls and exoskeleton of crustaceans and insects, making it a biodegradable and a generally recommended as safe polymer, with low cost of production and favourable characteristics for nucleic acid delivery systems (Karayianni et al. 2023). However, in certain concentrations and degrees of de-acetylation it was found to exhibit antimicrobial properties against a wide range of bacterial and fungal species (Ke et al. 2021). These antifungal properties could be a beneficial added effect, but it would as well eclipse the effect of RNAi by specific gene targeting using dsRNA. At the initial concentration of chitosan in the nanoparticles (0.9% w/v), a strong antifungal effect was observed when added to *V. longisporum* colonies in 6-well-plates (Figure 10.C-D).

Unloaded chitosan nanoparticles and formulated dsRNA completely blocked germination of conidia (Figure 10.F), as well as elimination of growing colonies within an hour of addition. This effect was confirmed using CLSM of colonies treated with chitosan nanoparticles (Figure 10.H), which shows multiple aggregates of these particles on the growing hyphae one hour after addition, which is later perforated most likely due to the binding of positively charged chitosan moieties to cell walls and thus disrupts normal growth.

This strong antifungal effect was avoided by drastically decreasing the concentration of chitosan in the final formulation (0.0029% w/v) and introducing washing steps during the formulation process to avoid unbound chitosan particles presence, while keeping the same charge ratio of formulated dsRNA. These changes led to a relatively more diluted solutions and thus limits the production of highly concentrated dsRNA formulation solutions. An average dsRNA concentration in the formulated nanoparticles of 12-20 ng/µl could be achieved by this method.

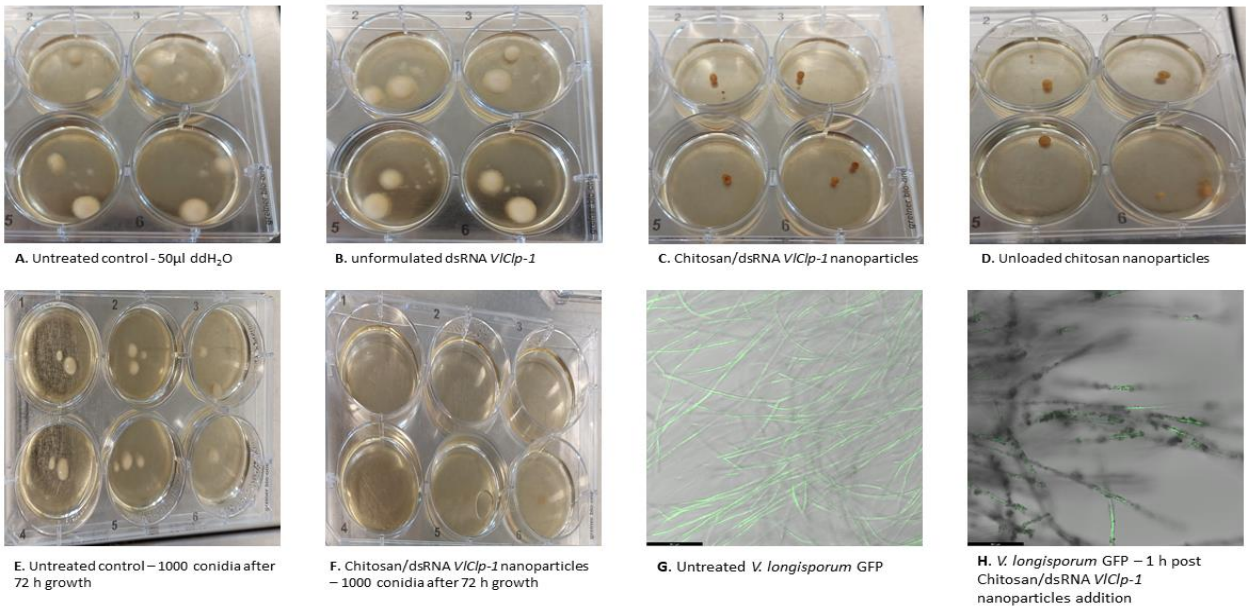

Figure 10. **A-D**: Growth of *V. longisporum GFP* (Vl43) in PDB medium under sterile conditions. 500 conidia were added to 2 ml liquid medium in each well, and allowed to grow for 72 h before addition of the equivalent of 1 µg dsRNA/formulation/unloaded controls to be observed. All samples containing chitosan - formulated dsRNA/chitosan nanoparticles and unloaded nanoparticles - showed browning of growing colonies and reduced biomass 24 h after treatment. **E-F**: Effect of dsRNA/chitosan nanoparticles on germination of *V. longisporum GFP* (Vl43) conidia, where no visible colonies are seen after 72 h in (**F**) when 1 µg dsRNA/chitosan nanoparticles are added alongside conidia to the liquid medium. **G-H**: CLSM imaging of treated *V. longisporum GFP* colonies showing aggregates of dsRNA/chitosan nanoparticles, nanoparticles were added to *V. longisporum GFP* (Vl43) colonies growing for 72 h and observed 1 h after addition.

5.3.2 *In-vitro* gene silencing using formulated chitosan-alginate/dsRNA nanoparticles

The formulated dsRNA did not achieve the same levels of gene silencing observed with naked dsRNA targeting *VlClp-1* or *VlGFP* when the same concentration of dsRNA is used (Figure 11). One limitation for this concentration conversion is the absence of tools to quantify dsRNA in the final formulation, since nanodrop dsRNA concentration measurement is not possible for such formulated nanoparticles. Another possibility for the decreased gene silencing activity is the release of dsRNA from the formulated nanoparticles. It is hypothesized that the release of dsRNA would take place upon cellular uptake of the nanoparticles and exposure to slightly alkaline pH of the cytosol, thereby delaying the gene silencing effects compared to naked dsRNA which would directly be available for processing and integration in the RNAi cascade. Further technical details about the formulation strategy, preparation method and nanoparticles properties were published (Moorlach et al. 2024).

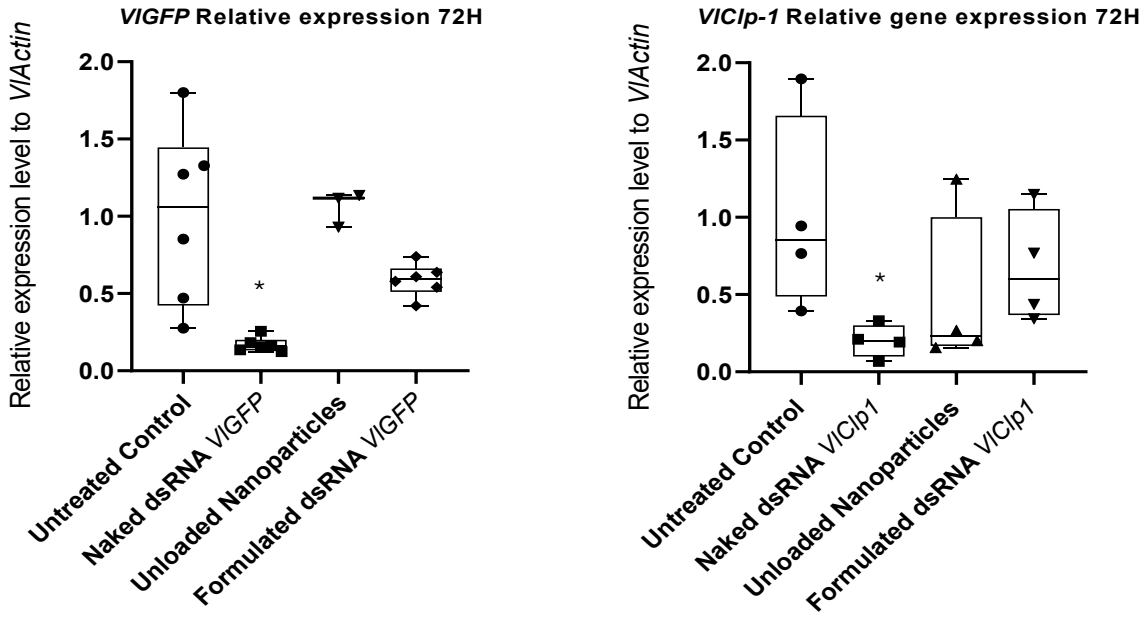

Figure 11. Relative gene expression analysis of *V. longisporum GFP* (left) and *V. longisporum Clp-1* (right) genes normalized to *V. longisporum Actin* gene expression levels, samples grown axenically in 2 ml of Xylem simulated medium (SXM) were treated with the equivalent of 1 µg dsRNA and harvested at 72 h after treatment. *VlActin* was used as a housekeeping gene for normalization of Ct values obtained from qRT-PCR analysis, and relative gene expression was calculated according to ΔΔCt method. Statistical significance was analysed with one-way ANOVA for 6 biological replicates; error bars represent standard deviation (SD) and stars demonstrate statistical significance from the control according to Dunnett's multiple comparisons test (* p≤0.05).

3.6 Growth assay in 96-well-plates

To assess the direct effects of different dsRNA molecules on the transgenic *V. longisporum* Vl43 growth in liquid cultures, GFP fluorescence intensity was measured for three different starting concentrations of *V. longisporum GFP* conidia (500, 2500, 5000 conidia/ml) in 200 µl SXM. GFP fluorescence intensity increased steadily up till the 11th day and started declining upon saturation of the wells and consumption of the culture medium. The comparison between starting conidia concentration and GFP fluorescence intensity showed a high correlation between 3 and 7 days with correlation coefficient (R^2) above 0.90. The wildtype strain *V. longisporum* Vl41 was used to compare the background fluorescence and did not show a similar increase in fluorescence intensity and no correlation to growth within the same timeframe, supporting the specificity of the measured fluorescence to GFP abundance and minimal background interference (Figure 12.A).

Using *in-vitro* transcribed dsRNA molecules around 500 bp in length, the selected gene targets (*VlClp-1*, *VlCYP1* and *VlIC*) were investigated for their direct effect on the growth rate of *V. longisporum* through GFP fluorescence intensity measurement. At a concentration of 2.5 ng/µl, a significant reduction (p-value 0.028) of *V. longisporum* growth was observed in *VlIC* treated wells after 7 days, with an overall growth reduction across all measured timepoints. *VlCYP1* targeting showed a potential for reducing growth at this concentration (p-value 0.08) after 7 days. In contrast, *VlClp1* treated wells rather showed an increase in GFP fluorescence when compared to untreated wells, implying an enhanced growth of *V. longisporum* upon silencing of *VlClp-1* protein (Figure 13.A). The lower concentration of dsRNA was 0.5 ng/µl, the observed effects on *V. longisporum* growth by dsRNA *VlClp1* and *VlIC* were not evident, while *VlCYP1* dsRNA caused a highly significant increase in growth (p-value<0.0001) at the lower concentration (Figure 13.B). The observed variation of responses from different molecules and concentrations of dsRNA requires further investigation, in order to identify the optimal dsRNA concentration and gene target - or

combination of targets - for efficient gene silencing and eventually a consistent growth reduction.

A

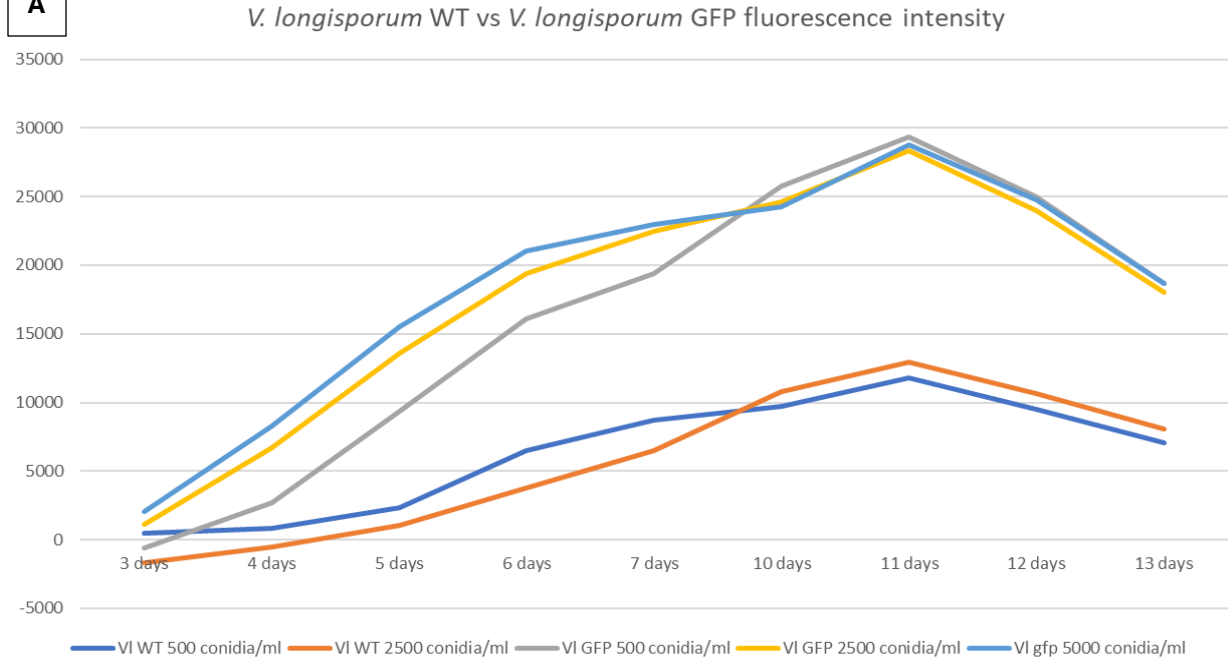

Time	3 days	4 days	5 days	6 days	7 days	10 days	11 days	12 days	13 days
R^2	0.940413	0.90397	0.927407	0.933261	0.802923	0.854186	0.269173	0.015065	0.011545

B

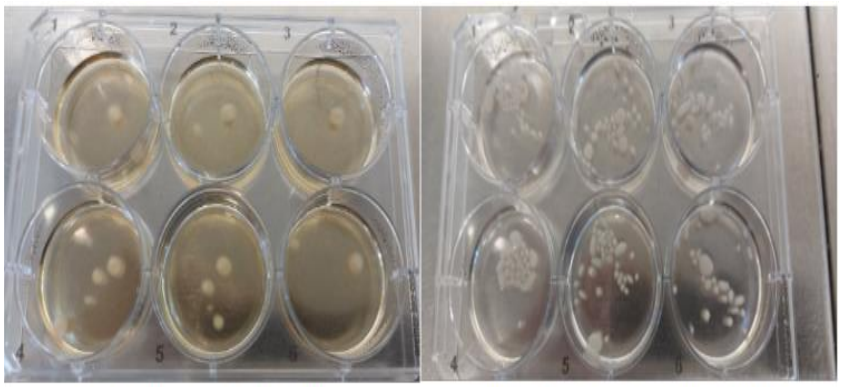

Figure 12. **A.** *GFP* fluorescence intensity recorded over days after *V. longisporum GFP* (Vl43) or *V. longisporum* WT (Vl41) conidia addition to Xylem simulated medium (SXM), average values obtained from six biological replicates are subtracted from blank wells containing only SXM growth medium were used to measure the correlation coefficient (R^2) between the number of starting conidia and the observed fluorescence intensity. **B.** Effect of growth medium on the morphology of *Verticillium longisporum* (Vl43) colonies and their average total RNA yields.

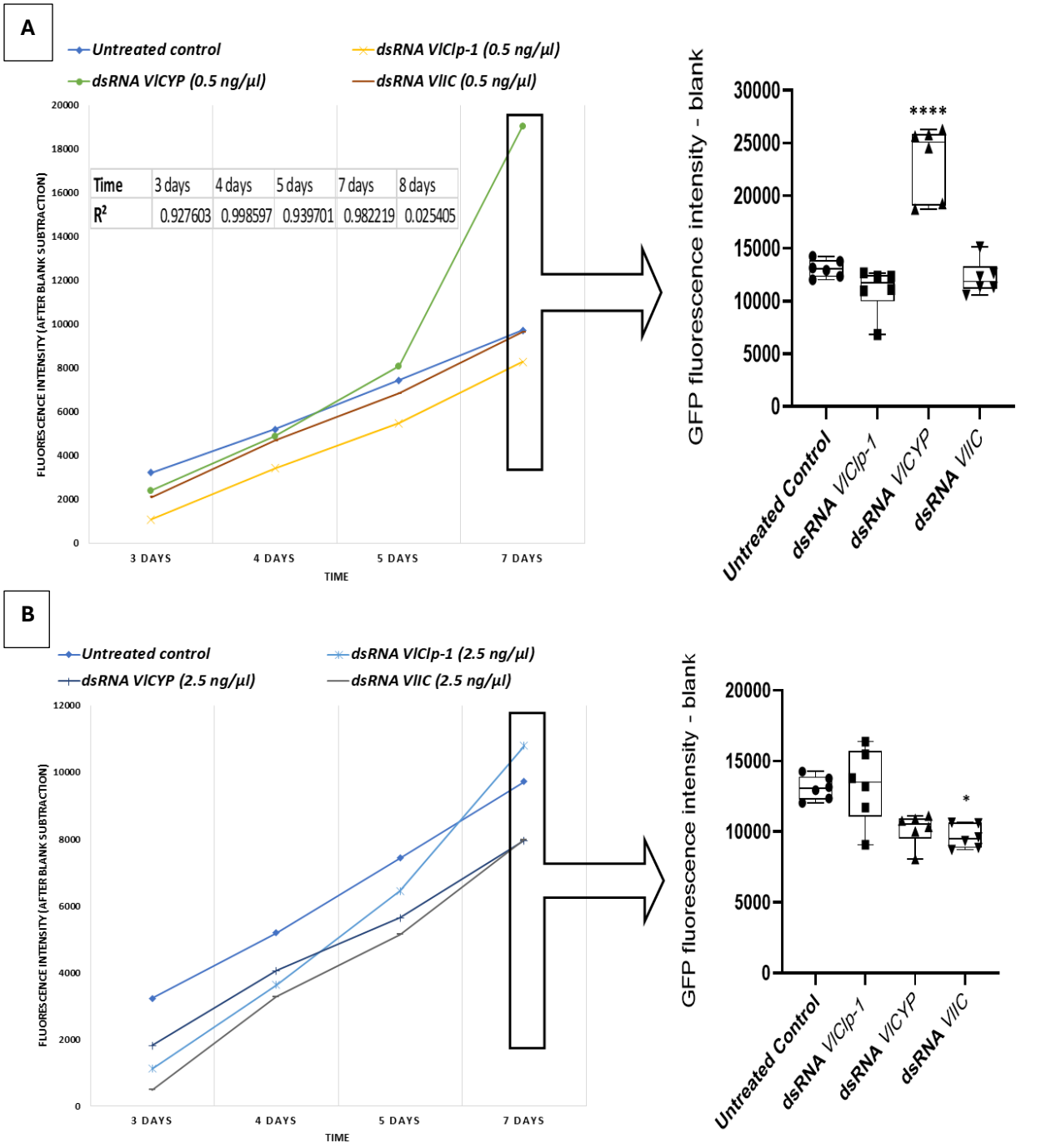

Figure 13. *GFP* fluorescence intensity recorded over days after *V. longisporum GFP* conidia addition to SXM, treated with different naked dsRNA molecules (dsRNA *VlClp-1*/ dsRNA *VlCYP1*/ dsRNA *VlIC)* and final concentrations of **A**. 0.5 ng/µl and **B.** 2.5 ng/µl. The presented values are the average obtained from six biological replicates after subtraction from blank wells (SXM and dsRNA only). The correlation coefficient (R^2) is calculated between the number of starting conidia and the observed fluorescence intensity. Statistical significance was analysed for 7 days after addition values with one-way ANOVA, error bars represent standard deviation (SD) and stars demonstrate statistical significance from the untreated control (* $p \leq 0.05$, **** $p \leq 0.00001$) using Dunnet test.

3.7. Hydroponic infection assay

3.7.1 *VlClp-1* silencing effect on *V. longisporum* infections in the hydroponic system

The effect of naked and formulated dsRNA targeting *VlClp-1* was tested on *A. thaliana* Col-0 plants grown in the hydroponic system. The initial trials tested positively charged formulated chitosan nanoparticles (data not shown) and an additional trial included both positively and negatively charged chitosan nanoparticles, to assess the effect of formulations charge on possible uptake by roots and leaves. It was demonstrated that nanocarriers charge influenced uptake, translocation and distribution differently in roots and leaves, with the negatively charged nanocarriers being better absorbed by roots and minimal to no root uptake of positively charged ones (Zhang et al. 2023). It is worth noting that these tested nanocarriers had considerably smaller particle size of around 10 nm.

A total of 125 µg dsRNA with a final concentration of 2.5 ng/µl or its equivalent of formulated and unloaded chitosan-alginate nanoparticles were applied 24 h before inoculation with *V. longisporum*, either directly to roots or through foliar spray. In almost all the root treated groups an increased chlorosis and wilting symptoms were observed when compared to the untreated infected plants, as well as a higher relative fungal biomass of *V. longisporum* in the harvested roots from the last timepoint. The results illustrate an enhanced growth of *V. longisporum* when in direct contact with naked/formulated dsRNA as shown with the increased disease severity index and higher relative fungal biomass in roots (Figure 14).

Root application exhibited higher incidence of chlorosis and thus a higher disease severity (Group 3, 5 and 7) when compared to foliar spray application (Group 2, 4 and 6), which might indicate limited uptake and translocation of dsRNA to roots after foliar spray. The results imply an enhanced growth of *V. longisporum* upon silencing of *VlClp-1* gene and matches the observed effects in the growth assay (Figure 13) using this concentration of dsRNA *VlClp-1* (2.5 ng/µl).

The only group with a reduced fungal biomass in roots was unloaded negatively charged nanoparticles (Group 8) when compared to the infected untreated plants (Group 1). However, the fungal biomass quantification in roots did not entirely reflect on chlorosis percentage and disease severity index, possibly due to partial growth of *V. longisporum* outside the roots (Root surface). The foliar spray of naked dsRNA *VlClp-1* resulted in the highest relative amounts of *V. longisporum* gDNA, suggesting a variable colonization and spreading activity of *V. longisporum* in the vasculature depending on the dsRNA application method.

3.7.2 *VlIC* / *VlCYP1* Hydroponic infection assay

In a separate experiment, further gene targets were evaluated for limiting infections caused by *V. longisporum*. Using the same concentration of dsRNA applied via root treatment, dsRNA targeting *VlIC* and *VlCYP1* dsRNA showed reduced chlorosis symptoms and overall reduction in disease severity index across the four weeks after infection, leading to an AUDPC similar to the uninfected plants. The analysis of relative fungal biomass showed a reduction of *V. longisporum* gDNA content in roots (-32%) and leaves (-38%) for *VlIC* treated plants, while only a reduction of *V. longisporum* gDNA content was observed in leaves (-93%) of *VlCYP1* treated plants, and rather an increase in *V. longisporum* gDNA content was observed in roots (+50%).

The separation of replicates and the root system growing in the hydroponic system is crucial for future experiments, to further understand the distribution of *V. longisporum* across vasculature in multiple replicates, and to investigate dsRNA effects on infection and migration dynamics in a clearer manner.

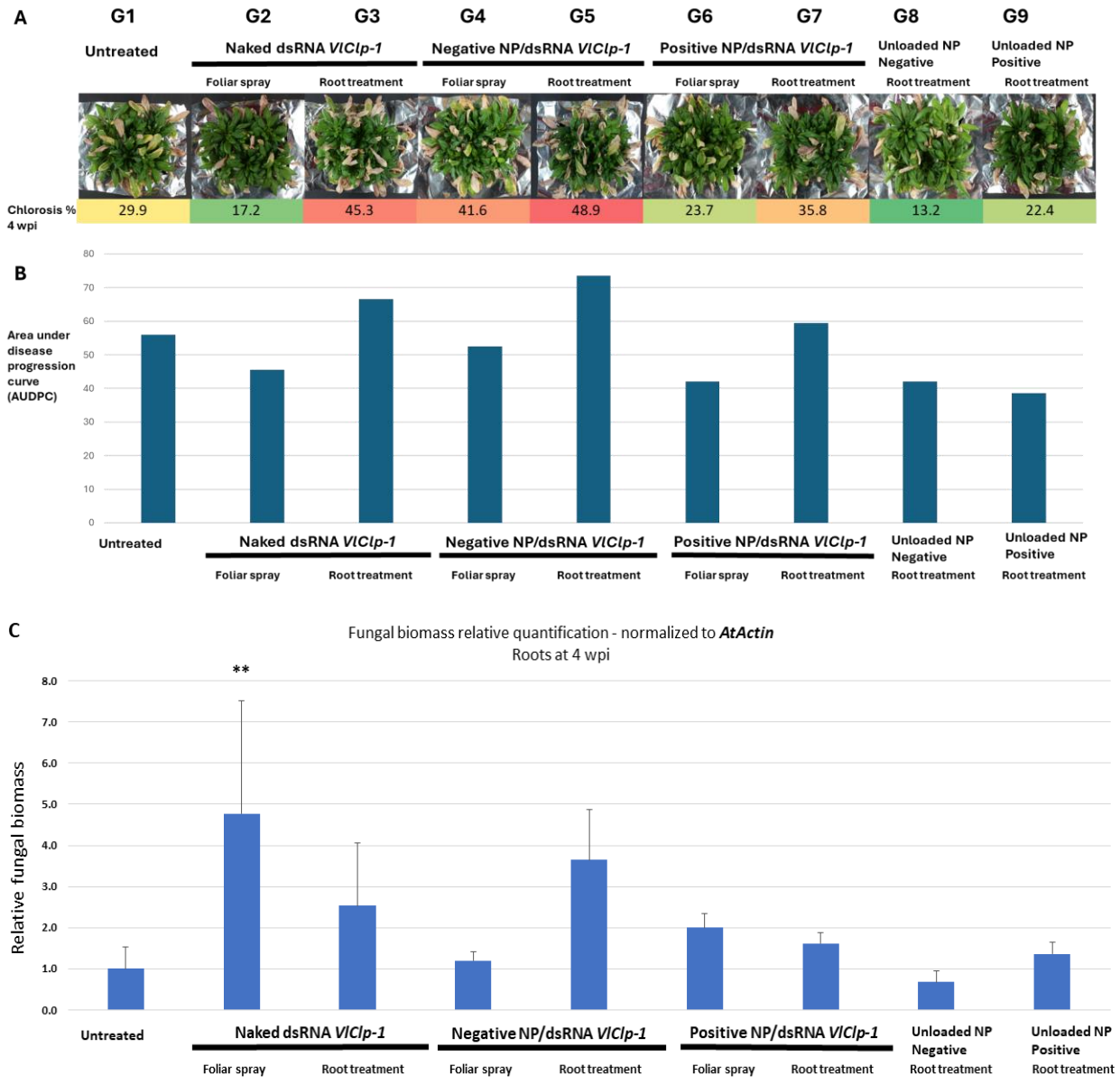

Figure 14. Hydroponic infection assay results at 4 weeks post inoculation using dsRNA targeting *VlClp-1,* either non-formulated "Naked" or formulated with chitosan-alginate nanoparticles (NP) with a positive or negative net charge, **A.** Images of different treatment groups were analysed using ImageJ to identify the overall chlorosis percentage **B.** Chlorosis percentages were used to calculate the area under disease progression curve (AUDPC) throughout the 4 wpi. **C.** Relative fungal biomass quantification in harvested roots of all treatment groups at 4 wpi, gDNA was extracted from 3 biological replicates, fungal biomass relative quantification was carried out using qRT-PCR, *AtActin* was used for normalization of Ct values, and relative fungal biomass was calculated according to ΔΔCt method, using the infected and untreated G1 samples as a reference. Statistical significance was analysed with one-way ANOVA for 3 biological replicates, error bars represents standard deviation (SD) and stars demonstrate statistical significance from the untreated control according to Dunnett test (** p ≤0.005)

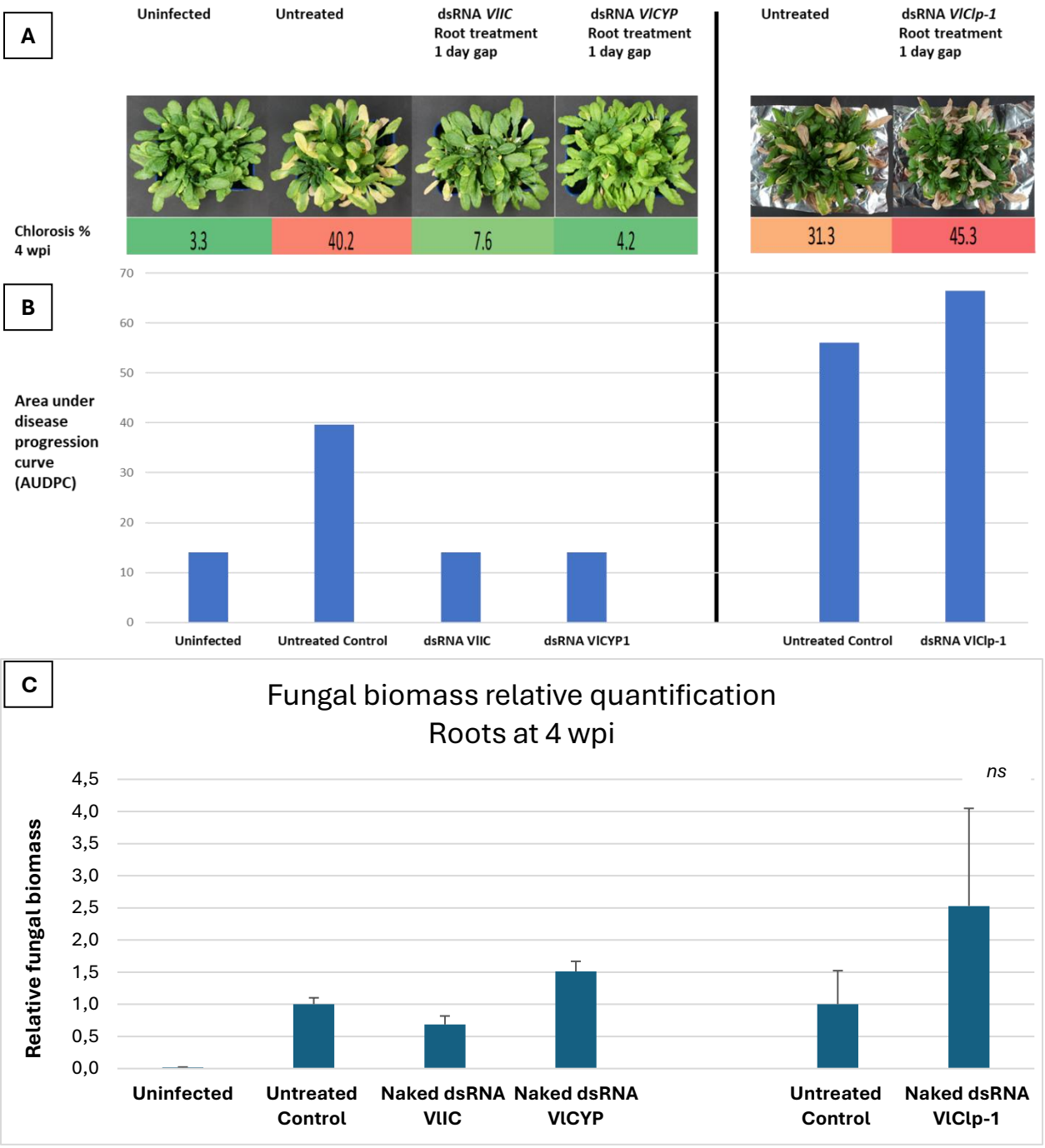

Figure 15. Hydroponic infection assay results at 4 weeks post inoculation using naked dsRNA targeting *VlIC, VlCYP1* and *VlClp-1* **A.** Images of different treatment groups were analysed using ImageJ to identify the overall chlorosis percentage **B.** Chlorosis percentages were used to calculate the area under disease progression curve (AUDPC) throughout the 4 wpi. **C.** Relative fungal biomass quantification in harvested roots of all treatment groups at 4 wpi, gDNA was extracted from 3 biological replicates, fungal biomass relative quantification was carried out using qRT-PCR, *AtActin* was used for normalization of Ct values, and relative fungal biomass was calculated according to ΔΔCt method, using the infected and untreated samples as a reference. Statistical significance was analysed with one-way ANOVA for 3 biological replicates, error bars represent standard deviation (SD) and stars demonstrate statistical significance from the untreated control according to Dunnett test (ns: not significant).

3.7.3 Time and method of application comparison (dsRNA *VlIC*)

To identify the best strategy for application in terms of application method (Foliar spray vs root treatment) and time of application (simultaneously with inoculation or with a 24 h gap before infection), dsRNA targeting *VlIC* showed the highest potential for limiting infections and thus was used for this purpose.

The highest reduction of disease symptoms was achieved using root treatment with one day gap between infection and dsRNA addition, where this protective effect was not achieved by foliar spray of the same amount of dsRNA prior to inoculation (Figure 16). A similar reduction of protection potential was observed when no gap is introduced in both root treatment and foliar spray between infection and dsRNA addition. The results indicate a better protective effect through root treatment with dsRNA *VlIC*, when applied 24 h before root inoculation with *V. longisporum* (Figure 16), which was found to also decrease the growth rate of *V. longisporum GFP* in the fluorescence-based growth assay (Figure 13). The gap between dsRNA application and more specific RNAi effects was also illustrated in other systems (Zheng et al. 2025), and might point towards an unspecific effect rising from the host recognition of dsRNA, through triggering an immune response that might interfere with the immune response against the invading fungal pathogen.

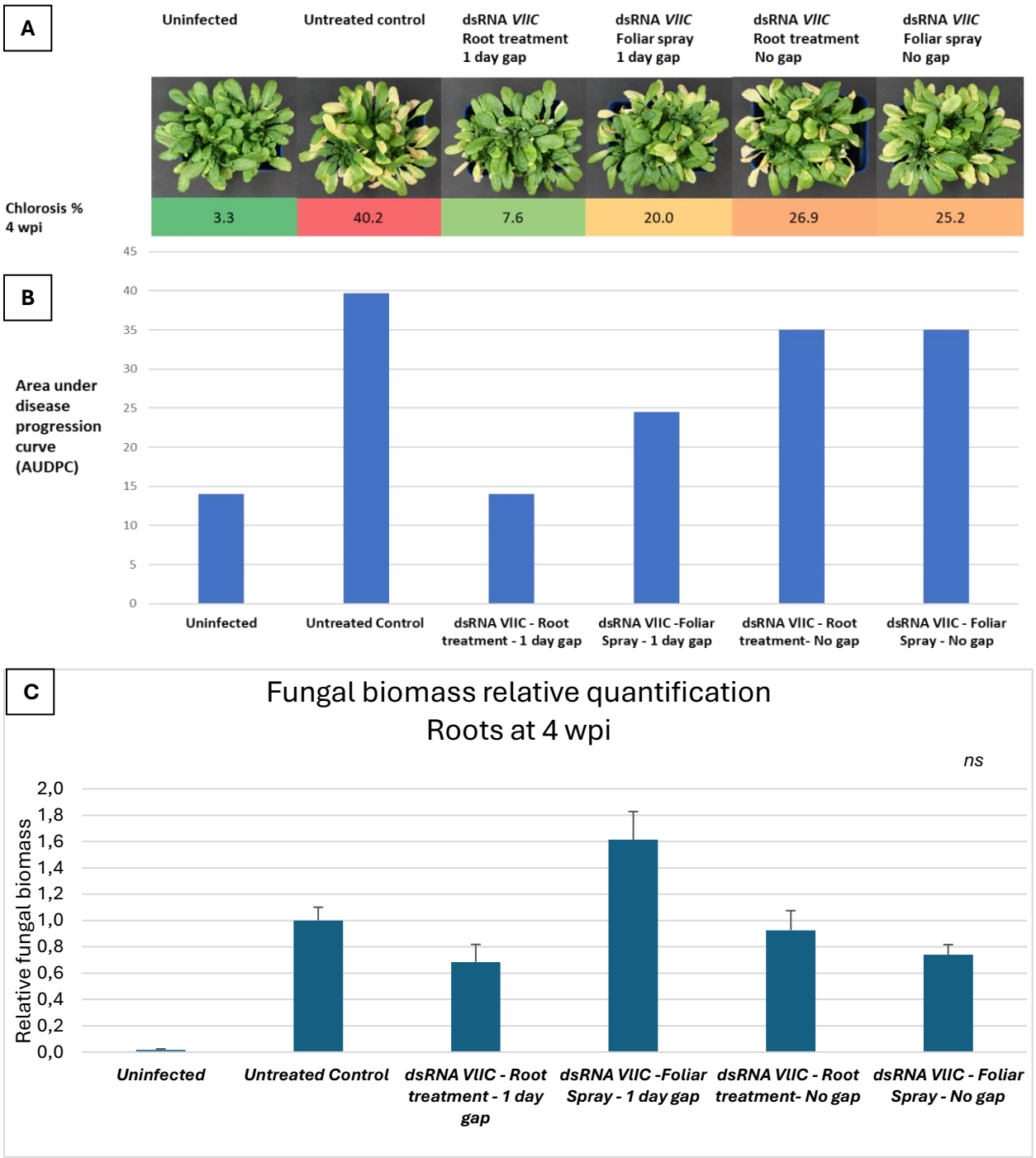

Figure 16. Hydroponic infection assay results at 4 weeks post inoculation using naked dsRNA targeting *VIIC* **A.** Images of different treatment groups were analysed using ImageJ to identify the overall chlorosis percentage **B.** Chlorosis percentages were used to calculate the area under disease progression curve (AUDPC) throughout the 4 wpi. **C.** Relative fungal biomass quantification in harvested roots of all treatment groups at 4 wpi, gDNA was extracted from 3 biological replicates, fungal biomass relative quantification was carried out using qRT-PCR, *AtActin* was used for normalization of Ct values, and relative fungal biomass was calculated according to ΔΔCt method, using the infected and untreated samples as a reference. Statistical significance was analysed with one-way ANOVA for 3 biological replicates, error bars represents standard deviation (SD) and stars demonstrate statistical significance from the untreated control according to Dunnett test (ns: not significant)

3.8. PTI response evaluation

Selected marker genes were investigated for transcriptional changes after foliar spray application of unformulated and formulated dsRNA, as well as the unloaded equivalents of nanoparticles. To simulate internalization of dsRNA and formulation nanoparticles, the same experiment was repeated after wounding of sprayed leaves using celite rubbing on leaf surfaces, which would lead to surface wounding and thus allow more dsRNA or formulation nanoparticles to cross the many barriers of leaf structure. The gene markers investigated were *Pathogenesis-related gene 2* (*AtPR2* - AT3G57260), *Pathogenesis-related gene 5* (*AtPR5* - AT1G75040), Zinc finger of *A. thaliana* 12 (*AtZAT12* - AT5G59820) and *Calmodulin-binding protein 60-like G* (*AtCBP60G* – AT5G26920).

AtPR2 and At*PR5* are known to be pathogen responsive genes, they are associated alongside At*PR1* with salicylic acid response in PTI. At*PR2* is a family of endo-1,3-β-glucanases found to regulate cell wall maintenance, and plays a role in callose deposition and pathogen cell wall degradation in response to biotic stress (Perrot et al. 2022). At*PR5* was found to be significantly upregulated after *A. thaliana* leaf disc exposure to synthetic dsRNA analogue Poly I:C (Niehl et al. 2016).

AtCBP60g is induced upon various bacterial and fungal pathogens identification, and was found to regulate multiple defence related genes in the immune response cascade as part of salicylic acid signalling pathway (Sun et al. 2022 and Wang et al. 2011). *AtZAT12* encodes a C_2H_2 type Zinc finger protein, it was found to be induced in response to various abiotic stress conditions and oxidative stress, as well as being involved in the defence response against fungal pathogens and induction of endochitinases (Davletova et al. 2005).

Table 03. Foliar spray applied groups, 4 weeks old *A. thaliana* plants were sprayed with 1.5 ml solution containing the equivalent of 20 µg dsRNA or formulations per plant, control group was sprayed with 1.5 ml sterile MilliQ H_2O. Three biological replicates were sprayed and timepoints of harvesting leaves were T1: 1 h, T2: 3 h, T3: 24 h, T4: 72 h after foliar spray.

Group #	Foliar spray treatment (1.5 ml/plant)
G1	MilliQ H_2O spray
G2	Naked dsRNA *VlClp-1*
G3	Positive Chitosan nanoparticles / dsRNA *VlClp-1*
G4	Positive unloaded Chitosan nanoparticles
G5	Negative Chitosan nanoparticles / dsRNA *VlClp-1*
G6	Negative unloaded Chitosan nanoparticles

3.8.1 Evaluation of responses to foliar spray of non-formulated vs formulated dsRNA molecules

Gene expression analysis showed a significant up-regulation of *AtPR5* 24 h after foliar spray with the positively charged chitosan-alginate formulation only, while negatively charged formulations showed up-regulation of *AtZAT12* 3 h after foliar spray application. This induction was not persistent and returned to normal levels at the next timepoints. The results suggest a different pathway of detection, or a different distribution of chitosan-alginate nanoparticles based on their net charge. Naked dsRNA showed higher variation in the setup between the replicates used for gene expression analysis, higher concentrations might be needed to reach a more uniform response. Only one out of the three biological replicates showed up-regulation of *AtPR2*, *AtPR5* and *AtZAT12* after naked dsRNA application in the earlier timepoints.

Further RNAi machinery genes were analysed like *AtRDR6, AtMAPK6, AtDCL2* and *AtDCL4* (data not shown), not showing any significant changes in gene expression levels across all time points. Their activation or regulation might be more evident on protein phosphorylation analysis level (Kurzynska-Kokorniak et al. 2015).

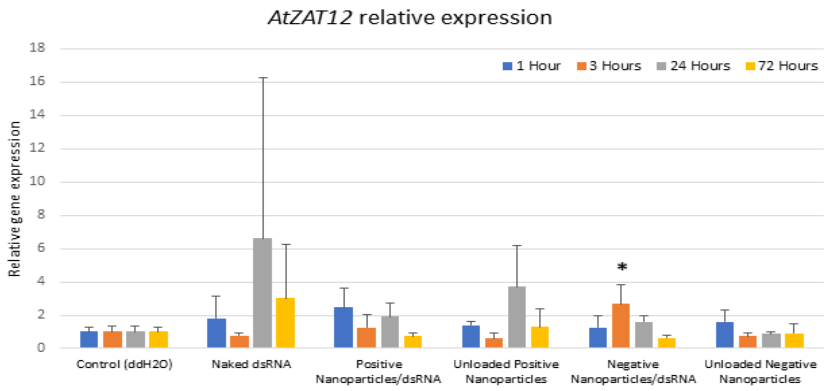

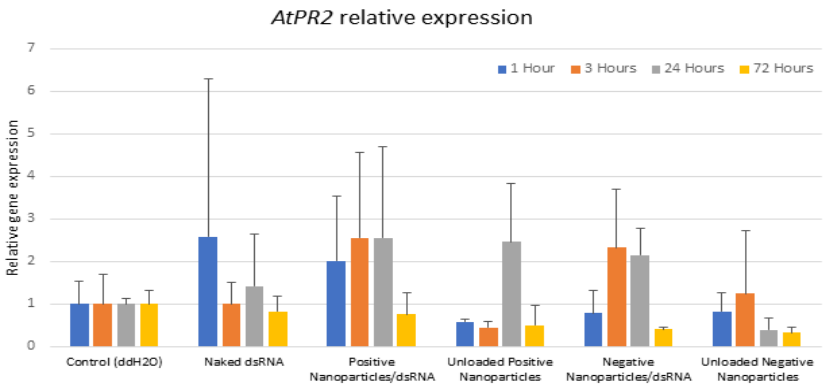

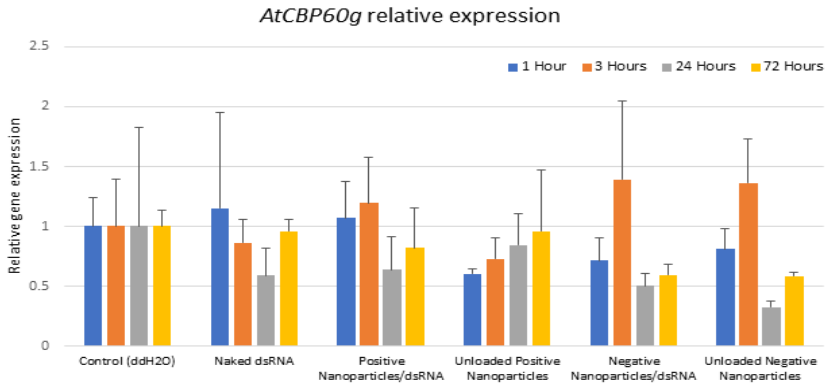

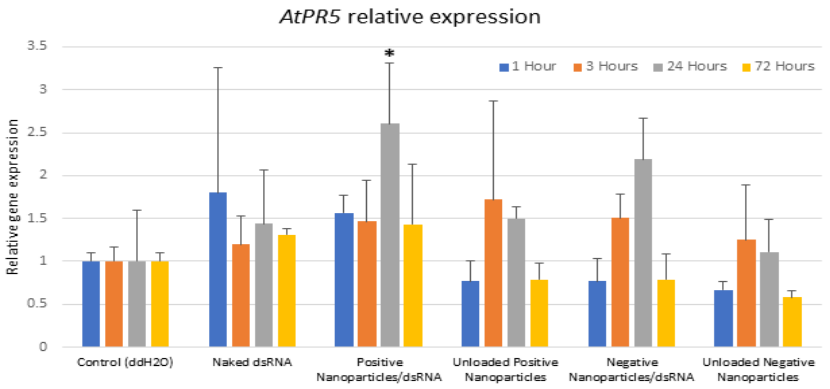

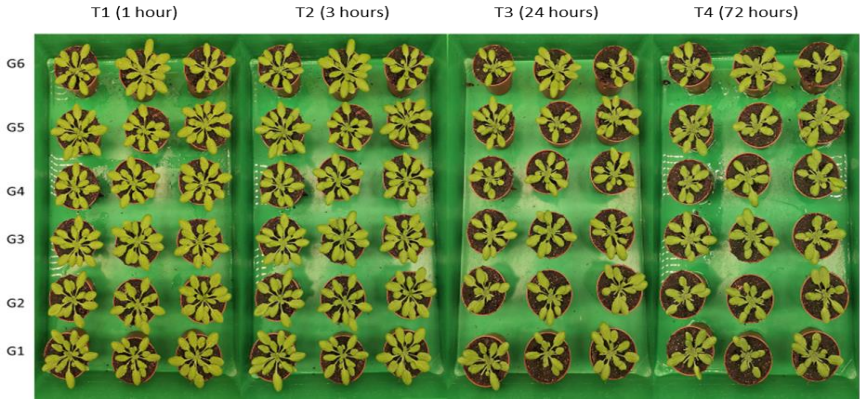

Figure 17. *A. thaliana* Col-0 plants used for foliar spray application for PTI markers analysis. Foliar spray treatments from table 03 were allowed to dry before harvesting two leaves from each plant at the stated timepoints. One of the two leaves was thoroughly washed using double distilled H_2O prior to freezing in liquid nitrogen. Total RNA extracted from 3 biological replicates was used to quantify relative transcript levels of target PTI markers. *AtActin* was used as a housekeeping gene for normalization of Ct values obtained from qRT-PCR analysis, and relative gene expression was calculated according to ΔΔCt method. Statistical significance was analysed with one-way ANOVA, error bars represent standard deviation (SD), stars demonstrate statistical significance from the untreated control using Dunnet test (* p≤0.05).

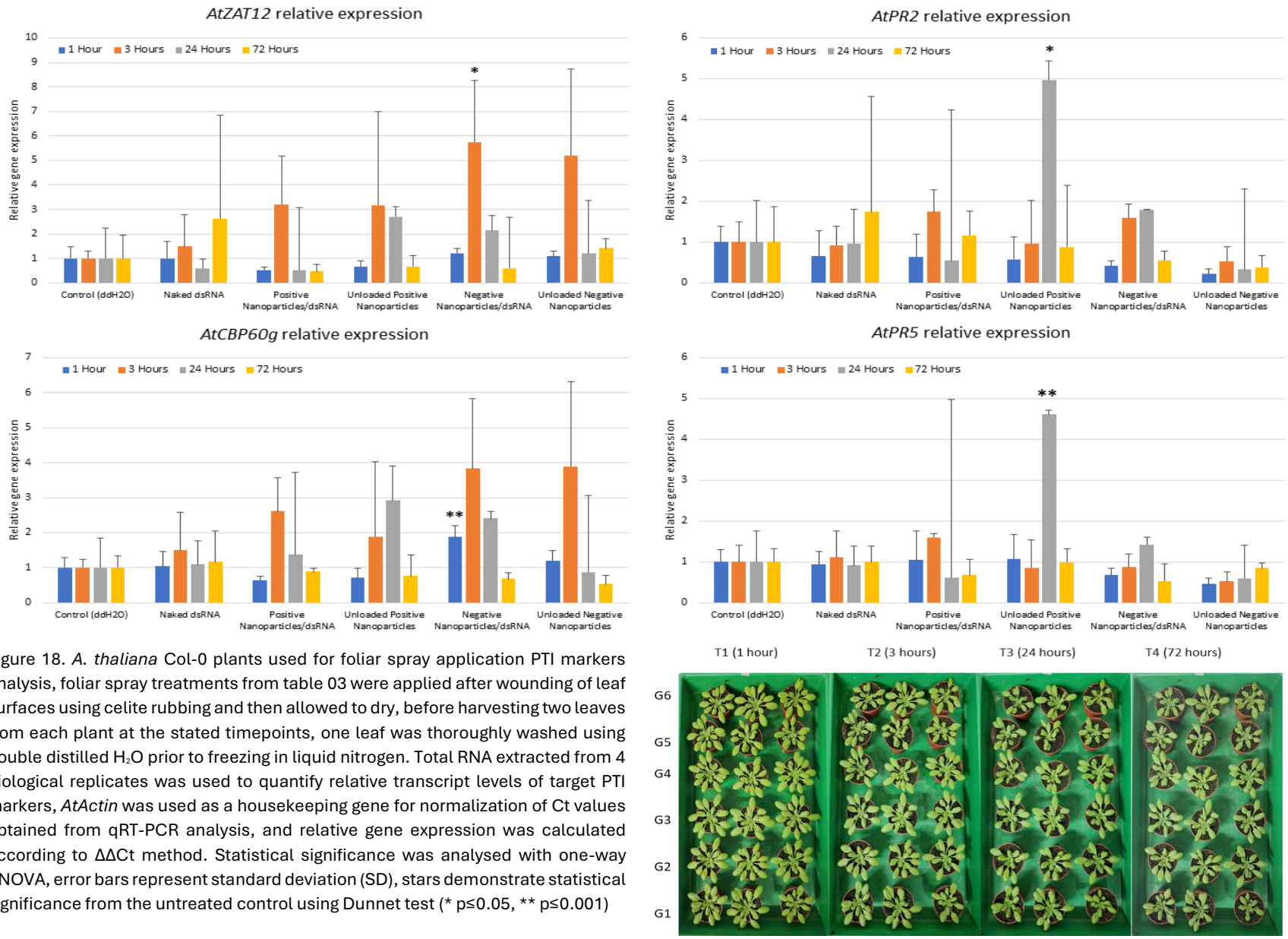

Figure 18. *A. thaliana* Col-0 plants used for foliar spray application PTI markers analysis, foliar spray treatments from table 03 were applied after wounding of leaf surfaces using celite rubbing and then allowed to dry, before harvesting two leaves from each plant at the stated timepoints, one leaf was thoroughly washed using double distilled H_2O prior to freezing in liquid nitrogen. Total RNA extracted from 4 biological replicates was used to quantify relative transcript levels of target PTI markers, *AtActin* was used as a housekeeping gene for normalization of Ct values obtained from qRT-PCR analysis, and relative gene expression was calculated according to ΔΔCt method. Statistical significance was analysed with one-way ANOVA, error bars represent standard deviation (SD), stars demonstrate statistical significance from the untreated control using Dunnet test (* p≤0.05, ** p≤0.001)

3.8.2 Evaluation of responses to foliar spray of non-formulated vs formulated dsRNA molecules after celite wounding

Using celite to induce wounding before spraying leaves yielded a faster and higher fold change in relative gene expression, represented in a more statistically significant response compared to the intact leaf spray results. Celite rubbing for 10 sec prior to foliar spray did not show signs of excessive stress up to one-week post wounding. Gene expression analysis (Figure 18) showed a significant up-regulation rapidly after spraying negatively charged formulations of *AtCBP60g* after 1 h and *AtZAT12* after 3 h. While positively charged unloaded nanoparticles showed a statistically significant up-regulation of *AtPR2* and *AtPR5* after 24 h. Similar to the intact leaf spray application, the results confirm a different transcriptional response depending on the charge of formulations used, with a higher fold change after celite wounding, implying a limited uptake of the sprayed particles on intact leaves. The activation of PTI specific gene markers indicates the recognition of chitosan-alginate nanoparticles as a possible PAMP, and raises a concern on the delivery of dsRNA upon this recognition, where an inert carrier might be more favourable to avoid triggering an unspecific immune response and might eclipse the anticipated effects from RNAi pathway.

3.9. dsRNA stability assay

J2 monoclonal antibodies are considered the “gold standard” for dsRNA detection, the antibody binds dsRNA in a sequence non-specific manner starting from 40 bp length. The antibody was used for various purposes, including the detection of dsRNA contaminations during mRNA synthesis, as well as monitoring viral infections in plants where dsRNA is either originating from viral genome or produced during viral replication process (Kariko et al. 2011 and Richardson et al. 2010).

First, the specificity of detected signals from various nucleic acid samples directly applied to a positively charged nylon membrane was validated, showing high specificity towards samples containing *in-vitro* transcribed dsRNA around 500 bp in length and no visible signals for total RNA extracted from *V. longisporum* and *A. thaliana* untreated samples, as well as no signals from genomic DNA. Additionally, negatively charged formulated dsRNA showed stronger signals when compared to positively charged formulated dsRNA, as expected from the nature of the membrane positive charge, that would only bind negatively charged free dsRNA in the case of the later (Figure 19).

Next, the possibility of detecting dsRNA from treated *V. longisporum* colonies in liquid SXM cultures was established. The growing colonies were separated from liquid medium by centrifugation, followed by RNA precipitation from the supernatant using ethanol and high salt concentration, and total RNA extraction from the pelleted colonies. The detection of dsRNA after RNA precipitation from the supernatant was possible and showed stronger signals after immunoblotting with increasing the amount of dsRNA added (1, 2 & 4 µg) to the liquid growth medium. Similar pattern was also observed when precipitated RNA was checked using gel electrophoresis on a 1% agarose gel (Figure 20.A).

Sample#	Descripion
1	Nuclease free H_2O
2	100 ng Naked dsRNA *VlClp-1*
3	Positively charged nanoparticles + 100ng dsRNA *VlClp-1*
4	unloaded positively charged nanoparticles
5	Negatively charged nanoparticles + 100 ng dsRNA *VlClp-1*
6	Unloaded negatively charged nanoparticles
7	Total RNA *V. longisporum* (200 ng)
8	gDNA *V. longisporum* (200 ng)

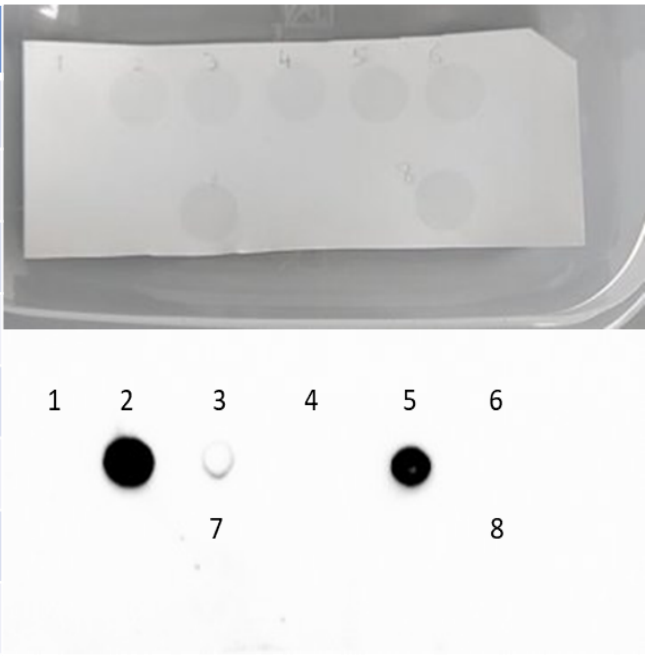

Figure 19. Direct application of various nucleic acid samples and formulated chitosan-alginate nanoparticles on a positively charged nylon membrane, to determine specificity of J2 monoclonal antibodies in the dot blot approach. The equivalent of 100 ng dsRNA was diluted in 8 µl nuclease free H_2O and left to dry before proceeding to the membrane blocking and antibodies binding steps.

The same approach was used on *V. longisporum* growing in liquid culture, samples were harvested and centrifuged after several timepoints (5 min, 15 min, 1, 6, 18 & 24 h) to track the presence of dsRNA in each fraction, the immunoblot showed that dsRNA was present in the liquid medium for up to 6 h after addition and no signals of dsRNA associated with the pellet, while the later timepoints at 18 and 24 h after dsRNA addition has the opposite pattern with no more dsRNA detected in the liquid fraction and a signal from the pelleted colonies (Figure 20.B). The results suggest an initial phase where dsRNA is only detectable in liquid cultures, followed by dsRNA uptake by growing colonies, where it should be processed in the RNAi pathway or degraded leading to absence of the signals detected in that initial phase.

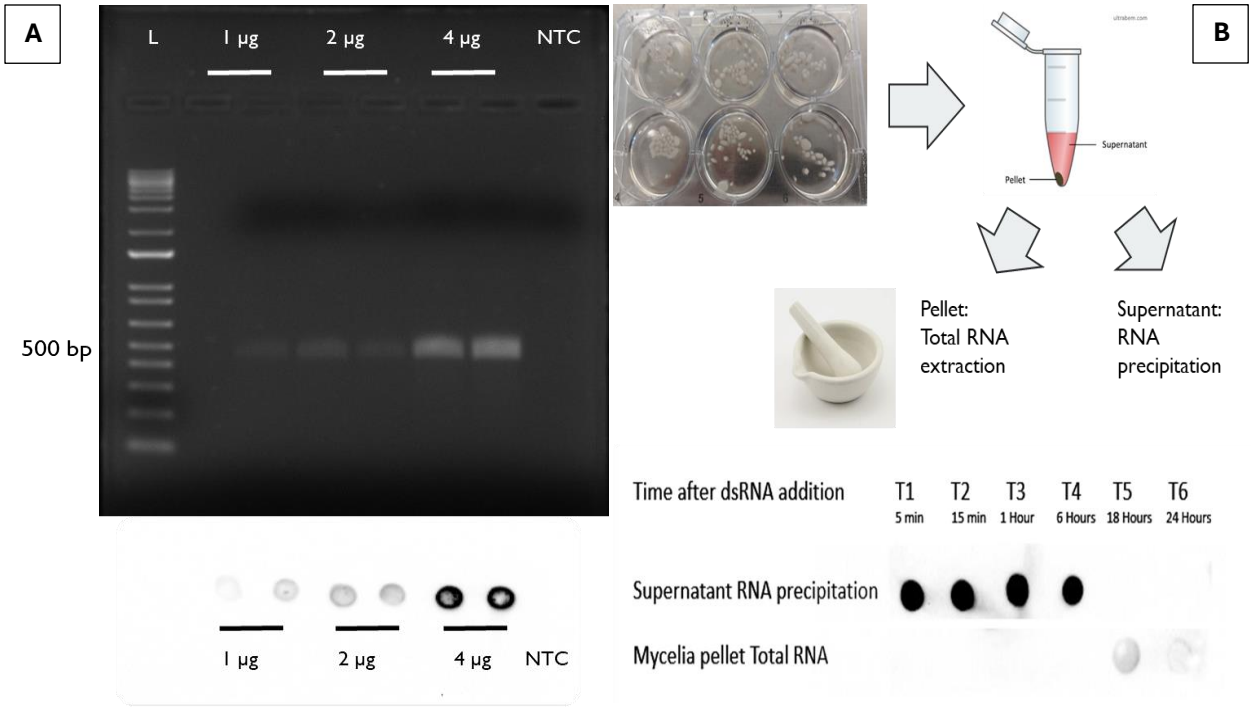

Figure 20. **A**. Upper panel: 1% agarose gel electrophoresis of precipitated dsRNA from SXM medium, 3M Sodium acetate and ethanol were used to trigger precipitation of nucleic acids. The observed bands correspond to the size of dsRNA used (476 bp) and band intensity corresponds to different amounts of dsRNA used (1, 2 & 4 µg). Lower panel: The same samples were used to perform the dot blot approach on positively charged nylon membrane using J2 mAb, intensity of the detected signal matches band intensity after gel electrophoresis. **B**. dsRNA detection after treatment of *V. longisporum* colonies growing in SXM medium, six well plates are aseptically handled in a sterile bench to harvest components of each well to 2 ml Eppendorf tubes, centrifugation is then used to separate the liquid supernatant for RNA precipitation, while total RNA is extracted from the pellet.

The dot blot method was also used to evaluate the protective effect of formulating dsRNA for foliar spray applications, and the effect of formulations net charge on dsRNA retention on leaf surface. *A. thaliana* Col-0 plants were sprayed with different dsRNA formulations (Table 03) and leaves were harvested at several timepoints. Immunoblotting of the total RNA extracted from washed and unwashed leaves (Figure 21) revealed a rapid degradation of unformulated dsRNA, with detectable dsRNA only up to 3 h after spray, while formulated dsRNA with a negative net charge could retain dsRNA up to 3 days after spray, and formulated dsRNA with a positive net charge showing faint signals up to 1 day after spray. Control groups included ddH_2O, unloaded positive and negatively charged nanoparticles did not show any background signals, confirming the high specificity of this approach for dsRNA detection.

While the positively charged formulated dsRNA did not show strong binding to the positively charged nylon membrane when directly applied (Figure 19), it is more likely that dsRNA is released from formulations during total RNA extraction process and thus represents the whole amount of dsRNA remaining at the specified timepoints. Further characterization of dsRNA release kinetics from the formulated nanoparticles is required for a more objective comparison between net charge effect on formulations uptake, stability and release profile.

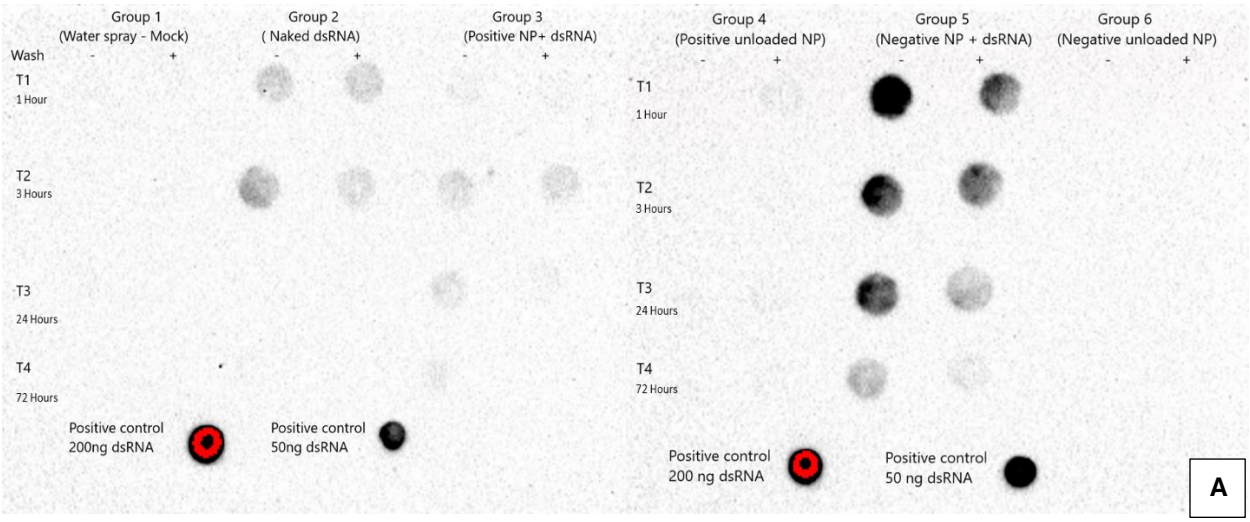

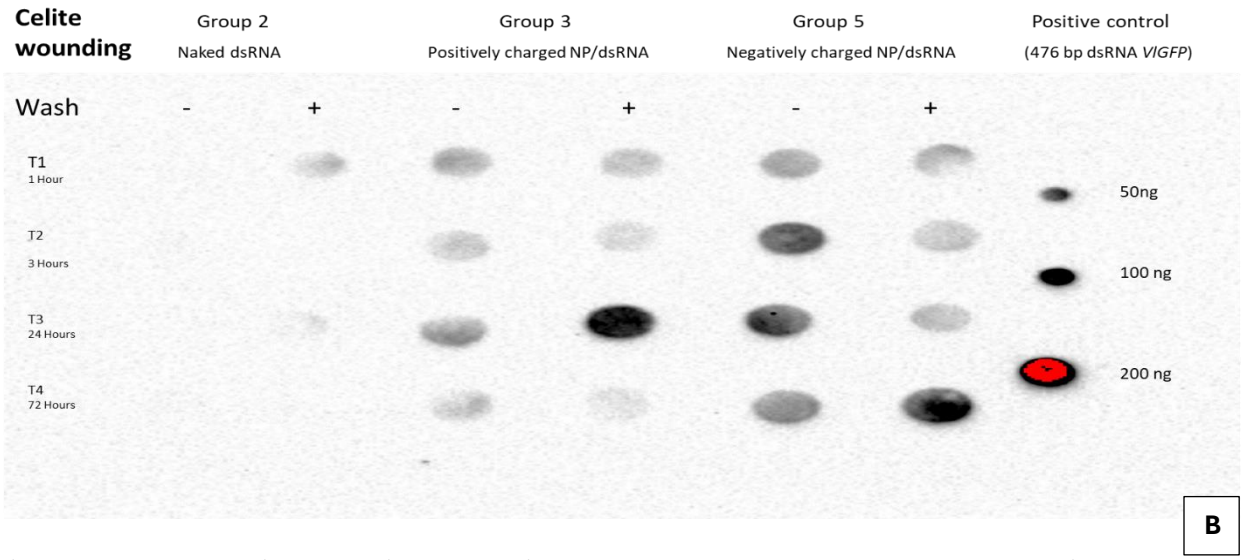

Figure 21. Dot blot analysis for detection of dsRNA in total RNA extracted from harvested leaves, *A. thaliana* Col-0 plants **A.** intact leaves or **B.** after celite wounding were sprayed with an equivalent of 20 µg dsRNA per plant and leaves harvested at four timepoints (T1=1 h after spraying, T2=3 h after spraying, T3=24 h after spraying, T4=72 h after spraying). An equivalent of 1 µg total RNA was directly pipetted on a positively charged nylon membrane. J2 mAB was used to bind dsRNA and Goat anti-mouse IgG was used as secondary antibody followed by Chemiluminescence imaging. Positive controls are 476 bp dsRNA and they showed comparable signal in both blots, while all groups containing no dsRNA did not show any signal. Two leaves were harvested at each time point, one was directly frozen in liquid nitrogen (Wash -) and the other leaf was washed thoroughly (Wash +)

The detection of dsRNA size was explored using north-western blotting, however the blotting step usually led to big losses in nucleic acids transferred from the non-denaturing polyacrylamide gels used for separation according to size, as well as the presence of strong background signals that interfere with results interpretation. The only available commercial dsRNA ladder was tested, and better results were obtained after UV crosslinking of the blotted nucleic acids, however biological samples treated with dsRNA did not come up with similar clarity (Figure 22). Further optimization of this approach is needed to study the timeframe of dsRNA processing and differentiation between dsRNA degradation by nucleases and dsRNA processing to siRNA in the RNAi pathway, where the later scenario should theoretically give rise to various lengths of dsRNA molecules after processing by DCL enzymes, as opposed to the complete degradation expected in case of by RNA nucleases.

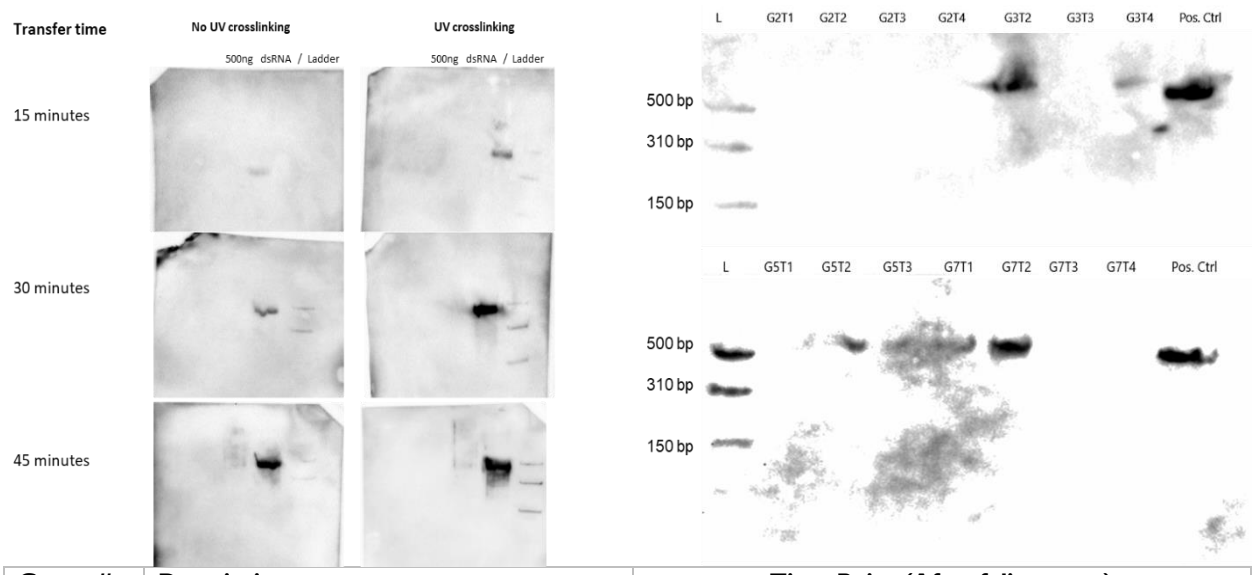

Group #	Description	Time Point (After foliar spray)	
G2	ddH_2O spray	T1	1 Hour
G3	20 µg Naked dsRNA *VlClp-1*	T2	3 Hours
G4	Positive unloaded Nanoparticles	T3	24 Hours
G5	20 µg Positive NP/dsRNA *VlClp-1*	T4	72 Hours
G6	Negative unloaded NP Nanoparticles		
G7	20 µg Negative NP/dsRNA *VlClp-1*		

Figure 22. North-western blotting for size determination of the detected dsRNA after foliar spray of *A. thaliana* Col-0 plants, total RNA is extracted from sprayed leaves and loaded with 6x orange loading dye on 12% Native Polyacrylamide gel. The gel is then used to transfer separated RNA to a positively charge nylon membrane for immunoblotting using J2 mAb as a primary antibody and goat anti-mouse IgG as a secondary antibody. UV crosslinking was found to be essential for retention of dsRNA on the membrane after a 45 min electrophoretic transfer.

3.10. Off-target analysis using *pssRNAit*

Off-target effect is considered to be one of the main challenges facing RNAi as a novel tool for plant protection applications, especially when spray induced gene silencing is considered due to the concern arising from off-targets in open field setting, potentially all organisms in a field could be affected by dsRNA after spraying, given that these dsRNAs are uptaken and processed. The off-target prediction is based on predicting all possible 21 bp siRNAs that could be generated by DICER enzymes upon uptake of long dsRNA, which is then aligned to cDNA sequence libraries from target species. The analysis on default settings with a maximum of 20 off-target results for each predicted siRNAs showed a large number of predicted off-targets for all sequences (Table 04), the number of possible off-targets increased with increasing length of dsRNA while keeping a similar ratio to the dsRNA size in bp, as well as an increase of total number of siRNAs and predicted off-targets based on genome size of plant species in inquiry, reflected in the number of off-targets difference between *A. thaliana* vs *B. napus*. The sequence of dsRNA *VlGFP* showed the highest predicted number of off-targets per bp in both *A. thaliana (0.157 Gbp)* and *B. napus (1.2 Gbp),* due to a higher number of predicted siRNAs and thus more off-target possibilities.

The results are expected to have a similar pattern with every genome checked, since the probabilities of matching any 21 bp sequence to a whole cDNA library is high, alongside the reported tolerance of mismatches in the RISC complex cleavage process (Chen et al. 2021), with a variable allowance of mismatches depending on the biological system in question.

Table 04. Off-target analysis for V. longisporum dsRNA targets on cDNA libraries for *A. thaliana* Col-0 and *B. napus*, using default settings on pssRNAit online tool

		***A. thaliana* Col-0**			
Sequence	**Length (bp)**	**Predicted siRNAs#**	**Predicted off- targets**	**Off-target/bp**	**Top 5 targets (Based on target site accessibility score)**
dsRNA2 *VlClp-1*	467	31	441	0.94	AT4G36680.1, AT3G22660.1, AT2G45640.1, AT2G28190.1, AT2G45000.1
dsRNA *VlCYP1*	472	30	407	0.86	AT2G05630.1, AT3G05130.1, AT2G04062.1, AT5G47050.1, AT2G02300.1
dsRNA *VlIC*	473	28	407	0.86	AT1G05230.5, AT5G49010.2, AT1G48120.1, AT1G32640.1, AT2G20890.1
dsRNA3 *VlClp-1*	477	14	229	0.48	AT2G17410.3, AT1G69280.3, AT3G45110.1, AT1G19460.1, AT3G63270.1
dsRNA *VlGFP*	479	33	503	1.05	AT2G29800.1, AT4G20870.1, AT4G04020.1, AT5G59050.4, AT1G40129.1
dsRNA1 *VlClp-1*	510	24	379	0.74	AT5G53486.4, AT4G32710.1, AT4G13615.1, AT2G43110.1, AT2G47800.1
dsRNA *VlCYP1* *(Full length)*	1784	115	1637	0.92	AT3G62980.1, AT4G30390.1, AT5G07930.2, AT1G18900.3, AT1G31760.1
dsRNA *VlClp-1* *(Full length)*	2904	141	2155	0.74	AT5G53486.4, AT4G32710.1, AT4G36680.1, AT3G26610.1, AT2G45640.1
dsRNA *VlClp-1* *(Full length+ intron)*	4022	193	2881	0.72	AT5G53486.4, AT1G75550.1, AT5G53486.1, AT4G32710.1, AT1G76490.1

		B. napus			
Sequence	**Length (bp)**	**Predicted siRNAs#**	**Predicted off- targets**	**Off-target/bp**	**Top 5 targets (Based on target site accessibility score)**
dsRNA2 *VlClp-1*	467	113	1636	3.5	BnaC09g37030D, BnaA07g12150D, BnaC06g38150D, BnaCnng37900D, BnaC08g08280D
dsRNA *VlCYP1*	472	98	1497	3.2	BnaA08g11330D, BnaC07g26640D, BnaC04g30900D, BnaA04g08660D, BnaC01g36930D
dsRNA *VlIC*	473	134	2095	4.4	BnaA08g25130D, BnaC01g01280D, BnaA10g21010D, BnaA07g09040D, BnaC09g37960D
dsRNA3 *VlClp-1*	477	120	1919	4.0	BnaC04g36330D, BnaA05g01370D, BnaA06g25520D, BnaAnng31060D, BnaA01g23480D
dsRNA *VlGFP*	479	135	2230	4.7	BnaC03g76030D, BnaA08g17700D, BnaC03g22910D, BnaCnng11840D, BnaC09g01530D
dsRNA1 *VlClp-1*	510	83	1289	2.5	BnaA09g00350D, BnaCnng01360D, BnaC06g28960D, BnaA01g28270D, BnaC06g25210D
dsRNA *VlCYP1 (Full length)*	1784	418	6251	3.5	BnaC06g31100D, BnaC05g38100D, BnaA06g08460D, BnaA08g13090D, BnaC05g09840D
dsRNA *VlClp-1 (Full length)*	2904	672	10394	3.6	BnaC09g37030D, BnaA07g12150D, BnaCnng37900D, BnaC08g08280D, BnaC05g18930D
dsRNA *VlClp-1 (Full length+ intron)*	4022	867	13414	3.3	BnaC09g37030D, BnaA07g12150D, BnaCnng37900D, BnaC08g08280D, BnaC05g18930D

Table 05. Summary of different dsRNA gene targets in *V. longisporum* investigated and their effect on gene expression levels (Figure 02), growth pattern (Figure 13) and infection severity in the hydroponic infection assay (Figures 14/15/16). Chlorosis percentage is calculated by comparing yellow pixels area to the overall area of infected *A. thaliana* Col -0 plants at 4 weeks post infection. N/A = not available.

Gene target	***In-vitro* gene silencing (0.5 ng/µl)**	**Growth assay Lower dsRNA conc. (0. 5 ng/µl)**	**Growth assay Higher dsRNA conc. (2.5ng/µl)**	**Hydroponic infection assay (2.5 ng/µl) Foliar Spray**		**Hydroponic infection assay (2.5 ng/µl) Root treatment**	
				Chlorosis percentage 4 wpi (Uninfected Control 3.3%)	Relative Fungal biomass	Chlorosis percentage 4 wpi (Uninfected Control 3.3%)	Relative Fungal biomass
VlClp-1	Down-regulation trend after 72 h	No change in growth	Enhanced growth	17%	Root: 4.77 Leaves: N/A	45%	Root: 2.5 Leaves: N/A
VlCYP1	Down-regulation trend after 72 h	Significant increase in growth	Reduction of growth	20%	N/A N/A	4.2%	Root: 1.51 Leaves: 0.07
VlIC	Not available	No change in growth	Significant reduction of growth	25.2%	Root: 1.6 Leaves: 1.25	7.6%	Root: 0.68 Leaves: 0.63
VlGFP	Down-regulation trend after 72 h	N/A	N/A	N/A		N/A	

Chapter IV. Discussion and outlook

While the RNAi machinery is established in a wide range of eukaryotes to function in immune response and gene regulation, some fungal species such as *Saccharomyces cerevisiae* and *Ustilago maydis* have lost this machinery and do not respond as expected to exogenous dsRNA application (Drinnenberg et al. 2011 and Laurie et al. 2008). Another exception is *Zymoseptoria tritici*, which was found to have lost the ability to uptake exogenous dsRNA, but has a non-canonical RNAi machinery able to produce siRNAs even after knocking out DCL and AGO genes (Kettles et al. 2019). Thus, the ability of *V. longisporum* to uptake exogenous dsRNA was investigated using fluorescently labeled UTP (Figure 01). This approach was found to be more reliable in demonstrating that the observed fluorescence signal comes from intact dsRNA molecules, since the free nucleotides did not associate with *V. longisporum* colonies in the same manner. End labelling of dsRNA using Cy3 was less reliable, due to the uncertainty rising from the ability of this fluorescent tag to associate on its own with cell walls (Supplementary figure 01).

RNAi proteins have been characterized in *Verticillium* genus, supporting the conclusion that dsRNA can be used to target specific genes (Jeseničnik et al. 2019). Furthermore, it was recently demonstrated that *V. dahliae* hyphae can uptake exogenously applied dsRNA (21bp and 500 bp). The dsRNA uptake was found to be mediated through endocytosis, since the use of both clathrin mediated endocytosis and endocytosis inhibitors reduced the observed uptake level. However, it remains unclear whether these internalized dsRNA molecules can escape endosomes to access the cytoplasm and RNAi pathway, or if an alternative active transport mechanism exists in parallel (Liu et al. 2025). Following the internalization of exogenously applied dsRNA in a cell cytoplasm with a functioning RNAi machinery, it is expected that 20-30 nt siRNAs will be produced to target mRNA with complementary sequences. This was confirmed for a transgene (*VlGFP*) in Figure 02.A and two endogenous genes *VlClp-1* and *VlCYP1* in Figure 02.B and 02.C respectively.

The reduction of the targeted gene transcripts followed a similar trend, with a statistically significant reduction observed after 72 h from dsRNA addition. This indicates an expected gap between the time of application and the observation of down-regulation effect, due to the time needed for dsRNA processing, recruitment of RNAi machinery and finally degradation of complementary transcripts.

For the evaluation of RNAi-mediated gene silencing effects on *V. longisporum* virulence, a reliable patho-system was needed. Previous studies of SIGS application to limit *Verticillium* wilt focused on *V. dahliae* (Qiao et al. 2021 and Tao et al. 2025), in both cases dsRNA was applied alongside the inoculation step and thus a single dsRNA application point is possible. Repeated application of dsRNA could offer a more prolonged protection period and simulating this in the lab setting is challenging using plants grown in soil. *V. longisporum* is able to infect the well characterised model dicot plant *A. thaliana* through root dipping. After uprooting and a short inoculation time, the plants could be returned to soil without major stress signals. Infection symptoms like chlorosis and stunting could be observed 2 wpi, and *V. longisporum* gDNA could be detected by PCR from infected leaves gDNA starting from 3 wpi, and to a higher extent in 4th week. However, roots were not accessible for similar detection and the method was time consuming and not scalable, since every single plant requires careful handling and repotting.

Being a root pathogen, a hydroponic system offered a practical alternative to study this interaction and virulence using different gene targets and dsRNA application methods (i.e. root treatment or foliar spray). *V. longisporum* could still infect *A. thaliana* plants grown in the hydroponic system, using rockwool for seed germination and a simple setup, whilst having a direct access to root tissue during the whole incubation time. Detection of *V. longisporum* gDNA was possible from both roots and leaves at 4 wpi (Figure 04.B), with an infection severity depending on the amount of conidia incubated with roots overnight (Figure 04.A). The hydroponic system can be further optimized to enable the evaluation of separate plants leaves and roots, where in the used format the roots of all growing replicates were

inseparable and overlapping rosettes at 4 wpi, limiting infection analysis precision from individual biological replicates.

The bottleneck for gene silencing analysis in *V. longisporum* is the RNA extraction. Fungal colonies are within the "hard to lyse" group of tissues, extracting high quality total RNA required homogenizing individual biological replicates using liquid nitrogen grinding in sterilized mortar and pestle. The yield of total RNA was significantly higher when SXM was used in 6-well-plates compared to PDB, most likely due to the nature of growth with multiple smaller colonies that are easier to break down (Figure 12.B). High-throughput automated RNA extraction platforms could enable screening wider range of dsRNA targets and application strategies, especially when multiple dsRNA sequences could have different gene silencing efficiencies for the same gene (Wang et al. 2019 and Yang et al. 2021). However, it remains a challenge to standardize RNA extraction for fungi on large scale, given the complex cell wall structures and huge diversity of RNases and polyphenols that in some cases limit RNA yields and quality (Cortés-Maldonado et al. 2020).

Gene target selection is a crucial first step for an effective pathogen control using RNAi mechanism, known gene targets of conventional fungicides can be a good starting point for such screening in most cases. In the case of *V. longisporum,* chemical fungicides offer no significant protection, and very limited information is available about virulence mechanisms so far. Therefore, virulence genes identified from *V. dahliae* HIGS studies were selected, based on their size suitability for the *in-vivo* dsRNA production platform and homologues identification in *V. longisporum*. The three tested gene targets from *V. dahliae (VdCYP1, VdClp-1, VdIC)* were identified in *V. longisporum* with high identity matches of protein sequences (≥96%), making it a reliable source for gene targets to be screened. However, the first challenge in the transferability of gene targets lies in the mechanistic difference between SIGS and HIGS approaches, in terms of the number of siRNAs available for gene silencing and their consistent presence, which is more favorable in case of HIGS. On the other hand, in SIGS, the longer dsRNA constructs could provide stronger gene silencing

levels in some cases due to the presence of more than one siRNA targeting the same mRNA sequence (Koch et al. 2019).

The transfer of siRNAs from host to pathogen (and vice versa) was well documented in many different plant-fungi interactions (Zhang Tao et al. 2016, Wang et al. 2016), but the direct comparison between the two systems remains objectively impossible; given the lack of tools to match siRNA concentrations from both approaches, as well as mechanistic differences since the sprayed dsRNA can be uptaken directly by the pathogen, where the RNAi machinery will be alerted and all proteins recruited for further gene silencing processes to take place. In HIGS the transferred siRNA wouldn't trigger the same strong immune response and would be in a competitive disadvantage (Kakiyama et al. 2019). The lack of secondary amplification of gene silencing effect by RDRs was illustrated in *V. dahliae* targeted by HIGS in *A. thaliana* (Zhang et al. 2022), but it remains unclear if using longer dsRNA constructs would lead to secondary amplification of gene silencing effects, given that three RDRs are predicted in *V. dahliae* (Jin et al. 2019).

The second challenge in the transferability of gene targets is the genomic differences between the haploid *V. dahliae* genome and nearly diploid genome of *V. longisporum*, which can influence the efficiency of gene silencing on disease severity. To address these challenges and the throughput limitation of RT-qPCR based evaluation, the GFP fluorescence-based approach was developed to investigate the effects of different dsRNA molecules on the growth rates of *V. longisporum GFP* in 96-well-plates (Figure 12/13). This approach enables a preliminary screening stage of gene target(s) leading to *in-vitro* growth reduction, and thus would have a higher potential as a virulence limiting gene targets. Obtaining uniform fluorescence values relied on consistent number of conidia in each well, dilution of the conidia solution led to lower standard deviation between similar treatment groups.

The growth medium selection was based on medium background fluorescence, SXM had the lowest influence on background fluorescence compared to PDB and HA mediums, SXM was also found to better simulate the transcriptional state expected *in-planta* (Leonard et al. 2020). The correlation coefficient between the number of starting conidia and GFP fluorescence was highest between 3 and 7 days, which corresponds to the exponential growth phase, with a peak growth and depletion of the liquid medium observed after 11 days.

Sterile conditions could be maintained throughout the measurement days and re-addition of dsRNA can be done under aseptic conditions, which adds to the flexibility of this approach and high throughput screening of various gene targets or dsRNA concentrations, thereby speeding up the target selection process. Similar approaches have been reported for bacterial *in-vitro* growth estimation based on fluorescence intensity measurement, showing comparable results to cell counting and optical density (OD) methods, and providing even lower variation coefficients in some cases (Blay et al. 2020 and Krishnamurthi et al. 2021).

The tested gene targets (*VlClp-1*, *VlCYP1* and *VlIC*) showed variable effects on growth curves of *V. longisporum*, based on the concentration of dsRNA used (Figure 13). While silencing of *VlClp-1* was expected to reduce virulence of *V. longisporum* as in the case reported in *V. dahliae,* rather an increase in growth was observed in the *in-vitro* growth assay (Figure 13) and higher AUDPC in the hydroponic infection assay (Figure 14). Different variants of the calpain protein family were found to affect growth, conidiation and pathogenicity of *M. oryzae* differently (Liu et al. 2016), the knockout of certain calpain protein variants showed a faster growth rate and could be explained by the absence of autophagy and growth regulating roles carried out by this protein family. These results also showcase the genome complexity of the amphidiploid *V. longisporum*, targeting a crucial homeostasis gene might trigger transcriptional changes or increase expression of an alternative "redundant" variants, highlighting the importance of an initial screening step when *V. dahliae* gene targets are investigated.

The interaction between dsRNA and fungi can also be seen in the case of mycoviruses, these viruses were found to infect a wide range of fungal species and affect their virulence levels, either hypervirulence or hypovirulence can occur depending on the virus and infected fungal species (Kotta-Loizou et al. 2021). RNA silencing is in the centre of this interaction, viral dsRNA can be processed by the fungal RNAi machinery leading to transcriptional silencing of fungal genes, an off-target effect in this case, or RNA silencing inhibition by viral proteins leading to limited gene regulation.

The observed changes in growth rates were concentration dependant, lower dsRNA *VlCYP1* (0.5 ng/µl) concentration led to a significant increase in growth as opposed to the higher concentration (2.5 ng/µl) showing slower growth. These variable responses might be due to triggering transcriptional changes associated with the anti-viral immune response without efficiently silencing the target gene in the former scenario, compared to a more profound RNA silencing of target gene in the latter case.

However, in the case of dsRNA *VlIC,* lower concentration (0.5 ng/µl) did not lead to faster rates of growth, and the higher concentration (2.5 ng/µl) significantly reduced growth after seven days. Therefore, the observed changes in growth rates of *V. longisporum* were sequence based, given that all three gene targets tested resulted in different responses at the same concentration, dsRNA length and fluorescence measuring conditions (Table 05). Beside the sequence specific responses, sequence unspecific effects were observed in a recent study on *M. oryzae* following exogenous dsRNA application (Zheng et al. 2025), dsRNA triggered reactive oxygen species (ROS) production, influenced germ tube length and activated the high osmolarity glycerol (HOG) stress pathway, all pointing towards the detection of dsRNA longer than 30 bp and the initiation of stress responses.

More in-depth studies on different systems are needed to fully understand the fungal responses to dsRNA application, to identify all involved factors and design dsRNA with maximum efficacy, through uncoupling of sequence specific intended effects and sequence unspecific stress responses. Poly I:C can play a big role in such investigations, the synthetic

analogue for dsRNA with polyinosinic-polycytidylic acid base pairing, it can trigger the same immune response to gene specific dsRNA without proceeding to any gene silencing actions. dsRNA targeting a non-endogenous gene like GFP is commonly used as a non-specific dsRNA for confirming the observed beneficial effects in SIGS experiments, while *in-silico* off-target analysis predicts the highest off-targets/bp for *VlGFP* dsRNA (Table 04). The only limitation to be addressed for Poly I:C use is matching the size of dsRNA used, since the commercially available Poly I:C contains a mixture of different lengths – 200 to 1000 bp for low molecular weight Poly I:C - and would therefore affect precise estimation of the sequence unspecific effects (Kato et al. 2008).

The observed effects of dsRNA application on growth rates of *V. longisporum* at a concentration of 2.5 ng/µl were also observed on the disease severity in the hydroponic infection assay after root treatment. Addition of dsRNA *VlClp-1* led to more severe infection reflected in the elevated chlorosis and overall AUDPC when compared to the infected and untreated control group.

While both dsRNA *VlCYP1* and *VlIC* root treatment led to decreased chlorosis and overall lower AUDPC closest to uninfected control group, and reduced relative fungal biomass in the case of dsRNA *VlIC*. These effects were achieved when dsRNA was applied 24 hours before infection with conidia of *V. longisporum* as root treatment, simultaneous application of dsRNA and conidia or foliar spray application did not match the reduction in disease severity or relative fungal biomass. The hydroponic infection assay provides a good benchmark for developing efficient dsRNA delivery systems against root pathogens, which requires “cross-kingdom RNAi” through uptake and translocation of large amounts of dsRNA in the case of foliar spray application (Wang et al. 2016). Alternatively, formulations designed for root application might be a more realistic approach, given the complex life cycle and resilience of *Verticillium* microsclerotia in the soil. The hydroponic infection system can be improved through separating individual biological replicates for better imaging and root fungal biomass analysis on a larger scale (Wang et al. 2019).

The selected *in-vivo* dsRNA big scale production in *P. syringae* was not suitable for fungal gene constructs for yet unknown reasons. The size of gene inserts was excluded as a limiting criterion for polymerase complex (PC) stability and successful dsRNA *in-vivo* production, through matching the original phi6 genome sizes (*pMS2/VlClp-1* 4 kb) and using only one cloned vector in combination with the original phi6 vectors (Table 02). Furthermore, the integrity of cloned vectors was confirmed through *in-vitro* dsRNA expression (Figure 08) and sanger sequencing (Data not shown). These results points towards a yet unknown factors involved in the packaging step of ssRNA to PC and the stability of these PCs, possibly through uncharacterized sequence elements that are present in viral sequences and absent from fungal ones. Another possible cause could be a higher susceptibility to recombination or a significantly different prevalence of secondary structures in fungal sequences that interferes with ssRNA packaging to PCs.

E. coli HT115 (DE3) based systems are continuously optimized for better yields of dsRNA, minimizing costs of purification and exploring alternative non-toxic inducers (da Rosa et al. 2024), the strain was originally developed for studying gene silencing in *C. elegans* (Timmons et al. 2001), the suppression of RNase III in this strain allows cellular accumulation of dsRNA produced from cloned vectors by T7 polymerase that is inducible by IPTG.

One major advantage of this system is the specificity of dsRNA produced, the absence of unneeded phi6 specific dsRNA produced from the L-segment of phi6 genome in the *P. syringae* system, purification of such biproduct raises the cost and affects the yield of dsRNA production. Second advantage is the size flexibility of the produced dsRNA molecules, *P. syringae* system produces three dsRNAs from each vector (L – M – S segments) with relatively large sizes; 7599 bp, 4063 bp and 2948 bp respectively. While targeting the whole sequence of a certain gene might lead to a stronger knock-down effect and wider availability of siRNAs for a sustained effect, it also means a higher probability of unintended off-target effects. Additional enzymatic digestion or extensive purification steps would considerably raise the price of dsRNA production, and would miss the point of the production system.

More commonly, dsRNA molecules around 200-800 bp are becoming the benchmark for RNAi studies. The recent advancement and decreasing cost/g of dsRNA production and purification addresses this hurdle and shifts the focus towards developing efficient dsRNA delivery systems (Figueiredo Prates et al. 2023).

Chitosan/alginate nanoparticles provided protection of dsRNA against RNase III and MNase degradation, and showed extended stability of long dsRNA after foliar spray application (Figure 21), especially for the negatively charged formulated nanoparticles. The charge of the formulated nanoparticles impacted the PTI response after foliar spray, seen more significantly after surface wounding using celite (Figures 17/18), as well as triggering different immune pathways depending on the nanoparticles net charge. These results imply a limited systematic uptake of dsRNA when applied to intact leaf surface and therefore limits their SIGS potential use against root pathogens.

Another aspect to consider in formulation development should be immunogenicity of the materials used, due to the intertwined and antagonistic relationship between plant immune response and plant development functions (Brown 2002, Nakano and Shimasaki 2024 and Ning et al. 2017), and the simultaneous activation of multiple immune pathways in the infection assay setting - pathogen, dsRNA and formulation particles – which might trigger a growth trade-off (He et al. 2022). Positively charged chitosan/alginate formulations showed a significant upregulation of *AtPR2* and *AtPR5* after celite wounding, both pathogenesis related (PR) genes are linked to salicylic acid response to biotrophic pathogens in systemic acquired resistance (Durrant and Dong 2004). On the other hand, negatively charged chitosan/alginate formulations showed no significant upregulation of PR genes with or without wounding, significant upregulation of *AtZAT12* and *AtCBP60g* was short lived and their expression levels returned back to basal levels within 24 hours after foliar spray. The differences between both formulations highlights the relationship between the surface charge and their perception by plant cells, in this context negatively charged formulations would be preferred, given their lower immunogenicity, better uptake by roots and longer

duration of protecting dsRNA from degradation. The release kinetics of dsRNA from the formulated nanoparticles was not sufficiently characterized.

It is reasonable to expect that a longer time for gene silencing effects will be needed compared to naked dsRNA, which is directly available for uptake and processing by RNAi machinery. This delay in action was reflected in the *in-vitro* gene silencing results for both dsRNA *VlGFP* and dsRNA *VlClp-1* (Figure 11). It remains unclear how long exactly is needed and how much dsRNA will be available for gene silencing action from the formulated nanoparticles. The delay in release of dsRNA after formulations was also reported in other formulation strategies like BioClay (Niño-Sánchez et al. 2022), where uptake of formulated fluorescently labeled dsRNA was not visible after 3 h and 16 h post addition to *B. cinerea* growing conidia, while naked fluorescently labeled dsRNA was.

Methods for dsRNA detection are developing to offer a better understanding of its fate in different systems. These methods include labeling dsRNA using fluorescent tags for microscopic observation to evaluate their uptake and distribution, immunoblotting using dsRNA specific mAB (Schonborn et al. 1991), digestion of single stranded RNA using RNase A followed by agarose gel electrophoresis (Poynter et al. 2017), and northern blotting using radioactively or non-radioactively labeled probes matching the dsRNA sequence (Mitter et al. 2017).

While many of these methods were intended for viral dsRNA detection or to avoid dsRNA contamination as an immunogenic byproduct during *in-vitro* mRNA synthesis, the re-purposed dsRNA detection dot-blot for monitoring dsRNA stability provides a practical solution to further study release kinetics and half-life of dsRNA in various setups (Figure 20/21). The approach showed high sensitivity and specificity to dsRNA longer than 40 bp, regardless of their sequence (Figure 19). Further analytical methods need to be developed for differentiating intact dsRNA and processed dsRNA, in order to have an objective comparison between different formulation strategies and to ensure that the applied dsRNA could achieve its intended purpose. The challenge lies in the ability to extract such processed products of long dsRNA at detectable concentrations and their efficient transfer

following gel electrophoresis prior to immunoblotting. A potential solution to select only cells affected by dsRNA is fluorescence activated cell sorting (FACS), applying this technique after using fluorescently labelled dsRNA would lead to separating cell fractions based on dsRNA uptake. This enrichment would potentially lead to a more objective analysis and a wider understanding of the interaction between dsRNA and the targeted organism (Bleichrodt and Read 2019, Vlaardingerbroek et al. 2015).

Potential Off-targets in the treated host or NTO represents the major regulatory concern for RNAi based plant protectants. Bioinformatics online platforms are addressing this concern through aiding in designing dsRNA with the least potential matches outside the gene target of the investigated pathogen. A recent example is dsRIP, an online platform intended to find gene targets and design dsRNA for targeting insect pests and few fungal pathogens (Cedden et al. 2025).

The results of potential off-targets for *V. longisporum* gene targets in *A. thaliana* and *B. napus* (Table 04) reflects the necessity of sequence analysis to minimize that risk as much as possible. While the number of predicted off-targets is inflated due to using the conservative default parameters like off-target accessibility estimate, shorter dsRNA sequences will possess a smaller risk of off-targets in any environmental setting, where many different organisms will be subjected to potential gene knockdowns, with varying RNAi sensitivities and functions that are beyond bioinformatic estimation capabilities.

Therefore, *in-silico* predicted off-targets include many false positives and does not necessarily means a negative effect will take place if an off-target gene is silenced in the host plant or an NTO. Small RNA sequencing might give a better idea about the exact populations of siRNAs generated after dsRNA application in a given system, and will provide a more precise estimate of potential off-targets based on the actual siRNAs pool. Alternatively, *in-vitro* assays aiming to simulate processes like dsRNA conversion to siRNAs and target mRNA cleavage were developed for designing the most efficient gene silencing sequences against *Cucumber mosaic virus* (CMV), beside the efficacy screening, it can be a useful approach to understand how different plant systems will react to dsRNA application

(Knoblich et al. 2025). However, this post application fate of dsRNA on non-target organisms remains unclear in most systems and hinders a complete risk assessment for using dsRNA in open field setting (Devisetty et al. 2025).

With a growing knowledge about the RNAi mechanism in different systems, advances in reducing production costs of dsRNA and multiple products in the regulatory pipeline, there is little doubt about the future availability of SIGS based plant protectant products as a less toxic alternative to chemical ones. Progress in the regulatory side is not moving with the same pace, mostly due to the lack of harmonized testing methods and definitive answers to the concerns surrounding this new technology (Gunasekara et al. 2025). Areas that could be harmonized in RNAi based research include size of dsRNA, amount of dsRNA, “unspecific” controls in efficacy experiments and frequency of application. Answering the off-targets effect dilemma and NTO exposure risk assessment should be the top priorities for advancing SIGS research, through defining its limitations and identifying the scope of potential uses for a clear way forward.

Establishing biosafety screens that includes the most relevant organisms (e.g. pollinators, invertebrates) will be highly beneficial, first to identify the maximum allowable concentrations that don't lead to negative environmental effects, and more importantly to gain public trust through showcasing that this new technology is indeed less toxic than conventional pesticides (Tardin-Coelho et al. 2025). This ecological risk assessment was prioritized by OECD conference participants including scientists, regulators and industry representatives in 2019 (Mendelsohn et al. 2019), however, progress in many sides of the eco-toxicological research is still not evident (Zarrabian and Sherif 2024).

N.B. The results from this thesis are not published.

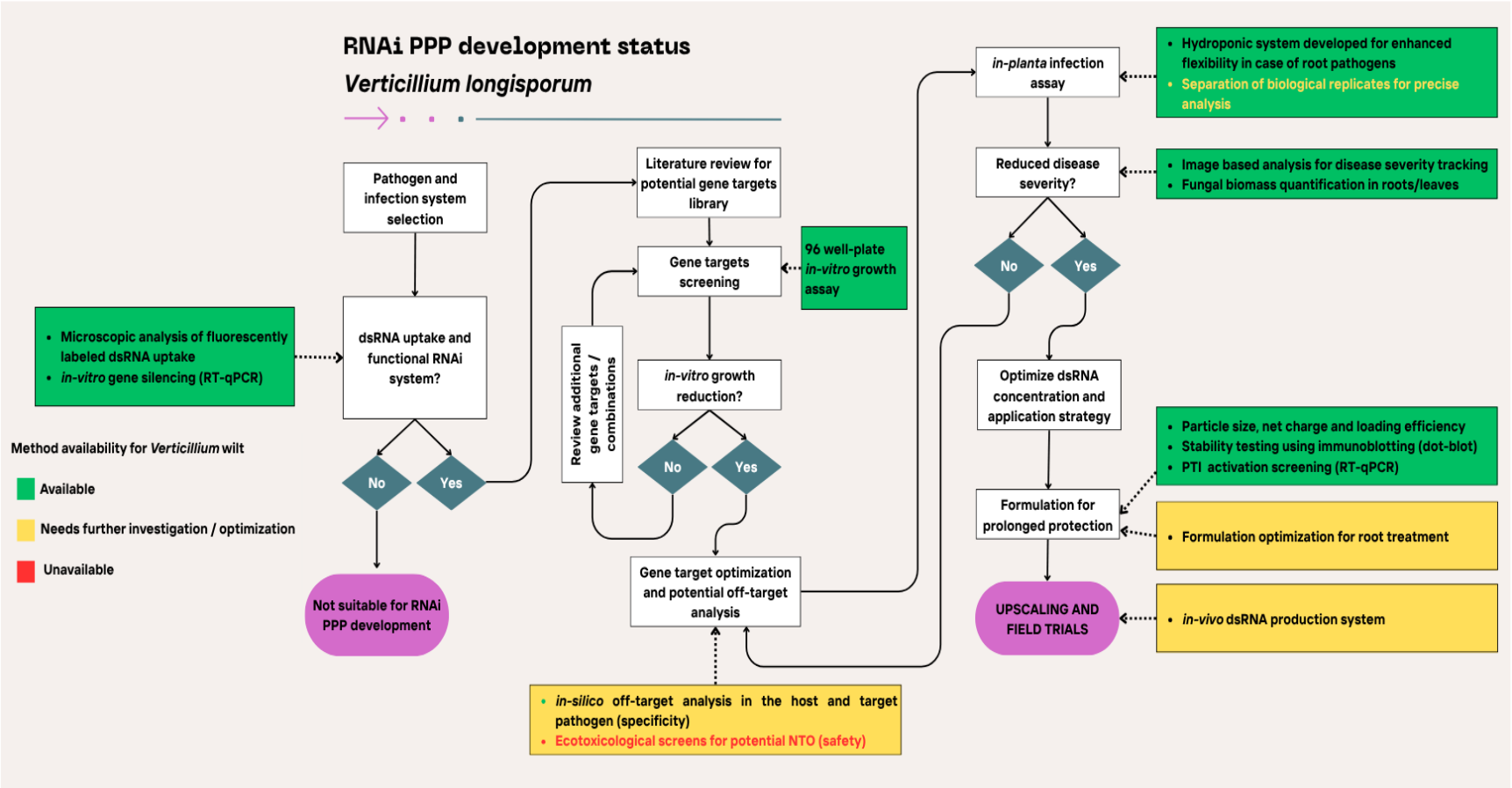

Figure 01: Flowchart for suggested processes in RNAi plant protection product (PPP) development and method availability for each step in *Verticillium* wilt management

Conclusion

RNAi has been demonstrated as an emerging mechanism in handling a wide range of plant pathogens and still holds a potential for even wider applications. In the case of *V. longisporum*, different outcomes have been observed based on dsRNA gene targets, site of application and concentrations. The high-throughput growth assay presents as an excellent opportunity to determine gene target(s) leading to *Verticillium* growth reduction or even lethality, thereby bringing this technology a step closer to field application. While large scale dsRNA production was not successful using the *P. syringae in-vivo* system, other cost-efficient platforms are available, shifting the focus towards dsRNA delivery and stabilization. Environmental considerations remain an important aspect in functionalized formulations for better dsRNA stability and uptake, due to the conserved RNAi machinery in almost all eukaryotes and the practically immeasurable NTO exposure consequences. Chitosan/alginate nanoparticles protected dsRNA from nuclease degradation and thus prolongs dsRNA presence on leaf surfaces, which makes it suitable for leaf pathogens or leaf ingesting insects. Immunogenicity of both chitosan and alginate limits their systemic use for root pathogens, where dsRNA uptake and translocation are needed prior to transfer to the invading fungal cells. General recommendations for dsRNA formulation for a root pathogen would be: i) Particle size in the range of passive diffusion ≈10-50 nm, ii) inert substance(s) to avoid priming effects and minimize unspecific effects and iii) clear dsRNA quantification and release kinetics from formulation.

Supplementary data

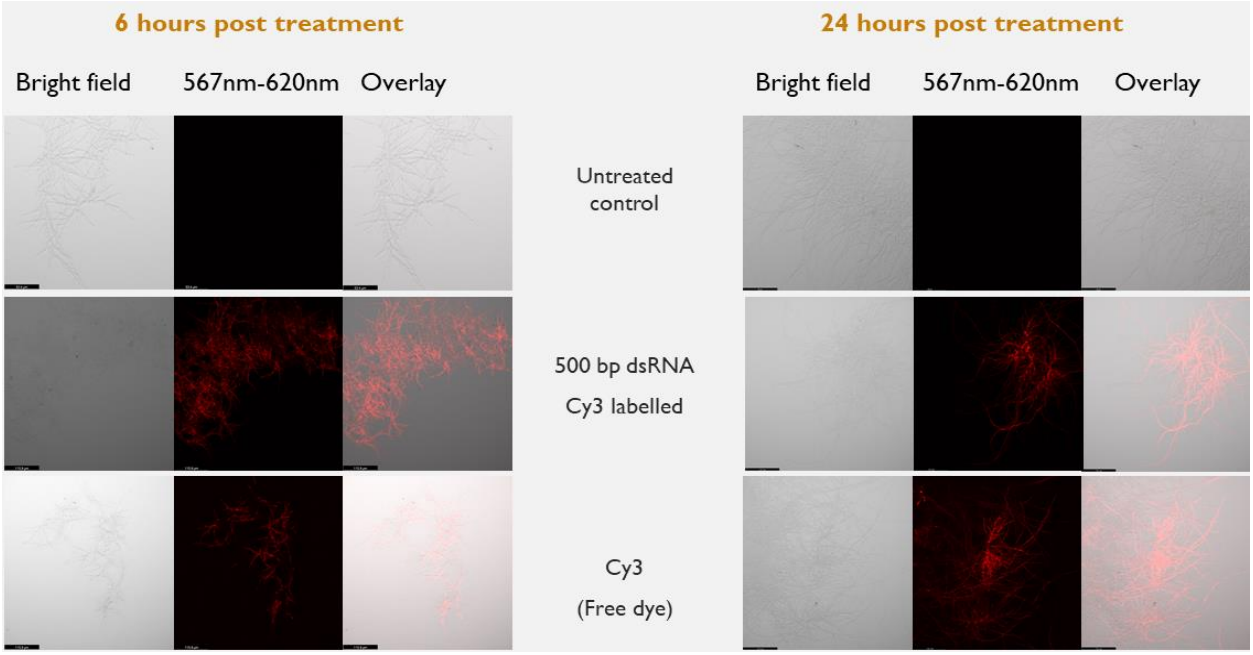

Supplementary figure 01. CLSM pictures of treated *V. longisporum* wildtype (Vl41) using Cy3 labelled dsRNA (476 bp) and the signal accumulation of free dye. Pictures were taken 6 h and 24 h post treatment of *V. longisporum* colonies in sterile conditions, scale bar is 116 µm.

Sequences

> dsRNA3 *VlClp1* (477bp)
CGTTGACAATGTCTTGGCCTCCATGATCACGTAGGCATGACCCTCACAGATACCGACACGGTCGCCATATCCGC
ATTCGAGCAAACCCGTGGAGCAGCCAAACATGAATTCTGAGTTCACCTTGGACAATTCATTATCCCAGAAGCTGTC
GAGATCCAGTATATCAGACGTCAAGATCTCCGCTGTGACGCCACCAGAGAGATCTTCCAAGGCCTCGCCAATCC
AGCCGCCCACCAGCGAAGCATAGTCGCCGTGGGCTTTGGCGTAGGCCTTCTCAAGAAGAGGGACCCAGGTTTC
ATTCTGGTCGATACACTTGCCGAAGTAGAGGGCTTTTGATCCTGTCTGGTACGTTTGACGGTACACGCGCTCCTGG
TCTTCGCGATCAATCTGCTGTAGCAGCTCCCGCTGCTTACTCCTCGAGTCCCAGGTGGGTGACTTGAGATAGAGC
TTATCGTCGATGATGGAGTAGACCCACTC

> dsRNA *VlCYP1* (472 bp)
TAATACGACTCACTATAGgGAGAACGGACATGGCAGGAGAGTGTCTTGATCACATGGCGGCCGGCATCGACACA
ACGGGCGATGGCCTTTGTTTCCTCATGTGGCAGCTGTCGCAGCCATCGTCGATGCACTGCCAGGAGAAGCTGCA
GCAGGAGCTGCGCAACAACCCAGATGCCGACTTTGACAAGCTGCCCTACCTGGATGCCGTGATCCAGGAAGGC
TTGCGATGCTTCCCCCCCATCCCCATGTCGCTTCCCCGACGAGTGCCGCAGGGCGGAAAGGTTGTGGACGGCT
TCATCGTGCCCGGAGGCACCATCGTCAGCTGCCAAGCGTACTCTGTGCACACAATCAACAGCCAGGTATTCCCT
GAGCCGGAGACATTCGATCCCGAGCGATGGACTGCCGCAGAGGGCGACGTGGAGCGAAAACGACTCATGTTTG
CGTTCGCTCTCcCTATAGTGAGTCGTATTA

> dsRNA *VlIC* (473 bp)
GGTTGAACGAGCACATGGCCGACGTCTTCAATGAAAATGCCATTAACGTTGCCGAAATGTTCAAGACGCCCGGAA
AGCTTCGGGGGGAAACGCCGCGAACCGCGAGAAAAGTCATCACAGGAGAACCTCGCGTTCCTCTCTCAGATAT
CTTCTCCTCCGCGTCGAAGGGAGCGCCGACACCGTTCACGCAGCAGCTAGGTCGCATGCAGTCGCCGAGGTTA
CAGGCTTCAAACTCCAGGTCGCCGCTCGCCAACAAGATCGCGTCCCCATTGAGACCTCTGCCGTCGATGCGGC
CTCAACCTACTAAGAATGCAGCACTTCCGGCGGACTCTGGCTATTATGGGAGCCAGTCTCAGGACGTGATGGATG
TTGACCATCACGTTTACGCGACGCAGTCTACACAGCCTTTCAGCCCTGTTCGAGAAGCCGACTTGAACGAAGAC
GTCGCGTTCCACGTCGATGAACCCTCAACA

> dsRNA *VlGFP* (479 bp)
ACCACATGAAGCAGCACGACTTCTTCAAGTCCGCCATGCCCGAAGGCTACGTCCAGGAGCGCACCATCTTCTTC
AAGGACGACGGCAACTACAAGACCCGCGCCGAGGTGAAGTTCGAGGGCGACACCCTGGTGAACCGCATCGAG
CTGAAGGGCATCGACTTCAAGGAGGACGGCAACATCCTGGGGCACAAGCTGGAGTACAACTACAACAGCCACA
ACGTCTATATCATGGCCGACAAGCAGAAGAACGGCATCAAGGTGAACTTCAAGATCCGCCACAACATCGAGGAC
GGCAGCGTGCAGCTCGCCGACCACTACCAGCAGAACACCCCCATCGGCGACGGCCCCGTGCTGCTGCCCGA
CAACCACTACCTGAGCACCCAGTCCGCCCTGAGCAAAGACCCCAACGAGAAGCGCGATCACATGGTCCTGCT
GGAGTTCGTGACCGCCGCCGGGATCACTCTCGGCATGGACGAG

> V*lClp-1* dsRNA1 (510 bp)
GGACATCTCTAGCAGAGCTCCTTCTCAGACTCTGCCGGTGTCGGCTGTGGTGTGACGAGCACACCTGGAGTACT
TGCGCCCGAGTCGAGTTTGTCAAAGTCGGAACTGCCAGAGCTCCTTTCCGACTTTGTGTCATCCTCTGGCTTAGTT
TGATCTTCGGTCTCGGGCGCGTCGTCGGCATCACCATCTCCCTGGACGGACGAAGGGGTCGGCGCAGGTTCC
GGCTCAGCCTCGTTGTCGCGCTCTCCTCCAGCGTTGACTTGAGCGTCATCTAGGTCGGCGCCGCCCTTCTTGCC
CATACCGCCCTCCTCGAGATCGCCACCCTCCAGGACCACCTTCAGCTCGAGATCTTCGTCCATTGTGTAGACGC
GAACACCGATGACGCAGATGGCATTCCACGGGTCAGGTGCATTCTCGTCTTCAGACTCGTAGATCTCGGCTTTGG
TTAAGGGAGGCCCAGCGGGTTTTGCCCTGGGTTTGCGTACGAAGTCATCGTCGCTGTACAAGAGC

> *VlClp-1* dsRNA2 (467 bp)
GGTGCAGGTGATGGAGTCGTCGCCTTTTCATCTTCAGCAGGCGGTTCCTTTTGGGTAATGACCTTCGGGGCATCC
TTGGCGTTCTGGCCCTGTTGGGTCCCCTCGTCCGCCTCATCATTCCCGCCCTCATCGTCGCCCTCTTCTGCTTCT
TCCTTGGCCTTGGTGGCCTTTCGTTCTTTCTTTTCGAGGTTCTTGGCCTTCTGTTGCTTGTTGACCTGACGTGTAAGA
CGGCGCCTCTCCCACTGTTTCCGGCGCTCCTCTTTGCGCAGTGCGGATGCCTTCTTCTGTTCCTTCTCCTTACGC
AGGCGGGAGACCTCCTCGAGATGAGCCGCGGCCTTGCTGTGGGCCAAGTCATAGGCGTAGCCCACCTGTGCA
AGCTTGGCGTTACCACTGCGGTGCTTACACTCGCGCTTAACGACGTCCTCGACAGAGTCAAGCTGCGTGTAGCG
CTCAGCTTTGACGCTGAT

> *VlClp*_4kb M-segment cloning insert
GCTCCTTTCCGACTTTGTGTCATCCTCTGGCTTAGTTTGATCTTCGGTCTCGGGCGCGTCGTCGGCATCACCATCT
CCCTGGACGGACGAAGGGGTCGGCGCAGGTTCCGGCTCAGCCTCGTTGTCGCGCTCTCCTCCAGCGTTGACTT
GAGCGTCATCTAGGTCGGCGCCGCCCTTCTTGCCCATACCGCCCTCCTCGAGATCGCCACCCTCCAGGACCA
CCTTCAGCTCGAGATCTTCGTCCATTGTGTAGACGCGAACACCGATGACGCAGATGGCATTCCACGGGTCAGGT
GCATTCTCGTCTTCAGACTCGTAGATCTCGGCTTTGGTTAAGGGAGGCCCAGCGGGTTTTGCCCTGGGTTTGCGT
ACGAAGTCATCGTCGCTGTACAAGAGCTCGTGGTCCTCAATAGGAGAATCCGATGACTCGCCGTCCGAGACTTCT

TCGACCTTTTTGGCAGCCTTTTTGGACGGTGCAGGTGATGGAGTCGTCGCCTTTTCATCTTCAGCAGGCGGTTCCT
TTTGGGTAATGACCTTCGGGGCATCCTTGGCGTTCTGGCCCTGTTGGGTCCCCTCGTCCGCCTCATCATTCCCGC
CCTCATCGTCGCCCTCTTCTGCTTCTTCCTTGGCCTTGGTGGCCTTTCGTTCTTTCTTTTCGAGGTTCTTGGCCTTCT
GTTGCTTGTTGACCTGACGTGTAAGACGGCGCCTCTCCCACTGTTTCCGGCGCTCCTCTTTGCGCAGTGCGGATG
CCTTCTTCTGTTCCTTCTCCTTACGCAGGCGGGAGACCTCCTCGAGATGAGCCGCGGCCTTGCTGTGGGCCAAG
TCATAGGCGTAGCCCACCTGTGCAAGCTTGGCGTTACCACTGCGGTGCTTACACTCGCGCTTAACGACGTCCTC
GACAGAGTCAAGCTGCGTGTAGCGCTCAGCTTTGACGCTGATGAAAATGCTGTAGTCACCAGCAGGCATGTCAG
GAATCTCGATGGATACGGAACGGCTCATCAAATAGTTCCCGTGAGACCGGACAATGTAGTCCTCGGCGTTTGGTC
GACCTTTCTCATGGACACGGAAGTGAAGCTCAAACCGGTATTGGCCGTGGAGTCCCTTGAAATACCGGTTATCCA
GTTGGGACAGGGAAATTACCATTGGCGAGTCCTTGGTGAGTTTGACTTGGAACTTCTCGTTGTACTGTGGCTTCCA
GGGAACATCGACGCCGATCCATCGTTGACAGCACCTCCACTTTGGGTCGTTGAATAGTCGCGTGCGGTCGAAAT
GCTGGAACTTGTTGAGAAAGTCCTCGTAAGAGATCCAGAAAACTGAATCGTTGCCGAATTGATGGCCTAGCTCTGC
CTGGATCTCAGGAGTCCAGTCTCGAGAACCATCGGACCAGGCTCCCTCCCAGATACCCTTACGAATTTTGCCCC
ACGGGTTCCTTTTGGGGTGTCAGCTCACAAATCACACCAGGAACAGAAGGTCGGGTCACATACCTGAGCTTGAC
GAGCCGCGTCCCCGTTGACAATGTCTTGGCCTCCATGATCACGTAGGCATGACCCTCACAGATACCGACACGGT
CGCCATATCCGCATTCGAGCAAACCCGTGGAGCAGCCAAACATGAATTCTGAGTTCACCTTGGACAATTCATTATC
CCAGAAGCTGTCGAGATCCAGTATATCAGACGTCAAGATCTCCGCTGTGACGCCACCAGAGAGATCTTCCAAGG
CCTCGCCAATCCAGCCGCCCACCAGCGAAGCATAGTCGCCGTGGGCTTTGGCGTAGGCCTTCTCAAGAAGAGG
GACCCAGGTTTCATTCTGGTCGATACACTTGCCGAAGTAGAGGGCTTTTGATCCTGTCTGGTACGTTTGACGGTAC
ACGCGCTCCTGGTCTTCGCGATCAATCTGCTGTAGCAGCTCCCGCTGCTTACTCCTCGAGTCCCAGGTGGGTGA
CTTGAGATAGAGCTTATCGTCGATGATGGAGTAGACCCACTCGCCGTCTTGTGTCCTGGTCAGTACCTGATGCAGT
CGATCCGAATGCCAGCCGCCACATTTACATACCTCTGTAAAAGACAAAGCCGTAGATGCCAACACGTGTGTCATA
TTCCACACAGATCCGCCGCAGACTCTCGGGCTCATTGGCCAGGGCCGTGAAACTGGCGATCAGCCAGCAATTG
CCGATGCTGCCTTGCTGGACGTCTCTGCCGTCGACATTCTTCATGAAAGTCGGCTTCTCGAAGATCTCGTGGACT
CGCTTCACAGCCTTGGGCACTGAGGCGCTGCTGTCGGCGAGGGTGGCCTTGTTGATCGACCAATCCGTGGCAC
CAAGCCTGTTGAGGCAGTGTCCCTTGTACCATTTGAGGTCCCAATCCTGTGGCGCGGGCAGCCGCGTTAGCGTT
CCGTGCTCCGTGCTCCGTGTTCGGCCAGAACATGTGGTGGCGAGGGGCCTGCTCTGCTTACCAGATCCCAGCC
CGGGTCCCTGTAGCGCTGGTTTACCCTGCGGCACTCCTTGATGATCTTTTTGACCTTGCGGCGGCACTCCTCGAC
GGCTCTCTCGTAGCCCGCAATCATGAGCTCATTGGGGCGTTCGGGGCTCACAGGTGGAGGCACGGGGTCGAAG
GGAAGTATTGCCAGCGCCTTGTTGAAGGTGCGCTTCTGGAACGTCTTCCAGATGTGGTTGATCGACTGCTGTGGC
GGCACCTTCTTCTTCTTTTTCACCTTCTTGTCGGTGGTGCTTGTTGCAGAGGCGGGCGGAGGCCTCGGCCTCTTG
GGGTCGTCGGACTCCTCGGAGGAGCTGTAGCCGTGCATAGTGGCGGTCGCGGCTCGAGTCAGGTTGCTGACGT
TATGTCGTTGAATCGCTGCAAGAGAGAACGTAGGAACAACGACAAAGTCTGCCGTTGAGATGAGAGTGAAAGTGT
ATATCACAGGAACACGTATCTAGACATTTGTCAGTGGTGCTGCCATCAGTCATGAAAGGCTCGAATGAGGCACGA
CTCACGCAGTAGCAAGGCCAATATCTCTTCAGCTCTAATCAAATACGCGAAACCAAACGGAGGAACAAAGGAGG
AACGAGCGACGAGGTGGCGGGGCGTTGAATCGAGCAGCGGATGGTCTTTATATGTGAAGCCAAAGGGGGCACC
AGAGCGAGCCTTGGTGCAATCAGGGGGCACACTTGGCATCCAGCGCGCCTCCCATCTTGTCAATGGCTGGCCA
CCCATGAAGAGTCATTACCCTGTCAGTAAGCTTGGTCCCACACCGCCGTGGACTGACAGGCGCAAGACGTGTAG
TCCGCCATCCAGGTTGCCATTCAGGAGGGGGCCTGGCGCATGGCGTTGGTGTTTCCGTCCCCGAGGTTCAAGA
CAAGAGACAAGCCATATGCCGGCCAAGTGGGCCACCAGCCAGGGGGGCAAGGCTCCATCCTGGCAGGAAGC
GGGTCACAGCGTTGAAACCAAGGGTCTTGTGAACAGGACACGGACAACGAAAACGGTTATCGATTCGTGCTCGA
ACTGGTCGGAGGGAATGGCGGTGGACAGGGCTGGAGGTCCAGATTTGGACCCTCAACAGAGCCGCGAAGTGG
AGTACGGTGTTAGGTGGAAAGAAGGAGGCAGGTCCGACAGATAGGTAGGTAGGTGCCTACCTAGGTACCTTAGG
TAGGTACCTAGGTACCTAAGTAAGGTACCTCTGACCACCCAGGGTAGTGCGTTTCCAGGGATTGTGCAGGCAGTC
CGGGTCCTCCCCTTGCCTTTCCAGATTGCGCCCGTGTCCGCGCCTCTCATCACAGGAATTGGATGGGCCGCATC

CTCATGGCGAGTCCAGAGTCTCACCTCGCCTCGTCCTGGGGTCCTGGGTATTCTAGGGGTCCTGCCAGTGGCC
CCTTTTAGCGGCTGACAGGGGGGGGGGGGGCAATGGCCCTCTGGTGGGTCTCCCCACGATTGCAGTCGCCGC
CAGTCCTGGGGTTAAGGGTACCTTGAATGCGGGAATTCGTACACTTTCCAGGTCTCGTGGTGCTACTCATCAGTTC
CCTCAGTTCCC

> *VlClp-1*_3kb M-segment cloning insert
CTTTCCGACTTTGTGTCATCCTCTGGCTTAGTTTGATCTTCGGTCTCGGGCGCGTCGTCGGCATCACCATCTCCCT
GGACGGACGAAGGGGTCGGCGCAGGTTCCGGCTCAGCCTCGTTGTCGCGCTCTCCTCCAGCGTTGACTTGAG
CGTCATCTAGGTCGGCGCCGCCCTTCTTGCCCATACCGCCCTCCTCGAGATCGCCACCCTCCAGGACCACCTT
CAGCTCGAGATCTTCGTCCATTGTGTAGACGCGAACACCGATGACGCAGATGGCATTCCACGGGTCAGGTGCAT
TCTCGTCTTCAGACTCGTAGATCTCGGCTTTGGTTAAGGGAGGCCCAGCGGGTTTTGCCCTGGGTTTGCGTACGA
AGTCATCGTCGCTGTACAAGAGCTCGTGGTCCTCAATAGGAGAATCCGATGACTCGCCGTCCGAGACTTCTTCGA
CCTTTTTGGCAGCCTTTTTGGACGGTGCAGGTGATGGAGTCGTCGCCTTTTCATCTTCAGCAGGCGGTTCCTTTTG
GGTAATGACCTTCGGGGCATCCTTGGCGTTCTGGCCCTGTTGGGTCCCCTCGTCCGCCTCATCATTCCCGCCCT
CATCGTCGCCCTCTTCTGCTTCTTCCTTGGCCTTGGTGGCCTTTCGTTCTTTCTTTTCGAGGTTCTTGGCCTTCTGTT
GCTTGTTGACCTGACGTGTAAGACGGCGCCTCTCCCACTGTTTCCGGCGCTCCTCTTTGCGCAGTGCGGATGCC
TTCTTCTGTTCCTTCTCCTTACGCAGGCGGGAGACCTCCTCGAGATGAGCCGCGGCCTTGCTGTGGGCCAAGTC
ATAGGCGTAGCCCACCTGTGCAAGCTTGGCGTTACCACTGCGGTGCTTACACTCGCGCTTAACGACGTCCTCGA
CAGAGTCAAGCTGCGTGTAGCGCTCAGCTTTGACGCTGATGAAAATGCTGTAGTCACCAGCAGGCATGTCAGGA
ATCTCGATGGATACGGAACGGCTCATCAAATAGTTCCCGTGAGACCGGACAATGTAGTCCTCGGCGTTTGGTCGA
CCTTTCTCATGGACACGGAAGTGAAGCTCAAACCGGTATTGGCCGTGGAGTCCCTTGAAATACCGGTTATCCAGTT
GGGACAGGGAAATTACCATTGGCGAGTCCTTGGTGAGTTTGACTTGGAACTTCTCGTTGTACTGTGGCTTCCAGGG
AACATCGACGCCGATCCATCGTTGACAGCACCTCCACTTTGGGTCGTTGAATAGTCGCGTGCGGTCGAAATGCTG
GAACTTGTTGAGAAAGTCCTCGTAAGAGATCCAGAAAACTGAATCGTTGCCGAATTGATGGCCTAGCTCTGCCTGG
ATCTCAGGAGTCCAGTCTCGAGAACCATCGGACCAGGCTCCCTCCCAGATACCCTTACGAATTTTGCCCCACGG
GTTCCTTTTGGGGTGTCAGCTCACAAATCACACCAGGAACAGAAGGTCGGGTCACATACCTGAGCTTGACGAGC
CGCGTCCCCGTTGACAATGTCTTGGCCTCCATGATCACGTAGGCATGACCCTCACAGATACCGACACGGTCGCC
ATATCCGCATTCGAGCAAACCCGTGGAGCAGCCAAACATGAATTCTGAGTTCACCTTGGACAATTCATTATCCCAG
AAGCTGTCGAGATCCAGTATATCAGACGTCAAGATCTCCGCTGTGACGCCACCAGAGAGATCTTCCAAGGCCTC
GCCAATCCAGCCGCCCACCAGCGAAGCATAGTCGCCGTGGGCTTTGGCGTAGGCCTTCTCAAGAAGAGGGAC
CCAGGTTTCATTCTGGTCGATACACTTGCCGAAGTAGAGGGCTTTTGATCCTGTCTGGTACGTTTGACGGTACACG
CGCTCCTGGTCTTCGCGATCAATCTGCTGTAGCAGCTCCCGCTGCTTACTCCTCGAGTCCCAGGTGGGTGACTT
GAGATAGAGCTTATCGTCGATGATGGAGTAGACCCACTCGCCGTCTTGTGTCCTGGTCAGTACCTGATGCAGTCG
ATCCGAATGCCAGCCGCCACATTTACATACCTCTGTAAAAGACAAAGCCGTAGATGCCAACACGTGTGTCATATTC
CACACAGATCCGCCGCAGACTCTCGGGCTCATTGGCCAGGGCCGTGAAACTGGCGATCAGCCAGCAATTGCC
GATGCTGCCTTGCTGGACGTCTCTGCCGTCGACATTCTTCATGAAAGTCGGCTTCTCGAAGATCTCGTGGACTCG
CTTCACAGCCTTGGGCACTGAGGCGCTGCTGTCGGCGAGGGTGGCCTTGTTGATCGACCAATCCGTGGCACCA
AGCCTGTTGAGGCAGTGTCCCTTGTACCATTTGAGGTCCCAATCCTGTGGCGCGGGCAGCCGCGTTAGCGTTCC
GTGCTCCGTGCTCCGTGTTCGGCCAGAACATGTGGTGGCGAGGGGCCTGCTCTGCTTACCAGATCCCAGCCCG
GGTCCCTGTAGCGCTGGTTTACCCTGCGGCACTCCTTGATGATCTTTTTGACCTTGCGGCGGCACTCCTCGACGG
CTCTCTCGTAGCCCGCAATCATGAGCTCATTGGGGCGTTCGGGGCTCACAGGTGGAGGCACGGGGTCGAAGGG
AAGTATTGCCAGCGCCTTGTTGAAGGTGCGCTTCTGGAACGTCTTCCAGATGTGGTTGATCGACTGCTGTGGCGG
CACCTTCTTCTTCTTTTTCACCTTCTTGTCGGTGGTGCTTGTTGCAGAGGCGGGCGGAGGCCTCGGCCTCTTGGG
GTCGTCGGACTCCTCGGAGGAGCTGTAGCCGTGCATAGTGGCGGTCGCGGCTCGAGTCAGGTTGCTGACGTTA
TGTCGTTGAATCGCTGCAAGAGAGAACGTAGGAACAACGACAAAGTCTGCCGTTGAGATGAGAGTGAAAGTGT

> *VlCYP1* S-segment cloning insert (1.8kb)

ATCAAGATCCCCACCGTACAGCCTTGCACTTGCTTCGCCTTTCTACTCCTCCGAAATAGGCACAAACCGAAGAAG
GCACTTCTGCCCCACGGGTCGCGAAGAAACCAGCTGGTCCGACATCTCCATTGACTCGGCCGTCATGGAAGGA
TCCGGCAGCGTTGTGTAGCGTGAGTAAACATCCTTAAGCAGAATCTTCATCTCAGCAAGGGCCAGGCTATACGCA
TGTCAGTGAAAAGGCTTTTGTCGTCTGTTGCCTCGAGACACGTACTGTTTCCCGACACAACCTCGGCCACCGTTG
GCGAACGCAAACATGAGTCGTTTTCGCTCCACGTCGCCCTCTGCGGCAGTCCATCGCTCGGGATCGAATGTCTC
CGGCTCAGGGAATACCTGGCTGTTGATTGTGTGCACAGAGTACGCTTGGCAGCTGACGATGGTGCCTCCGGGCA
CGATGAAGCCGTCCACAACCTTTCCGCCCTGCGGCACTCGTCGGGGAAGCGACATGGGGATGGGGGGGAAGC
ATCGCAAGCCTTCCTGGATCACGGCATCCAGGTAGGGCAGCTTGTCAAAGTCGGCATCTGGGTTGTTGCGCAGC
TCCTGCTGCAGCTTCTCCTGGCAGTGCATCGACGATGGCTGCGACAGCTGCCACATGAGGAAACAAAGGCCAT
CGCCCGTTGTGTCGATGCCGGCCGCCATGTGATCAAGACACTCTCCTGCCATGTCCGTCTGGTCTAGGGTGCC
GCCGCTCGCTGCCGCCTTCTCGTGCAATCGGCTGAGCAGCGTGAATGGAGACGGATCGGAGCGTTTGCTCGAC
TCCATCACGTAGTTGTCTGCCAGTGGTGTCTCACGAGGTTTGACGAAGAAGTACAGCACGCGCGCTGCGAGCTT
GTGCAACGTCGGATTGTAATGCTCAATGAGGCGGTCTACGATGATTGGTTATCTCCCCACTCAACGAACTGTCTGG
CCCGGCGGACGTACTCTGCAGGCTGTCATCGGATGCCACCTGGTGCATCATTTCTTCATCGTTCTTGTCCTGCAG
GCAGTTTGTGCCGTACGGGTTGAACAGATGGTGGGTGACACAATCGCATGCATATGCGTGCAGGGACATCTACA
GCCGTCAGTTACCACGAGGGACATGAAACTTAGGGTACTGCCTTTCATACGAAGATGTCATGACCTCCAGTGCCC
GATGAGAGACAGCGATCAAGGAACCTCCGAGACCTCTCCTGGATGCCCGACAACGGCGCCGGCTTAACAACGT
TGCTGTTGGCGTACCGATCCGCAATGATCCTCTTTCGCTTGGCATGCTGAGTTGTGTTAGGAGGACATGATTCAGA
GTTTTTAAAATTTCAAGCACTTACATCTTCTCTCTTCAGAGTCGTAAACATGGTCCTCCGGCCATATACCCTGAAAAG
GTCGTAGAATTCAGTCTTATCATACCCGCTACCACCGGAGCCATATATCTCCTTGACAGCGTCGTACGATGTGTAT
GACACCTCGTCAGGTGCTACCCGCACTACCGGGCCATATTTCTGGTGTAGTTGATGAATATACTTGGTCCGACTC
GCCTGGAAAGCGTGCCACTTCAGGAAGAGACCGGTGAAGACGGTATACCAGGGACCGGGGATCTTTCGGAGAG
GGGACGTGAGGCACTGGGCGAGATAGACAAGGAAGAGTGCGCCGCCAGCAGACAGCAGCAGAACTGGTGATA
GGAGCGCCATGATGA

Primers:

Cloning primers:

*VlClp-1*_4kb_fw1: GCTCCTTTCCGACTTTGTG
*VlClp-1*_4kb_rv1: GGGAACTGAGGGAACTGATG

*VlClp-1*_4kb_NheI_fw1: GGTTGCTAGCGCTCCTTTCCGACTTTGTG
*VlClp-1*_4kb_PstI_rv1: GGTTCTGCAGGGGAACTGAGGGAACTGATG

*VlClp-1*_4kb_NheI_fw2: GGTTGCTAGCAAAGTCGGAACTGCCAGAG
*VlClp-1*_4kb_PstI_rv2: GGTTCTGCAGGGGAACTGAGGGAACTGATG

*VlClp-1*_3kb_Fw_NheI: GGTTGCTAGCCTTTCCGACTTTGTGTCATCC
*VlClp-1_3kb*_Rv_PstI: GGTTCTGCAGACACTTTCACTCTCATCTCAAC

*VlCYP1*_Fw_NheI: GGTTGCTAGCATCAAGATCCCCACCGTACAG
*VlCYP1*_Rv_SacI: GGTTGAGCTCTCATCATGGCGCTCCTATCAC

Cloning insert size confirmation (pMS2 & pLD18)

M13_fw: GTAAAACGACGGCCAGT
M13_rv: AACAGCTATGACCATG

T7 dsRNA In-vitro transcription primers*:*

*VlClp-1*_dsRNA1_fw: TAATACGACTCACTATAGGGAGAGGTGCAGGTGATGGAGTCG
*VlClp-1*_dsRNA1_rv: TAATACGACTCACTATAGGGAGACATCAGCGTCAAAGCTGAGC

*VlClp-1*_dsrna2_fw: TAATACGACTCACTATAGGGAGAGGACATCTCTAGCAGAGCTCCTTC
*VlClp-1*_dsrna2_rv: TAATACGACTCACTATAGGGAGAGCTCTTGTACAGCGACGATGAC

*VlClp-1*_dsrna3_fw: TAATACGACTCACTATAGGGAGACGTTGACAATGTCTTGGCCTC
*VlClp-1*_dsrna3_rv: TAATACGACTCACTATAGGGAGAGAGTGGGTCTACTCCATCATCGAC

*VlCYP1*_dsRNA_fw: TAATACGACTCACTATAGGGAGAGCGAACGCAAACATGAGTCG
*VlCYP1*_dsRNA_rv: TAATACGACTCACTATAGGGAGAACGGACATGGCAGGAGAGTG

*VlGFP*_dsRNA_fw: TAATACGACTCACTATAGGGAGAACCACATGAAGCAGCACGAC
*VlGFP*_dsRNA_rv: TAATACGACTCACTATAGGGAGAGTCCATGCCGAGAGTGATC

*VlIC*_dsRNA_fw: TAATACGACTCACTATAGGGAGAGGTTGAACGAGCACATGG
*VlIC*_dsRNA_rv: TAATACGACTCACTATAGGGAGAGTTGAGGGTTCATCGACG

qPCR primers:

q*AtActin*_fw	GGAAGGATCTGTACGGTAAC	*AtActin* gene expression analysis *A. thaliana* Col-0 housekeeping gene
q*AtActin*_rv	TGTGAACGATTCCTGGACCT	
*qAtCBP60G*_fw	AAGAAGAATTGTCCGAGAGGAG	*AtCBP60g* gene expression analysis AT5G26920
*qAtCBP60G*_rv	GGCGAGTTTATGAAGCACAG	
q*AtCERK1*_fw	TACTATGCAGAGCTGAGAGGA	*AtCERK1* gene expression analysis AT3G21630
q*AtCERK1*_rv	ACACAATATCCAATCAGGCGA	
qAtDCL2_fw	GGTTGGATGGTTCCAGGTCA	*AtDCL2* gene expression analysis AT3G03300
qAtDCL2_rv	ACAACATCGGCCACACTCTT	
qAtDCL4_fw	AGGCTGCACAGCTGATGATT	*AtDCL2* gene expression analysis AT5G20320
qAtDCL4_rv	TCCAGCCCAACAAGATCCAC	
q*AtMAPK6*_fw	TCTCCTCCTGAACGCAAACT	*AtMAPK6* gene expression analysis AT2G43790
q*AtMAPK6*_rv	CACGGTACCATCTCGTGACA	
q*AtPR2*_fw	CGGTACATCAACGTTGGAA	*AtPR2* gene expression analysis AT3G57260
q*AtPR2*_rv	GCGTAGTCTAGATGGATGTT	
q*AtPR5*_fw	CGGTACAAGTGAAGGTGCTCGTT	*AtPR5* gene expression analysis AT1G75040
q*AtPR5*_rv	GCCTCGTAGATGGTTACAATGTCA	
q*AtRDR6*_fw	CCTCAGAAGAAAGCACAGACCC	*AtRDR6* gene expression analysis AT3G49500
q*AtRDR6*_rv	ACCTTGTATTGCCCAAGAAGACC	
q*AtZAT12*_fw	GTTTCATTCGTTCCAAGCCT	*AtZAT12* gene expression analysis AT5G59820
q*AtZAT12*_rv	GTGTCTCCTCATGTGTCCTC	
q*VlActin*_F	CCGATCCAGACGGAGTACTTG	*In-vitro* gene silencing analysis *V. longisporum* housekeeping gene
q*VlActin*_R	CCTGTACGGCAACATCGTCA	
q*VlClp1*_fw	TTGACAGCACCTCCACTTTGG	*In-vitro* gene silencing analysis *Vl Clp-1* gene expression
q*VlClp1*_rv	CGAGACTGGACTCCTGAGATCC	
q*VlCYP1*_fw	TGAGCAGCGTGAATGGAGAC	*In-vitro* gene silencing analysis *Vl CYP1* gene expression
q*VlCYP1*_rv	AGACACCACTGGCAGACAAC	
q*VlGFP*_fw	TGAGCAAGGGCGAGGAG	*In-vitro* gene silencing analysis *Vl GFP* gene expression
q*VlGFP*_rv	CCGGTGGTGCAGATGAAC	
q*VlGFP*_hydrop_fw	TACCCCGACCACATGAAGCAGCAC	Fungal biomass quantification (Hydroponic infection assay) *V. longisporum GFP*
q*VlGFP*_hydrop_rv	TGCCGTCCTCCTTGAAGTCGATGCC	

References

Ahmed, Firoz, Muthappa Senthil-Kumar, Xinbin Dai, Vemanna S. Ramu, Seonghee Lee, Kirankumar S. Mysore, and Patrick Xuechun Zhao. 'pssRNAit: A Web Server for Designing Effective and Specific Plant siRNAs with Genome-Wide Off-Target Assessment'. *Plant Physiology* 184, no. 1 (September 2020): 65–81. https://doi.org/10.1104/pp.20.00293.

Banno, Shinpei, Hidenari Saito, Hiroshi Sakai, Toshihiko Urushibara, Kentaro Ikeda, Takeshi Kabe, Isao Kemmochi, and Makoto Fujimura. 'Quantitative Nested Real-Time PCR Detection of Verticillium Longisporum and V. Dahliae in the Soil of Cabbage Fields'. *Journal of General Plant Pathology* 77, no. 5 (September 2011): 282–91. https://doi.org/10.1007/s10327-011-0335-9.

Blay, Vincent, Bhairavi Tolani, Sunita P. Ho, and Michelle R. Arkin. 'High-Throughput Screening: Today's Biochemical and Cell-Based Approaches'. *Drug Discovery Today* 25, no. 10 (1 October 2020): 1807–21. https://doi.org/10.1016/j.drudis.2020.07.024.

Bleichrodt, Robert-Jan, and Nick D. Read. 'Flow Cytometry and FACS Applied to Filamentous Fungi'. *Fungal Biology Reviews* 33, no. 1 (1 January 2019): 1–15. https://doi.org/10.1016/j.fbr.2018.06.001.

Bond, Jeff. 'More Gene Manipulations in Fungi. Edited by J. W. Bennett and L. L. Lasure. Academic Press. 1991. 470 Pages. £45.50. $75.00. ISBN 0 12 088642 1.' *Genetical Research* 60, no. 3 (December 1992): 236–37. https://doi.org/10.1017/S0016672300030998.

Brown, James K. M. 'Yield Penalties of Disease Resistance in Crops'. *Current Opinion in Plant Biology* 5, no. 4 (August 2002): 339–44. https://doi.org/10.1016/s1369-5266(02)00270-4.

Bui, Tri-Thuc, Rebekka Harting, Susanna A. Braus-Stromeyer, Van-Tuan Tran, Miriam Leonard, Annalena Höfer, Anja Abelmann, et al. 'Verticillium Dahliae Transcription Factors Som1 and Vta3 Control Microsclerotia Formation and Sequential Steps of Plant Root Penetration and Colonisation to Induce Disease'. *New Phytologist* 221, no. 4 (2019): 2138–59. https://doi.org/10.1111/nph.15514.

Carthew, Richard W., and Erik J. Sontheimer. 'Origins and Mechanisms of miRNAs and siRNAs'. *Cell* 136, no. 4 (20 February 2009): 642–55. https://doi.org/10.1016/j.cell.2009.01.035.

Cedden, Doga, Gözde Güney, Michael Rostás, and Gregor Bucher. 2025. 'Optimizing dsRNA Sequences for RNAi in Pest Control and Research with the dsRIP Web Platform'. *BMC Biology* 23 (1): 114. https://doi.org/10.1186/s12915-025-02219-6.

Chen, Jiasheng, Peng, Yingchuan, Zhang, Hainan, Wang, Kangxu, Zhao, Chunqing, Zhu, Guanheng, Reddy Palli, Subba, and Zhaojun and Han. 'Off-Target Effects of RNAi Correlate with the Mismatch Rate between dsRNA and Non-Target mRNA'. *RNA Biology* 18, no. 11 (2 November 2021): 1747–59. https://doi.org/10.1080/15476286.2020.1868680.

Chen, Y. Grace, and Sun Hur. 'Cellular Origins of dsRNA, Their Recognition and Consequences'. *Nature Reviews Molecular Cell Biology* 23, no. 4 (April 2022): 286–301. https://doi.org/10.1038/s41580-021-00430-1.

Chen, Yun-Ya, Chen Zhu, Jian-Hua Zhao, Ting Liu, Feng Gao, Ying-Chao Zhang, and Cheng-Guo Duan. 'DNA Methylation-Dependent Epigenetic Regulation of Verticillium Dahliae Virulence in Plants'. *aBIOTECH* 4, no. 3 (1 September 2023): 185–201. https://doi.org/10.1007/s42994-023-00117-5.

Cortés-Maldonado, Leyda, Jaime Marcial-Quino, Saúl Gómez-Manzo, Francisco Fierro, and Araceli Tomasini. 'A Method for the Extraction of High-Quality Fungal RNA Suitable for RNA-Seq'. *Journal of Microbiological Methods* 170 (1 March 2020): 105855. https://doi.org/10.1016/j.mimet.2020.105855.

Cunningham, Drew S., Daniel MacEachran, James Robbins Abshire, Himanshu Dhamankar, Ifeyinwa Iwuchukwu, Mehak Gupta, Matthew Eduardo Moura, et al. Methods and compositions for nucleoside triphosphate and ribonucleic acid production. United States US10858385B2, filed 20 November 2018, and issued 8 December 2020. https://patents.google.com/patent/US10858385B2/en.

Dalakouras, Athanasios, Venetia Koidou, and Kalliope Papadopoulou. 'DsRNA-Based Pesticides: Considerations for Efficiency and Risk Assessment'. *Chemosphere* 352 (1 March 2024): 141530. https://doi.org/10.1016/j.chemosphere.2024.141530.

Davletova, Sholpan, Karen Schlauch, Jesse Coutu, and Ron Mittler. 'The Zinc-Finger Protein Zat12 Plays a Central Role in Reactive Oxygen and Abiotic Stress Signaling in Arabidopsis'. *Plant Physiology* 139, no. 2 (October 2005): 847–56. https://doi.org/10.1104/pp.105.068254.

Deketelaere, Silke, Katrijn Spiessens, Sabien Pollet, Lien Tyvaert, Luc De Rooster, Danny Callens, Soraya C. França, and Monica Höfte. 'Towards Practical Application of Verticillium Isaacii Vt305 to Control Verticillium Wilt of Cauliflower: Exploring Complementary Biocontrol Strategies'. *Plants* 9, no. 11 (30 October 2020): 1469. https://doi.org/10.3390/plants9111469.

Deketelaere, Silke, Lien Tyvaert, Soraya C. França, and Monica Höfte. 'Desirable Traits of a Good Biocontrol Agent against Verticillium Wilt'. *Frontiers in Microbiology* 8 (6 July 2017): 1186. https://doi.org/10.3389/fmicb.2017.01186.

Deleris, Angélique, Javier Gallego-Bartolome, Jinsong Bao, Kristin D. Kasschau, James C. Carrington, and Olivier Voinnet. 'Hierarchical Action and Inhibition of Plant Dicer-Like Proteins in Antiviral Defense'. *Science* 313, no. 5783 (7 July 2006): 68–71. https://doi.org/10.1126/science.1128214.

Depotter, Jasper R. L., Silke Deketelaere, Patrik Inderbitzin, Andreas Von Tiedemann, Monica Höfte, Krishna V. Subbarao, Thomas A. Wood, and Bart P. H. J. Thomma. '*Verticillium Longisporum* , the Invisible Threat to Oilseed Rape and Other Brassicaceous Plant Hosts'. *Molecular Plant Pathology* 17, no. 7 (September 2016): 1004–16. https://doi.org/10.1111/mpp.12350.

Depotter, Jasper R. L., Fabian Van Beveren, Luis Rodriguez-Moreno, H. Martin Kramer, Edgar A. Chavarro Carrero, Gabriel L. Fiorin, Grardy C. M. Van Den Berg, Thomas A. Wood, Bart P. H. J. Thomma, and Michael F. Seidl. 'The Interspecific Fungal Hybrid *Verticillium Longisporum* Displays Subgenome-Specific Gene Expression'. Edited by Joseph Heitman. *mBio* 12, no. 4 (31 August 2021): 10.1128/mbio.01496-21. https://doi.org/10.1128/mbio.01496-21.

Devisetty, Upendra K., Emma De Neef, Eric R.L. Gordon, Valeria Velásquez-Zapata, Kenneth Narva, Laurent Mézin, Peter Mc Cahon, Kenneth W. Witwer, and Krishnakumar Sridharan. 'A Bioinformatics Framework for Human Health Risk Assessment of Externally Applied dsRNA-Based Biopesticides'. *Computational Toxicology* 33 (March 2025): 100340. https://doi.org/10.1016/j.comtox.2024.100340.

Dommes, Anna B, Thomas Gross, Denise B Herbert, Kimmo I Kivivirta, and Annette Becker. 'Virus-Induced Gene Silencing: Empowering Genetics in Non-Model Organisms'. *Journal of Experimental Botany* 70, no. 3 (5 February 2019): 757–70. https://doi.org/10.1093/jxb/ery411.

Doyle, Jeffrey. 'DNA Protocols for Plants'. In *Molecular Techniques in Taxonomy*, edited by Godfrey M. Hewitt, Andrew W. B. Johnston, and J. Peter W. Young, 283–93. Berlin, Heidelberg: Springer Berlin Heidelberg, 1991. https://doi.org/10.1007/978-3-642-83962-7_18.

Drinnenberg, Ines A., Gerald R. Fink, and David P. Bartel. 'Compatibility with Killer Explains the Rise of RNAi-Deficient Fungi'. *Science* 333, no. 6049 (16 September 2011): 1592–1592. https://doi.org/10.1126/science.1209575.

Durrant, W. E., and X. Dong. 'SYSTEMIC ACQUIRED RESISTANCE'. *Annual Review of Phytopathology* 42, no. Volume 42, 2004 (8 September 2004): 185–209. https://doi.org/10.1146/annurev.phyto.42.040803.140421.

Enebak, Scott A. 'Update on Soil Fumigation: MBr Alternatives and Reregistration Decisions', 2011. https://api.semanticscholar.org/CorpusID:134619144.

Erdmann, Robert M., and Colette L. Picard. 'RNA-Directed DNA Methylation'. *PLoS Genetics* 16, no. 10 (October 2020): e1009034. https://doi.org/10.1371/journal.pgen.1009034.

Eynck, C., B. Koopmann, G. Grunewaldt-Stoecker, P. Karlovsky, and A. von Tiedemann. 'Differential Interactions of Verticillium Longisporum and V. Dahliae with Brassica Napus Detected with Molecular and Histological Techniques'. *European Journal of Plant Pathology* 118, no. 3 (1 July 2007): 259–74. https://doi.org/10.1007/s10658-007-9144-6.

Figueiredo Prates, Lucas Henrique, Maximilian Merlau, Johanna Rühl-Teichner, Marc F. Schetelig, and Irina Häcker. 'An Optimized/Scale Up-Ready Protocol for Extraction of Bacterially Produced dsRNA at Good Yield and Low Costs'. *International Journal of Molecular Sciences* 24, no. 11 (January 2023): 9266. https://doi.org/10.3390/ijms24119266.

Fire, Andrew, SiQun Xu, Mary K. Montgomery, Steven A. Kostas, Samuel E. Driver, and Craig C. Mello. 'Potent and Specific Genetic Interference by Double-Stranded RNA in Caenorhabditis Elegans'. *Nature* 391, no. 6669 (February 1998): 806–11. https://doi.org/10.1038/35888.

Fradin, Emilie F., Zhao Zhang, Juan C. Juarez Ayala, Christian D.M. Castroverde, Ross N. Nazar, Jane Robb, Chun-Ming Liu, and Bart P.H.J. Thomma. 'Genetic Dissection of Verticillium Wilt Resistance Mediated by Tomato Ve1'. *Plant Physiology* 150, no. 1 (1 May 2009): 320–32. https://doi.org/10.1104/pp.109.136762.

Gibeaut, D. M., J. Hulett, G. R. Cramer, and J. R. Seemann. 'Maximal Biomass of Arabidopsis Thaliana Using a Simple, Low-Maintenance Hydroponic Method and Favorable Environmental Conditions'. *Plant Physiology* 115, no. 2 (1 October 1997): 317–19. https://doi.org/10.1104/pp.115.2.317.

Goessling, Helge F., Thomas Rackow, and Thomas Jung. 'Recent Global Temperature Surge Intensified by Record-Low Planetary Albedo'. *Science* 387, no. 6729 (3 January 2025): 68–73. https://doi.org/10.1126/science.adq7280.

Gunasekara, Sandya, Pedro Fidelman, Stephen Fletcher, et al. 2025. 'The Future of dsRNA-Based Biopesticides Will Require Global Regulatory Cohesion'. *Nature Plants* 11 (4): 664–67. https://doi.org/10.1038/s41477-025-01953-7.

Hammond, S. M., A. A. Caudy, and G. J. Hannon. 'Post-Transcriptional Gene Silencing by Double-Stranded RNA'. *Nature Reviews. Genetics* 2, no. 2 (February 2001): 110–19. https://doi.org/10.1038/35052556.

Hashiro, Shuhei, and Hisashi Yasueda. 'RNA Interference-Based Pesticides and Antiviral Agents: Microbial Overproduction Systems for Double-Stranded RNA for Applications in Agriculture and Aquaculture'. *Applied Sciences* 12, no. 6 (January 2022): 2954. https://doi.org/10.3390/app12062954.

Hayes, Ryan J., Leah K. McHale, Gary E. Vallad, Maria Jose Truco, Richard W. Michelmore, Steve J. Klosterman, Karunakaran Maruthachalam, and Krishna V. Subbarao. 'The Inheritance of Resistance to Verticillium Wilt Caused by Race 1 Isolates of Verticillium Dahliae in the Lettuce Cultivar La Brillante'. *Theoretical and Applied Genetics* 123, no. 4 (August 2011): 509–17. https://doi.org/10.1007/s00122-011-1603-y.

He, Li, Yifan Zhou, Qin Mo, Yanna Huang, and Xueming Tang. 'Spray-Induced Gene Silencing in Phytopathogen: Mechanisms, Applications, and Progress'. *Advanced Agrochem* 3, no. 4 (1 December 2024): 289–97. https://doi.org/10.1016/j.aac.2024.06.001.

He, Zuhua, Shanice Webster, and Sheng Yang He. 'Growth–Defense Trade-Offs in Plants'. *Current Biology* 32, no. 12 (20 June 2022): R634–39. https://doi.org/10.1016/j.cub.2022.04.070.

Heick, Thies Marten, Annemarie Fejer Justesen, and Lise Nistrup Jørgensen. 'Anti-Resistance Strategies for Fungicides against Wheat Pathogen Zymoseptoria Tritici with Focus on DMI Fungicides'. *Crop Protection* 99 (September 2017): 108–17. https://doi.org/10.1016/j.cropro.2017.05.009.

Henderson, Ian R., Xiaoyu Zhang, Cheng Lu, Lianna Johnson, Blake C. Meyers, Pamela J. Green, and Steven E. Jacobsen. 'Dissecting Arabidopsis Thaliana DICER Function in Small RNA Processing, Gene Silencing and DNA Methylation Patterning'. *Nature Genetics* 38, no. 6 (June 2006): 721–25. https://doi.org/10.1038/ng1804.

Huang, Caiping, Ana Rocío Sede, Laura Elvira-González, Yan Yan, Miguel Eduardo Rodriguez, Jérôme Mutterer, Emmanuel Boutant, Libo Shan, and Manfred Heinlein. 'dsRNA-Induced Immunity Targets Plasmodesmata and Is Suppressed by Viral Movement Proteins'. *The Plant Cell* 35, no. 10 (1 October 2023): 3845–69. https://doi.org/10.1093/plcell/koad176.

Ikeda, Kentaro, Shinpei Banno, Akiko Furusawa, Satoshi Shibata, Kazuhiro Nakaho, and Makoto Fujimura. 'Crop Rotation with Broccoli Suppresses Verticillium Wilt of Eggplant'. *Journal of General Plant Pathology* 81, no. 1 (January 2015): 77–82. https://doi.org/10.1007/s10327-014-0559-6.

Inderbitzin, Patrik, Richard M. Bostock, R. Michael Davis, Toshiyuki Usami, Harold W. Platt, and Krishna V. Subbarao. 'Phylogenetics and Taxonomy of the Fungal Vascular Wilt Pathogen Verticillium, with the Descriptions of Five New Species'. Edited by Alexander Idnurm. *PLoS ONE* 6, no. 12 (7 December 2011): e28341. https://doi.org/10.1371/journal.pone.0028341.

Inderbitzin, Patrik, and Krishna V. Subbarao. '*Verticillium* Systematics and Evolution: How Confusion Impedes Verticillium Wilt Management and How to Resolve It'. *Phytopathology®* 104, no. 6 (June 2014): 564–74. https://doi.org/10.1094/PHYTO-11-13-0315-IA.

Jeseničnik, Taja, Nataša Štajner, Sebastjan Radišek, and Jernej Jakše. 'RNA Interference Core Components Identified and Characterised in Verticillium Nonalfalfae, a Vascular Wilt Pathogenic Plant Fungi of Hops'. *Scientific Reports* 9, no. 1 (17 June 2019): 8651. https://doi.org/10.1038/s41598-019-44494-8.

Jin, Yun, Jian-Hua Zhao, Pan Zhao, Tao Zhang, Sheng Wang, and Hui-Shan Guo. 'A Fungal milRNA Mediates Epigenetic Repression of a Virulence Gene in Verticillium Dahliae'. *Philosophical Transactions of the Royal Society B: Biological Sciences* 374, no. 1767 (4 March 2019): 20180309. https://doi.org/10.1098/rstb.2018.0309.

Joga, Mallikarjuna R., Moises J. Zotti, Guy Smagghe, and Olivier Christiaens. 'RNAi Efficiency, Systemic Properties, and Novel Delivery Methods for Pest Insect Control: What We Know So Far'. *Frontiers in Physiology* 7 (17 November 2016): 553. https://doi.org/10.3389/fphys.2016.00553.

Kakiyama, Sayaka, Midori Tabara, Yuki Nishibori, Hiromitsu Moriyama, and Toshiyuki Fukuhara. 2019. 'Long DCL4-Substrate dsRNAs Efficiently Induce RNA Interference in Plant Cells'. *Scientific Reports* 9 (1): 6920. https://doi.org/10.1038/s41598-019-43443-9.

Karapapa, V.K., B.W. Bainbridge, and J.B. Heale. 'Morphological and Molecular Characterization of Verticillium Longisporum Comb, Nov., Pathogenic to Oilseed Rape'. *Mycological Research* 101, no. 11 (November 1997): 1281–94. https://doi.org/10.1017/S0953756297003985.

Karayianni, Maria, Theodore Sentoukas, Athanasios Skandalis, Natassa Pippa, and Stergios Pispas. 'Chitosan-Based Nanoparticles for Nucleic Acid Delivery: Technological Aspects, Applications, and Future Perspectives'. *Pharmaceutics* 15, no. 7 (July 2023): 1849. https://doi.org/10.3390/pharmaceutics15071849.

Karikó, Katalin, Hiromi Muramatsu, János Ludwig, and Drew Weissman. 'Generating the Optimal mRNA for Therapy: HPLC Purification Eliminates Immune Activation and Improves Translation of Nucleoside-Modified, Protein-Encoding mRNA'. *Nucleic Acids Research* 39, no. 21 (1 November 2011): e142. https://doi.org/10.1093/nar/gkr695.

Kato, Hiroki, Osamu Takeuchi, Eriko Mikamo-Satoh, et al. 2008. 'Length-Dependent Recognition of Double-Stranded Ribonucleic Acids by Retinoic Acid–Inducible Gene-I and Melanoma Differentiation–Associated Gene 5'. *Journal of Experimental Medicine* 205 (7): 1601–10. https://doi.org/10.1084/jem.20080091.

Kawchuk, Lawrence M., John Hachey, Dermot R. Lynch, Frank Kulcsar, Gijs Van Rooijen, Doug R. Waterer, Albert Robertson, et al. 'Tomato *Ve* Disease Resistance Genes Encode Cell Surface-like Receptors'. *Proceedings of the National Academy of Sciences* 98, no. 11 (22 May 2001): 6511–15. https://doi.org/10.1073/pnas.091114198.

Ke, Cai-Ling, Fu-Sheng Deng, Chih-Yu Chuang, and Ching-Hsuan Lin. 'Antimicrobial Actions and Applications of Chitosan'. *Polymers* 13, no. 6 (15 March 2021): 904. https://doi.org/10.3390/polym13060904.

Kettles, Graeme J., Bernhard J. Hofinger, Pingsha Hu, Carlos Bayon, Jason J. Rudd, Dirk Balmer, Mikael Courbot, Kim E. Hammond-Kosack, Gabriel Scalliet, and Kostya Kanyuka. 'sRNA Profiling Combined With Gene Function Analysis Reveals a Lack of Evidence for Cross-Kingdom RNAi in the Wheat – Zymoseptoria Tritici Pathosystem'. *Frontiers in Plant Science* 10 (4 July 2019). https://doi.org/10.3389/fpls.2019.00892.

Knoblich, Marie, Torsten Gursinsky, Selma Gago-Zachert, Claus Weinholdt, Jan Grau, and Sven-Erik Behrens. 2025. 'A New Level of RNA-Based Plant Protection: dsRNAs Designed from Functionally Characterized siRNAs Highly Effective against Cucumber Mosaic Virus'. *Nucleic Acids Research* 53 (5): gkaf136. https://doi.org/10.1093/nar/gkaf136.

Koch, Aline, Lisa Höfle, Bernhard Timo Werner, et al. 2019. 'SIGS vs HIGS: A Study on the Efficacy of Two dsRNA Delivery Strategies to Silence Fusarium FgCYP51 Genes in Infected Host and Non-Host Plants'. *Molecular Plant Pathology* 20 (12): 1636–44. https://doi.org/10.1111/mpp.12866.

Koch, Aline, and Michael Wassenegger. 'Host-Induced Gene Silencing - Mechanisms and Applications'. *The New Phytologist* 231, no. 1 (July 2021): 54–59. https://doi.org/10.1111/nph.17364.

Kotta-Loizou, Ioly. 'Mycoviruses and Their Role in Fungal Pathogenesis'. *Current Opinion in Microbiology* 63 (1 October 2021): 10–18. https://doi.org/10.1016/j.mib.2021.05.007.

Krishnamurthi, Venkata Rao, Isabelle I. Niyonshuti, Jingyi Chen, and Yong Wang. 'A New Analysis Method for Evaluating Bacterial Growth with Microplate Readers'. *PLOS ONE* 16, no. 1 (12 January 2021): e0245205. https://doi.org/10.1371/journal.pone.0245205.

Kurzynska-Kokorniak, Anna, Natalia Koralewska, Maria Pokornowska, Anna Urbanowicz, Aleksander Tworak, Agnieszka Mickiewicz, and Marek Figlerowicz. 'The Many Faces of Dicer: The Complexity of the Mechanisms Regulating Dicer Gene Expression and Enzyme Activities'. *Nucleic Acids Research* 43, no. 9 (19 May 2015): 4365–80. https://doi.org/10.1093/nar/gkv328.

Laurie, John D., Rob Linning, and Guus Bakkeren. 'Hallmarks of RNA Silencing Are Found in the Smut Fungus Ustilago Hordei but Not in Its Close Relative Ustilago Maydis'. *Current Genetics* 53, no. 1 (1 January 2008): 49–58. https://doi.org/10.1007/s00294-007-0165-7.

Leonard, Miriam, Anika Kühn, Rebekka Harting, Isabel Maurus, Alexandra Nagel, Jessica Starke, Harald Kusch, et al. 'Verticillium Longisporum Elicits Media-Dependent Secretome Responses With Capacity to Distinguish Between Plant-Related Environments'. *Frontiers in Microbiology* 11 (2020): 1876. https://doi.org/10.3389/fmicb.2020.01876.

Li, Sisi, and Dinshaw J. Patel. 'Drosha and Dicer: Slicers Cut from the Same Cloth'. *Cell Research* 26, no. 5 (May 2016): 511–12. https://doi.org/10.1038/cr.2016.19.

Li, Yan, QingQing Zhang, Jiangguang Zhang, Liang Wu, Yijun Qi, and Jian-Min Zhou. 'Identification of MicroRNAs Involved in Pathogen-Associated Molecular Pattern-Triggered Plant Innate Immunity'. *Plant Physiology* 152, no. 4 (1 April 2010): 2222–31. https://doi.org/10.1104/pp.109.151803.

Lindbo, J. A., L. Silva-Rosales, W. M. Proebsting, and W. G. Dougherty. 'Induction of a Highly Specific Antiviral State in Transgenic Plants: Implications for Regulation of Gene Expression and Virus Resistance.' *The Plant Cell* 5, no. 12 (1 December 1993): 1749–59. https://doi.org/10.1105/tpc.5.12.1749.

Liu, Chuanhui, Chen Cui, Guanyin Zhou, Feng Gao, Jianhua Zhao, Huishan Guo, and Yun Jin. 'The Endocytic Pathway for Absorption of Exogenous RNAs in Verticillium Dahliae'. *mLife* 4, no. 1 (2025): 45–54. https://doi.org/10.1002/mlf2.12149.

Liu, Xiao-Hong, Guo-Ao Ning, Lu-Yao Huang, Ya-Hui Zhao, Bo Dong, Jian-Ping Lu, and Fu-Cheng Lin. 'Calpains Are Involved in Asexual and Sexual Development, Cell Wall Integrity and Pathogenicity of the Rice Blast Fungus'. *Scientific Reports* 6, no. 1 (9 August 2016): 31204. https://doi.org/10.1038/srep31204.

Livak, K. J., and T. D. Schmittgen. 'Analysis of Relative Gene Expression Data Using Real-Time Quantitative PCR and the 2(-Delta Delta C(T)) Method'. *Methods (San Diego, Calif.)* 25, no. 4 (December 2001): 402–8. https://doi.org/10.1006/meth.2001.1262.

Lv, Junyuan, Shichao Liu, Jinglong Zhou, Zili Feng, Feng Wei, Lihong Zhao, Haiqiang Li, Heqin Zhu, Yalin Zhang, and Hongjie Feng. 'The Glycoside Hydrolase 7 Member VdGH7a Regulates *Verticillium Dahliae* Pathogenicity and Induces Host Defenses by Interacting with GhOLP11'. *Journal of Integrative Agriculture*, 2 March 2024. https://doi.org/10.1016/j.jia.2024.03.002.

Mitter, Neena, Elizabeth A. Worrall, Karl E. Robinson, Peng Li, Ritesh G. Jain, Christelle Taochy, Stephen J. Fletcher, Bernard J. Carroll, G. Q. (Max) Lu, and Zhi Ping Xu. 'Clay Nanosheets for Topical Delivery of RNAi for Sustained Protection against Plant Viruses'. *Nature Plants* 3, no. 2 (9 January 2017): 1–10. https://doi.org/10.1038/nplants.2016.207.

Moorlach, Benjamin W., Ana R. Sede, Katharina M. Hermann, Alesia A. Levanova, Minna M. Poranen, Michael Westphal, Martin Wortmann, et al. 'Interpolyelectrolyte Complexes of in Vivo Produced dsRNA with Chitosan and Alginate for Enhanced Plant Protection against Tobacco Mosaic Virus'. *International Journal of Biological Macromolecules* 306 (1 May 2025): 141579. https://doi.org/10.1016/j.ijbiomac.2025.141579.

Mosquera, Sandra, Mireille Ginésy, Irene Teresa Bocos-Asenjo, Huma Amin, Sergio Diez-Hermano, Julio Javier Diez, and Jonatan Niño-Sánchez. 'Spray-Induced Gene Silencing to Control Plant Pathogenic Fungi: A Step-by-Step Guide'. *Journal of Integrative Plant Biology* 67, no. 3 (2025): 801–25. https://doi.org/10.1111/jipb.13848.

Müller, Henry, and Gabriele Berg. 'Impact of Formulation Procedures on the Effect of the Biocontrol Agent Serratia Plymuthica HRO-C48 on Verticillium Wilt in Oilseed Rape'. *BioControl* 53, no. 6 (December 2008): 905–16. https://doi.org/10.1007/s10526-007-9111-3.

Nakano, Ryohei Thomas, and Tomohisa Shimasaki. 'Long-Term Consequences of PTI Activation and Its Manipulation by Root-Associated Microbiota'. *Plant and Cell Physiology* 65, no. 5 (1 May 2024): 681–93. https://doi.org/10.1093/pcp/pcae033.

Napoli, C., C. Lemieux, and R. Jorgensen. 'Introduction of a Chimeric Chalcone Synthase Gene into Petunia Results in Reversible Co-Suppression of Homologous Genes in Trans.' *The Plant Cell*, 1 April 1990, 279–89. https://doi.org/10.1105/tpc.2.4.279.

Neumann, M. 'Sequence Tag Analysis of Gene Expression during Pathogenic Growth and Microsclerotia Development in the Vascular Wilt Pathogen Verticillium Dahliae'. *Fungal Genetics and Biology* 38, no. 1 (February 2003): 54–62. https://doi.org/10.1016/S1087-1845(02)00507-8.

Niazi, Adnan, Shahid Manzoor, Shashidar Asari, Sarosh Bejai, Johan Meijer, and Erik Bongcam-Rudloff. 'Genome Analysis of Bacillus Amyloliquefaciens Subsp. Plantarum UCMB5113: A Rhizobacterium That Improves Plant Growth and Stress Management'. Edited by Mark Gijzen. *PLoS ONE* 9, no. 8 (13 August 2014): e104651. https://doi.org/10.1371/journal.pone.0104651.

Niehl, Annette, Marjukka Soininen, Minna M. Poranen, and Manfred Heinlein. 'Synthetic Biology Approach for Plant Protection Using Ds RNA'. *Plant Biotechnology Journal* 16, no. 9 (September 2018): 1679–87. https://doi.org/10.1111/pbi.12904.

Niehl, Annette, Ines Wyrsch, Thomas Boller, and Manfred Heinlein. 'Double-Stranded RNAs Induce a Pattern-Triggered Immune Signaling Pathway in Plants'. *New Phytologist* 211, no. 3 (2016): 1008–19. https://doi.org/10.1111/nph.13944.

Ning, Yuese, Wende Liu, and Guo-Liang Wang. 'Balancing Immunity and Yield in Crop Plants'. *Trends in Plant Science* 22, no. 12 (1 December 2017): 1069–79. https://doi.org/10.1016/j.tplants.2017.09.010.

Niño-Sánchez, Jonatan, Prabhakaran T. Sambasivam, Anne Sawyer, et al. 2022. 'BioClay™ Prolongs RNA Interference-Mediated Crop Protection against Botrytis Cinerea'. *Journal of Integrative Plant Biology* 64 (11): 2187–98. https://doi.org/10.1111/jipb.13353.

OECD. *Considerations for the Environmental Risk Assessment of the Application of Sprayed or Externally Applied Ds-RNA-Based Pesticides*. Series on Pesticides and Biocides. OECD, 2020. https://doi.org/10.1787/576d9ebb-en.

OECD. *Considerations for the Human Health Risk Assessment of Externally Applied dsRNA-Based Pesticides*. Series on Pesticides and Biocides. OECD, 2023. https://doi.org/10.1787/54852048-en.

Palanga, Koffi Kibalou, Ruixian Liu, Qun Ge, Juwu Gong, Junwen Li, Quanwei Lu, Pengtao Li, Youlu Yuan, and Wankui Gong. 'Current Advances in Pathogen-Plant Interaction between Verticillium Dahliae and Cotton Provide New Insight in the Disease Management'. *Journal of Cotton Research* 4, no. 1 (December 2021): 25. https://doi.org/10.1186/s42397-021-00100-9.

Pallis, Samuel, Andrei Alyokhin, Brian Manley, Thais Rodrigues, Ethann Barnes, and Kenneth Narva. 'Effects of Low Doses of a Novel dsRNA-Based Biopesticide (Calantha) on the Colorado Potato Beetle'. *Journal of Economic Entomology* 116, no. 2 (1 April 2023): 456–61. https://doi.org/10.1093/jee/toad034.

Pegg, George F., and Beryl L. Brady. *Verticillium Wilts*. CABI Books. Wallingford: CABI, 2002. https://doi.org/10.1079/9780851995298.0000.

Perrot, Thomas, Markus Pauly, and Vicente Ramírez. 'Emerging Roles of β-Glucanases in Plant Development and Adaptative Responses'. *Plants* 11, no. 9 (20 April 2022): 1119. https://doi.org/10.3390/plants11091119.

Poynter, Sarah J., and Stephanie J. DeWitte-Orr. 'Visualizing Virus-Derived dsRNA Using Antibody-Independent and -Dependent Methods'. In *Innate Antiviral Immunity*, edited by Karen Mossman, 1656:103–18. Methods in Molecular Biology. New York, NY: Springer New York, 2017. https://doi.org/10.1007/978-1-4939-7237-1_5.

Qiao, Lulu, Chi Lan, Luca Capriotti, Audrey Ah-Fong, Jonatan Nino Sanchez, Rachael Hamby, Jens Heller, et al. 'Spray-Induced Gene Silencing for Disease Control Is Dependent on the Efficiency of Pathogen RNA Uptake'. Microbiology, 2 February 2021. https://doi.org/10.1101/2021.02.01.429265.

Regulation (EC) No 1829/2003 of the European Parliament and of the Council of 22 September 2003 on genetically modified food and feed (OJ L 268, 18.10.2003, pp. 1–23)

Richardson, Sarah J., Abby Willcox, David A. Hilton, Sisko Tauriainen, Heikki Hyoty, Adrian J. Bone, Alan K. Foulis, and Noel G. Morgan. 'Use of Antisera Directed against dsRNA to Detect Viral Infections in Formalin-Fixed Paraffin-Embedded Tissue'. *Journal of Clinical Virology: The Official Publication of the Pan American Society for Clinical Virology* 49, no. 3 (November 2010): 180–85. https://doi.org/10.1016/j.jcv.2010.07.015.

Rosa, Cristina, Yen-Wen Kuo, Hada Wuriyanghan, and Bryce W. Falk. 'RNA Interference Mechanisms and Applications in Plant Pathology'. *Annual Review of Phytopathology* 56, no. Volume 56, 2018 (25 August 2018): 581–610. https://doi.org/10.1146/annurev-phyto-080417-050044.

Rosa, Juliana da, Américo José Carvalho Viana, Fernando Rafael Alves Ferreira, Alessandra Koltun, Liliane Marcia Mertz-Henning, Silvana Regina Rockenbach Marin, Elibio Leopoldo Rech, and Alexandre Lima Nepomuceno. 'Optimizing dsRNA Engineering Strategies and Production in E. Coli HT115 (DE3)'. *Journal of Industrial Microbiology & Biotechnology* 51 (16 August 2024): kuae028. https://doi.org/10.1093/jimb/kuae028.

Rosskopf, Erin, Francesco Di Gioia, Isaac Vincent, Jason Hong, and Xin Zhao. 'Impacts of the Ban on the Soil-Applied Fumigant Methyl Bromide'. *Phytopathology®* 114, no. 6 (June 2024): 1161–75. https://doi.org/10.1094/PHYTO-09-23-0345-IA.

Sanan-Mishra, Neeti, A. Abdul Kader Jailani, Bikash Mandal, and Sunil K. Mukherjee. 'Secondary siRNAs in Plants: Biosynthesis, Various Functions, and Applications in Virology'. *Frontiers in Plant Science* 12 (2021): 610283. https://doi.org/10.3389/fpls.2021.610283.

Savary, Serge, Laetitia Willocquet, Sarah Jane Pethybridge, Paul Esker, Neil McRoberts, and Andy Nelson. 'The Global Burden of Pathogens and Pests on Major Food Crops'. *Nature Ecology & Evolution* 3, no. 3 (4 February 2019): 430–39. https://doi.org/10.1038/s41559-018-0793-y.

Schonborn, J., J. Oberstraβ, E. Breyel, J. Tittgen, J. Schumacher, and N. Lukacs. 1991. 'Monoclonal Antibodies to Double-Stranded RNA as Probes of RNA Structure in Crude Nucleic Acid Extracts'. *Nucleic Acids Research* 19 (11): 2993–3000. https://doi.org/10.1093/nar/19.11.2993.

Schrader, C., A. Schielke, L. Ellerbroek, and R. Johne. 'PCR Inhibitors - Occurrence, Properties and Removal'. *Journal of Applied Microbiology* 113, no. 5 (November 2012): 1014–26. https://doi.org/10.1111/j.1365-2672.2012.05384.x.

Singh, Brajesh K., Manuel Delgado-Baquerizo, Eleonora Egidi, Emilio Guirado, Jan E. Leach, Hongwei Liu, and Pankaj Trivedi. 'Climate Change Impacts on Plant Pathogens, Food Security and Paths Forward'. *Nature Reviews Microbiology* 21, no. 10 (October 2023): 640–56. https://doi.org/10.1038/s41579-023-00900-7.

Song, Yin, and Bart P. H. J. Thomma. 'Host-Induced Gene Silencing Compromises Verticillium Wilt in Tomato and Arabidopsis'. *Molecular Plant Pathology* 19, no. 1 (2018): 77–89. https://doi.org/10.1111/mpp.12500.

Stapleton, James J. 'Soil Solarization in Various Agricultural Production Systems'. *Crop Protection* 19, no. 8–10 (September 2000): 837–41. https://doi.org/10.1016/S0261-2194(00)00111-3.

Stark, Christian. 'Das Auftreten der Verticillium-Tracheomykosen in Hamburger Gartenbaukulturen: Ein Beitrag zur Kenntnis ihrer Erreger'. *Die Gartenbauwissenschaft* Vol. 26 (8), no. No. 4 (1961): 493–528.

Steinberg, Gero, and Sarah J. Gurr. 'Fungi, Fungicide Discovery and Global Food Security'. *Fungal Genetics and Biology* 144 (November 2020): 103476. https://doi.org/10.1016/j.fgb.2020.103476.

Su, Xiaofeng, Guoqing Lu, Xiaokang Li, Latifur Rehman, Wende Liu, Guoqing Sun, Huiming Guo, Guoliang Wang, and Hongmei Cheng. 'Host-Induced Gene Silencing of an Adenylate Kinase Gene Involved in Fungal Energy Metabolism Improves Plant Resistance to Verticillium Dahliae'. *Biomolecules* 10, no. 1 (January 2020): 127. https://doi.org/10.3390/biom10010127.

Subbarao, K. V., Z. Kabir, F. N. Martin, and S. T. Koike. 'Management of Soilborne Diseases in Strawberry Using Vegetable Rotations'. *Plant Disease* 91, no. 8 (August 2007): 964–72. https://doi.org/10.1094/PDIS-91-8-0964.

Sun, Lifan, Jun Qin, Xiaoyun Wu, Jinghan Zhang, and Jie Zhang. 'TOUCH 3 and CALMODULIN 1/4/6 Cooperate with Calcium-Dependent Protein Kinases to Trigger Calcium-Dependent Activation of CAM-BINDING PROTEIN 60-LIKE G and Regulate Fungal Resistance in Plants'. *The Plant Cell* 34, no. 10 (1 October 2022): 4088–4104. https://doi.org/10.1093/plcell/koac209.

Tao, Yuan, Tingli Liu, Lingchao Cai, et al. 2025. 'Controlling Verticillium Wilt in *Acer Mollo* Maxim with a Star Polycation dsRNA Delivery System Targeting *Verticillium Dahliae VDAG_03333*'. *Journal of Cleaner Production* 492 (February): 144827. https://doi.org/10.1016/j.jclepro.2025.144827.

Timmons, Lisa, Donald L. Court, and Andrew Fire. 2001. 'Ingestion of Bacterially Expressed dsRNAs Can Produce Specific and Potent Genetic Interference in *Caenorhabditis Elegans*'. *Gene* 263 (1): 103–12. https://doi.org/10.1016/S0378-1119(00)00579-5.

US EPA, OCSPP. 'EPA Registers Novel Pesticide Technology for Potato Crops'. Announcements and Schedules, 26 December 2023. https://www.epa.gov/pesticides/epa-registers-novel-pesticide-technology-potato-crops.

Vega-Marin, Marta, Christian Obermeier, Birger Koopmann, Xiaorong Zheng, Rod Snowdon, and Andreas Von Tiedemann. 'Phenotypic and Phylogenetic Analysis of *Verticillium Longisporum* Strains from European and Canadian Oilseed Rape Fields'. *Plant Pathology* 74, no. 1 (January 2025): 196–209. https://doi.org/10.1111/ppa.14009.

Vega-Marin, Marta, and Andreas Von Tiedemann. 'Cross-Protection of Oilseed Rape against Verticillium Longisporum by the Non-Aggressive Lineage A1/D2'. *BioControl* 67, no. 4 (August 2022): 419–31. https://doi.org/10.1007/s10526-022-10147-5.

Vergani-Junior, Carlos A., Guilherme Tonon-da-Silva, Mehmet Dinçer Inan, and Marcelo A. Mori. 'DICER: Structure, Function, and Regulation'. *Biophysical Reviews* 13, no. 6 (16 November 2021): 1081–90. https://doi.org/10.1007/s12551-021-00902-w.

Wang, Dan, Dan-Dan Zhang, Jian Song, Jun-Jiao Li, Jun Wang, Ran Li, Steven J. Klosterman, et al. 'Verticillium Dahliae CFEM Proteins Manipulate Host Immunity and Differentially Contribute to Virulence'. *BMC Biology* 20, no. 1 (23 February 2022): 55. https://doi.org/10.1186/s12915-022-01254-x.

Wang, Jie, Lieqiong Kuang, Xinfa Wang, Guihua Liu, Xiaoling Dun, and Hanzhong Wang. 'Temporal Genetic Patterns of Root Growth in Brassica Napus L. Revealed by a Low-Cost, High-Efficiency Hydroponic System'. *Theoretical and Applied Genetics* 132, no. 8 (1 August 2019): 2309–23. https://doi.org/10.1007/s00122-019-03356-7.

Wang, K., Y. Peng, W. Fu, Z. Shen, and Z. Han. 'Key Factors Determining Variations in RNA Interference Efficacy Mediated by Different Double-Stranded RNA Lengths in Tribolium Castaneum'. *Insect Molecular Biology* 28, no. 2 (2019): 235–45. https://doi.org/10.1111/imb.12546.

Wang, Lin, Kenichi Tsuda, William Truman, Masanao Sato, Le V. Nguyen, Fumiaki Katagiri, and Jane Glazebrook. 'CBP60g and SARD1 Play Partially Redundant Critical Roles in Salicylic Acid Signaling'. *The Plant Journal* 67, no. 6 (2011): 1029–41. https://doi.org/10.1111/j.1365-313X.2011.04655.x.

Wang, Ming, Arne Weiberg, Feng-Mao Lin, Bart P. H. J. Thomma, Hsien-Da Huang, and Hailing Jin. 'Bidirectional Cross-Kingdom RNAi and Fungal Uptake of External RNAs Confer Plant Protection'. *Nature Plants* 2, no. 10 (19 September 2016): 16151. https://doi.org/10.1038/nplants.2016.151.

Wang, Zhiwen, Yu Li, Borui Zhang, Xiang Gao, Mengru Shi, Sicong Zhang, Shan Zhong, Yang Zheng, and Xili Liu. 'Functionalized Carbon Dot-Delivered RNA Nano Fungicides as Superior Tools to Control Phytophthora Pathogens through Plant RdRP1 Mediated Spray-Induced Gene Silencing'. *Advanced Functional Materials* 33, no. 22 (2023): 2213143. https://doi.org/10.1002/adfm.202213143.

Wilhelm, Stephen. 'Longevity of the Verticillium Wilt Fungus in the Laboratory and Field.', 1955.

Xue, Lei, Quanhong Xue, Qin Chen, Chaofeng Lin, Guanghui Shen, and Juan Zhao. 'Isolation and Evaluation of Rhizosphere Actinomycetes with Potential Application for Biocontrol of Verticillium Wilt of Cotton'. *Crop Protection* 43 (January 2013): 231–40. https://doi.org/10.1016/j.cropro.2012.10.002.

Yang, Peng, Shu-Yuan Yi, Jun-Na Nian, Qing-Song Yuan, Wei-Jie He, Jing-Bo Zhang, and Yu-Cai Liao. 'Application of Double-Strand RNAs Targeting Chitin Synthase, Glucan Synthase, and Protein Kinase Reduces Fusarium Graminearum Spreading in Wheat'. *Frontiers in Microbiology* 12 (9 July 2021). https://doi.org/10.3389/fmicb.2021.660976.

Zarrabian, Mohammad, and Sherif M. Sherif. 2024. 'Silence Is Not Always Golden: A Closer Look at Potential Environmental and Ecotoxicological Impacts of Large-Scale dsRNA Application'. *Science of The Total Environment* 950 (November): 175311. https://doi.org/10.1016/j.scitotenv.2024.175311.

Zhang, Dan-Dan, Xin-Yan Wang, Jie-Yin Chen, Zhi-Qiang Kong, Yue-Jing Gui, Nan-Yang Li, Yu-Ming Bao, and Xiao-Feng Dai. 'Identification and Characterization of a Pathogenicity-Related Gene VdCYP1 from Verticillium Dahliae'. *Scientific Reports* 6, no. 1 (22 June 2016): 27979. https://doi.org/10.1038/srep27979.

Zhang, Qinghua, Long Yang, Jing Zhang, Mingde Wu, Weidong Chen, Daohong Jiang, and Guoqing Li. 'Production of Anti-Fungal Volatiles by Non-Pathogenic Fusarium Oxysporum and Its Efficacy in Suppression of Verticillium Wilt of Cotton'. *Plant and Soil* 392, no. 1–2 (July 2015): 101–14. https://doi.org/10.1007/s11104-015-2448-y.

Zhang, Tao, Jian-Hua Zhao, Yuan-Yuan Fang, Hui-Shan Guo, and Yun Jin. 'Exploring the Effectiveness and Durability of Trans-Kingdom Silencing of Fungal Genes in the Vascular Pathogen Verticillium Dahliae'. *International Journal of Molecular Sciences* 23, no. 5 (January 2022): 2742. https://doi.org/10.3390/ijms23052742.

Zhang, Tao, Yun-Long Zhao, Jian-Hua Zhao, Sheng Wang, Yun Jin, Zhong-Qi Chen, Yuan-Yuan Fang, Chen-Lei Hua, Shou-Wei Ding, and Hui-Shan Guo. 'Cotton Plants Export microRNAs to Inhibit Virulence Gene Expression in a Fungal Pathogen'. *Nature Plants* 2, no. 10 (26 September 2016): 1–6. https://doi.org/10.1038/nplants.2016.153.

Zhang, Weixiong, Shang Gao, Xiang Zhou, Padmanabhan Chellappan, Zheng Chen, Xuefeng Zhou, Xiaoming Zhang, et al. 'Bacteria-Responsive microRNAs Regulate Plant Innate Immunity by Modulating Plant Hormone Networks'. *Plant Molecular Biology* 75, no. 1 (1 January 2011): 93–105. https://doi.org/10.1007/s11103-010-9710-8.

Zhang, Xiaojian, Lihong Zhao, Shichao Liu, Jinglong Zhou, Yajie Wu, Zili Feng, Yalin Zhang, Heqin Zhu, Feng Wei, and Hongjie Feng. 'Identification and Functional Analysis of a Novel Hydrophobic Protein VdHP1 from Verticillium Dahliae'. *Microbiology Spectrum* 10, no. 2 (4 April 2022): e02478-21. https://doi.org/10.1128/spectrum.02478-21.

Zhang, Yan, Xingfen Wang, Shuo Yang, Jina Chi, Guiyin Zhang, and Zhiying Ma. 'Cloning and Characterization of a Verticillium Wilt Resistance Gene from Gossypium Barbadense and Functional Analysis in Arabidopsis Thaliana'. *Plant Cell Reports* 30, no. 11 (November 2011): 2085–96. https://doi.org/10.1007/s00299-011-1115-x.

Zhang, Yilin, Michael R. Martinez, Hui Sun, Mingkang Sun, Rongguan Yin, Jiajun Yan, Benedetto Marelli, et al. 'Charge, Aspect Ratio, and Plant Species Affect Uptake Efficiency and Translocation of Polymeric Agrochemical Nanocarriers'. *Environmental Science & Technology* 57, no. 22 (25 May 2023): 8269–79. https://doi.org/10.1021/acs.est.3c01154.

Zhang, Zhao, Emilie Fradin, Ronnie De Jonge, H. Peter Van Esse, Patrick Smit, Chun-Ming Liu, and Bart P. H. J. Thomma. 'Optimized Agroinfiltration and Virus-Induced Gene Silencing to Study Ve1-Mediated *Verticillium* Resistance in Tobacco'. *Molecular Plant-Microbe Interactions®* 26, no. 2 (February 2013): 182–90. https://doi.org/10.1094/MPMI-06-12-0161-R.

Zhao, Weisong, Shezeng Li, Lihong Dong, Peipei Wang, Xiuyun Lu, Xiaoyun Zhang, Zhenhe Su, Qinggang Guo, and Ping Ma. 'Effects of Different Crop Rotations on the Incidence of Cotton Verticillium Wilt and Structure and Function of the Rhizospheric Microbial Community'. *Plant and Soil* 485, no. 1–2 (April 2023): 457–74. https://doi.org/10.1007/s11104-022-05842-2.

Zheng, Ying, Benjamin Moorlach, Desiree Jakobs-Schönwandt, Anant Patel, Chiara Pastacaldi, Stefan Jacob, Ana R. Sede, et al. 'Exogenous dsRNA Triggers Sequence-Specific RNAi and Fungal Stress Responses to Control Magnaporthe Oryzae in Brachypodium Distachyon'. *Communications Biology* 8, no. 1 (25 January 2025): 121. https://doi.org/10.1038/s42003-025-07554-6.

Acknowledgement

I would like to first thank Prof. Dr. Karl-Heinz Kogel for giving me this immense learning opportunity, and for the continued guidance and supervision throughout the last four years. Thanks to Prof. Dr. Marc F. Schetelig for his invaluable input to finalize this work and for taking the time to be a second reviewer.

I would also like to thank all colleagues from the Phytopathology institute for their support and great company, special thanks to Prof. Dr. Schäfer, Ruth, Jens, Bernhard and Sabrine for their openness and for taking the time to answer my frequent random questions. Many thanks to the exchange students - Mert, Irene and Rebecca - who were a great help with the lab work. Thanks to Maria for coordinating the Bioprotect project work and for providing feedback during the writing process.

Thanks to Prof. Dr. Von Tiedemann for providing the *V. longisporum* GFP strain that was instrumental in the majority of experiments.

I am grateful to have such loving and supporting wife and family, I would not be able to reach this stage without them. Thank you Asiula for being so patient and understanding. I cannot thank my family enough for all the years of support and for enabling me to pursue a scientific career. Alhamdulillah.